THE TIME YOU ENJOY WASTING IS NOT WASTED TIME.

-------BERTRAND RUSSELL

FACULTY OF BIOSCIENCE ENGINEERING

Virus infection and host antiviral defense, a story between Israeli acute paralysis virus (IAPV) and bumblebees (*Bombus terrestris*)

Haidong Wang

Promoters:

Prof. Dr. ir. Guy Smagghe

Dr. Ivan Meeus

A dissertation submitted to Ghent University in partial fulfilment of the requirements for the degree of Doctor in Applied Biological Sciences

Academic year: 2016 - 2017

GHENT UNIVERSITY

Refer to this thesis as follows:

Wang, H. (2017) Virus infection and host antiviral defense, a story between Israeli acute paralysis virus (IAPV) and bumblebees (*Bombus terrestris*). PhD dissertation, Faculty of Bioscience Engineering, Ghent University, Belgium.

ISBN: 9789463570206

Cover illustration:

The tissue specific infection of eight common bee viruses in honeybees (*Apis* spp.) and bumblebees (*Bombus* spp.).

The authors and the promoters give the authorization to consult and copy parts of this work for personal use only. Every other use is subject to copy right laws. Permission to reproduce any material contained in this work should be obtained from the author.

Promoters:

Prof. Dr. ir. Guy Smagghe

Department of Crop Protection, Faculty of Bioscience Engineering

Ghent University, Belgium

Dr. Ivan Meeus

Department of Crop Protection, Faculty of Bioscience Engineering

Ghent University, Belgium

Dean: Prof. Dr. ir. Marc Van Meirvenne

Rector: Prof. Dr. Anne de Paepe

Members of the examination committee

Prof. dr. ir. Peter Bossier (Chairman)
Department of Animal Production, Faculty of Bioscience Engineering
Ghent University, Belgium

Dr. ir. Olivier Christiaens
Department of Crop Protection, Faculty of Bioscience Engineering
Ghent University, Belgium

Prof. Dirk de Graaf
Department of Biochemistry and Microbiology, Faculty of Science
Ghent University, Belgium

Dr. ir. Tom Defoirdt
Center for Microbial Ecology and Technology (CMET),
Faculty of Bioscience Engineering,
Ghent University, Belgium

Dr. Ivan Meeus (promoter)
Department of Crop Protection, Faculty of Bioscience Engineering
Ghent University, Belgium

Prof. dr. ir. Guy Smagghe (promoter)
Department of Crop Protection, Faculty of Bioscience Engineering
Ghent University, Belgium

Prof. Dr. Luc Swevers
Institute of Biosciences & Applications (IB-A), National Centre for Scientific Research "Demokritos", Aghia Paraskevi, Athens, Greece

Prof. Daisy Vanrompay
Department of Animal Production, Faculty of Bioscience Engineering,
Ghent University, Belgium

Table of Contents

List of abbreviations

ABPV	acute bee paralysis virus
Ago-2	Argonaute-2
AL	antennal lobes
AMPs	antimicrobial peptides
ANOVA	analysis of variance
BQCV	black queen cell virus
CBPV	chronic bee paralysis virus
CCs	coagulocytes
CCD	colony collapse disorder
CrPV	Cricket paralysis virus
DAPI	4', 6-diamidino-2-phenylindole
DCV	Drosophila C virus
DENV	dengue virus
dsRNA	double stranded RNA
DWV	deformed wing virus
DXV	Drosophila X virus
FISH	fluorescence *in situ* hybridization
FHV	Flock House virus
GNBP	Gram negative binding protein
GRs	granular cells
Hop	Hopscotch
IAPV	Israeli acute paralysis virus
IFN	interferon
IMD	immune deficiency
IRES	internal ribosome entry site
IRF	interferon regulator factors
Jak/Stat	Janus kinase/signal transducer and activator of transcription
KBV	Kashmir bee virus
KCs	Keyon cells
LSV	Lake Sinai virus
MES	2 - (N-morpholino) ethanesulfonic acid
miRNA	micro RNA
ModSP	modular serine protease
NF-κB	nuclear factor κB
OCs	oenocytes
PAMP	pathogen associated molecular pattern
Pfu	plague forming units
PGRPs	peptidoglycan receptor proteins
PI	propidium iodide
PLs	plasmatocytes
piwiRNA	piwi-interacting RNA
PPIA	peptidylprolyl isomerase A
PRs	prohemocytes
preRISC	pre-RNA induced silencing complex
PRRs	pattern recognition receptors

PTU	phenylthiourea
RdRp	RNA-depended RNA polymerase
RPL23	60S ribosomal protein L23
RNAi	RNA interference
RNQs	relative normalized quantities
RT-qPCR	reverse transcription quantitative real-time polymerase chain reaction
SBPV	slow bee paralysis virus
SBV	sacbrood virus
siRNA	small interfering RNA
STAT	signal transducer and activator of transcription
SVCs	single von Willebrand factor C-domain proteins
SVWC domain	single von Willebrand factor C-domain
Teps	thioester-containing proteins
UTR	untranslated region
vir-1	virus induced gene-1
vsiRNA	virus-derived small interfering RNA
VSV	vesicular virus
WGA	wheat germ agglutinin
WNV	West Nile virus

Scope

Bumblebees (*Bombus* spp.) can effectively pollinate wild plants and agricultural crops, and different *Bombus* species are commercially reared to perform pollinating services. Recent emerges of RNA viruses in bumblebee got particular attention as some of these viruses are notorious, known to be associated with colony losses in another well-known pollinator, the honeybee (*Apis mellifera*). Three picornaviruses, namely deformed wing virus (DWV), Kashmir bee virus (KBV) and Israeli acute paralysis virus (IAPV) have been reported to be pathogenic in both honeybee and bumblebee species. However, the interaction of these viruses with the bumblebee host is poorly understood. The main goals of this PhD dissertation are to investigate the viral infection dynamics of IAPV in the bumblebee, *Bombus terrestris* and host antiviral activities. **Chapter Ⅰ** gives a general introduction mainly on bee viruses and the bee's antiviral immune system. **Chapter Ⅱ** to **Ⅵ** are experimental chapters exploring the virus-host interactions between IAPV and *B. terrestris* (Figure 1), with a particular interest in understanding bee immunity.

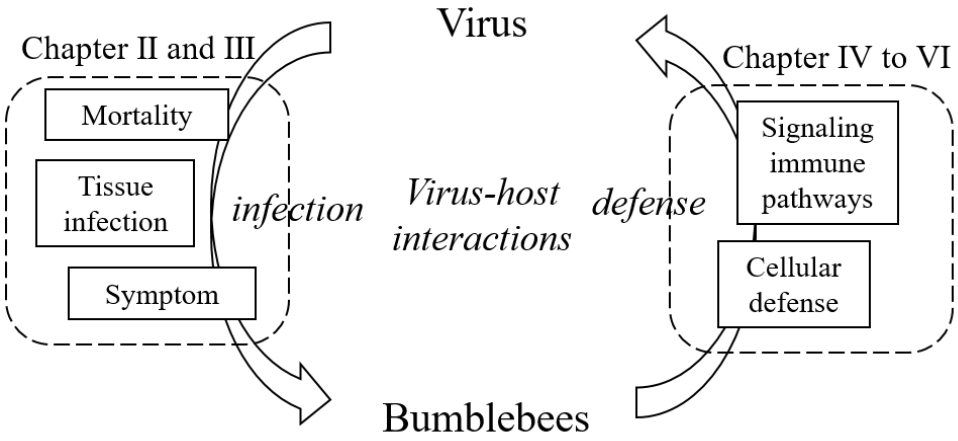

Figure 1. Schematic overview of the experimental chapters (Ⅱ-Ⅵ) in this thesis

A first requisite to study virus effects on bee health and immunity is understanding how infection methods could impact viral infection dynamics. Therefore, in **Chapter II**, we compared oral feeding and artificial injection of IAPV. Specifically, we looked at mortality, virus tissue distribution, and localization. Besides, for injection, we observed a new paralysis symptom and found that some bees exhibited front leg paralysis while others did not, yet all injected bees died within approximately 5 days. We tried to correlate this new paralysis symptom with viral tissues tropism in **Chapter III**.

Upon viral infection, insects rely on their innate immune system to defend themselves. Studies of the model insects *Drosophila* and mosquitos have revealed the involvement of two immune signaling pathways, RNAi and Jak/Stat, in the host antiviral activity. These two important pathways are linked to each other by an immune molecule, Vago belonging to a group of short proteins called single von Willebrand factor C-domain proteins (SVCs). Within hymenopteran species, the involvement of RNAi and Jak/Stat upon viral infection is described but the links between both are less known. We also noticed a reduced repertoire of SVCs in Hymenoptera, especially in most bee species there is only one SVC protein identified, and which function is not characterized. Therefore, in **Chapter IV**, we asked if this SVC in *B. terrestris* is an antiviral immune modulator. We exploited the silencing capacity of the RNAi pathway to specifically silence *BtSVC* and *BtDicer-2 in vivo*. We hypothesized that *BtSVC* silencing would increase the IAPV titers and *BtDicer-2* silencing would have impact on the *BtSVC* expression, which are the two core characteristics of the SVC protein Vago in *Drosophila*. Besides, seeing the different responsive character of SVCs to stressors, we also questioned whether this single *BtSVC* is involved in other immune pathways such as Toll and IMD. Based on the result of **Chapter IV**, where we reported a link between the antiviral immune modulator *BtSVC* and antimicrobial peptides (AMP)

genes expression, we asked ourselves if AMP expression could be related with virus infections (**Chapter Ⅴ**).

Aside from the recruitment of immune signaling pathways, insect immunity also invests in cellular defense to confront stresses. Here hemocytes are described as major components representing cellular immunity which are mainly associated with wounding healing and bacterial clearance. However, their roles in antiviral defense is poorly understood. Understanding the responses of hemocytes to viral infection can be critical first step to explore the role that these immune cells play upon viral infection. Therefore, in **Chapter Ⅵ**, we performed experiments to measure the staining patterns of hemocytes population of *B. terrestris* after virus infection by flow cytometry. We hypothesized that a virulent virus like IAPV would have severe damage on these immune cells. Besides, we also questioned whether phagocytosis, a major cellular immune activity can be involved in the host antiviral activity.

In the final **Chapter Ⅶ**, the main findings of our study and the future perspectives are discussed.

Chapter Ⅰ: General Introduction

1. Bumblebee

1.1 Important pollinators

Bumblebees (*Bombus* spp.) belong to the Apidae, the largest family within the super family Apoidea (Michener, 2007). They are primitive eusocial insects and have an annual life cycle, with queens single-handedly founding nests (Goulson, 2003). Bumblebees are important pollinators in temperate climate regions and considered as cold adapted bees. Aside from their pollination role in natural ecosystems they also provide valuable agriculture services, the most prominent being the pollination of agricultural plants (Goulson, Lye, and Darvill, 2008; Williams and Osborne, 2009). In Europe, the potential of bumblebee species to transfer pollen between flowers resulting in pollination has been recognized for a long time. For example, bumblebees are the main pollinator of most clover species and more than a century ago scientists believed it would be a good idea to introduce them in non-native regions. Shipments of hibernating wild bumblebee queens from U.K. to New Zealand were undertaken to improve seed set of red clover (Goulson, 2003). The current methodology is to rear different bumblebee species deprived from any outdoor environment. Rearing for commercial pollination purposes started in the late eighties, with a first focus on crops in green houses. It was the Belgian researcher Dr. de Jonghe who discovered the value of the bumblebee *Bombus terrestris* in pollinating greenhouse tomatoes and founded the company Biobest (Velthuis and van Doorn, 2006). Since then, many producers started rearing bumblebees for pollination service. Now, commercial bumblebee hives are used for greenhouse pollination over the globe (Goulson et al., 2008). Here, bumblebees had an added value in comparison to another well-known pollinator, the European honeybee (*Apis mellifera*). This is because of their robust size, less disorientated in greenhouses and buzz-pollination behavior (high-frequency

buzzing to release pollen from flowers; crucial to release the pollen from the tomato stamens) (De Luca and Vallejo-Marin, 2013). Besides, bumblebees can endure more harsh weather conditions. They can forage in very cold conditions and even have been noticed foraging in raining conditions (Corbet et al., 1993). Therefore, they are a reliable workforce providing robust pollination service in open field despite the unpredictable climate conditions.

1.2 Life with challenges

Although bumblebees are blessed with a pollination ability, which has led to a multi-billion-euro industry (e.g. the value of the bumblebee pollinated tomato crops is estimated to be 12 billion euros in 2004 and the total value of rearing bumblebee along is estimated to be 55 million (Velthuis and van Doorn, 2006)), many wild species are threatened. It is actually a diverse pollinator community that leads towards the highest fruit set when looking at the different crops in different regions of the world (Garibaldi et al., 2014). Thereby bee diversity is not only crucial to support pollination of the wild plant community, but it also has a direct economic added value. There is mounting evidence that the richness of these important pollinators has declined in recent decades with few species gone extinct in Western Europe (Goulson et al., 2015) and North American (Cameron et al., 2011).

These declines seem to be driven by multiple interacting stressors (Figure 1). Habitat loss[1] is a major long-term stressor. Aside from the loss of suitable environment, the reliance on agrochemicals also influences pollinator population. The use of herbicides

[1] Bumblebees need flower diversity as food resource, which need to provide season long forage around the nesting habitat (depending on the species within 1 km radius). Next to this, there can be spatially more distant and suitable hibernation sites.

results in diminished food resource availability and insecticides can have direct and indirect intoxication effects (Goulson et al., 2015). Besides, a more recent driver of bumblebee loss and one for future bumblebee generation is climate change (Kerr et al., 2015). It has lately become clear that these factors do not function in isolation and the combined effect seem to be more harmful (Goulson et al., 2015). Parasites and viruses are a good example. Pathogens are a natural part of an ecosystem, but

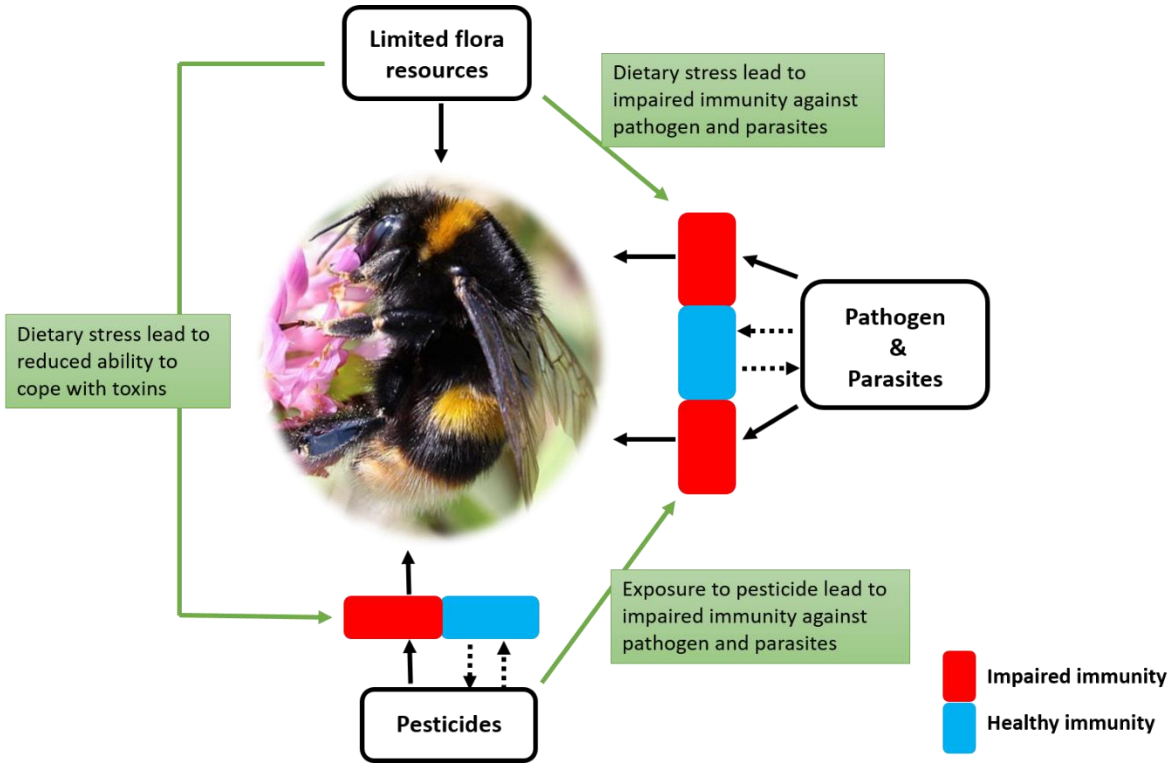

Figure 1. Multiple interacting stressors threat on the population of both managed and wild bumblebee species. The interaction (green arrows and boxes) of these stressors (black boxes) can have a combined effect on a bumblebee population. For example, exposure to pesticides reduces resistance to diseases and dietary stresses are likely to reduce the ability of bees to cope with both toxins and pathogens. Black arrow with solid line indicates harmful effect, black arrow with dash line indicates interactions between bee immunity and stressors. Red filled boxes indicate impaired immunity and blue filled boxes indicate healthy immunity.

because anthropogenic influences now also pose potential threats to bumblebees. For instance, *Crithidia bombi*, a natural parasite of bumblebee, causes little mortality in well-fed bumblebees but becomes virulent in those with a restricted diet (Brown, Loosli, and Schmid-Hempel, 2000). Besides, exposure to pesticides also reduces the resistance of bumblebee to diseases (Baron et al., 2014; Fauser-Misslin et al., 2014).

This indicates that dietary stress and pesticides exposure can lead to an impaired immunity, thus disturbing the natural host-parasites/pathogen dynamics (Figure 1). Besides, the introduction of non-native (bee) species (though commercial trading activities) which harbor parasites and viruses, can also interfer with natural host-parasite interactions. However, the interactions between these stressors are difficult to predict, owing to limited knowledge of the impact of these stressors on the bumblebee immune system. Therefore, to better understand the declines of bumblebees and other wide pollinators, researches into the interactions of these stressors with the bumblebee immune defense system are much needed.

2. Bee viruses

2.1 Viruses discovery, symptoms and tissues infection patterns

Bees naturally suffer from a broad range of viruses which symptoms can be observed in larvae, pupae and adults. Pioneering studies of isolating viruses from honeybees were performed by Bailey and Ball and their colleagues. In 1963, they identified two viruses from the infected honeybees and named them acute bee paralysis virus (ABPV) and chronic bee paralysis virus (CBPV), as both viruses can cause paralysis symptoms in adult honeybees (Bailey, Gibbs, and Wood, 1963). At that time the identification of bee viruses were mainly associated with the symptoms, the morphology of viral particles and binding properties of antisera. With the rapid development of sequencing techniques, the identification of bee viruses also stepped into the genome era. The first complete genome of a bee virus was from the Sacbrood virus (SBV) (Ghosh et al., 1999). To date there are around 23 viruses reported to infect honeybees and most of them are positive strand RNA viruses in the family of *Dicistroviridae* and *Iflaviridae* (Chen and Siede, 2007; Li et al., 2014; Runckel et al.,

2011). However, this number is not absolute, as some of the reported viruses are identified only *in silico* (Runckel et al., 2011).

The PCR primers designed based on viruses initially identified from the honeybee are often used for virus detection in other bee species, indicating that these viruses are not honeybee specific. Although the term "honeybee viruses" is in the collective memory of a big part of the research community, it is getting clear that most of them can also infect other bees, and even insects from different orders. Among the reported viruses infecting bees, eight of them namely, ABPV, SBPV, SBV, deformed wing virus (DWV), black queen cell virus (BQCV), Kashmir bee virus (KBV), slow bee paralysis virus (SBPV) and Israeli acute paralysis virus (IAPV) are the most common infection agents and objects of many ongoing research. By far, the majority virus studies have focused on virus interaction with the honeybee and to a lesser extent with the bumblebee (Figure 2). Thus, the following paragraphs will mainly describe research findings obtained from honeybees with references to bumblebees when possible.

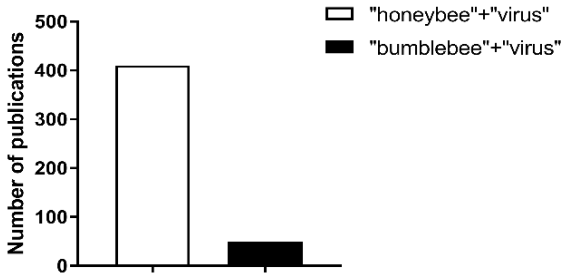

Figure 2. Number of publications in Web of Science core collection database. Unfilled bar represents search result using key words, "honeybee" and "virus"; black filled bar represents search results using key words, "bumblebee" and "virus". Data retrieved from http://apps.webofknowledge.com in May, 2017.

Bee viruses can cause visible symptoms on both individual level and colony level (Table 1). These symptoms range from brood to adult and some of them can be obvious and easily recognized, such as the paralysis symptom (ABPV, CBPV, SBPV and IAPV), wing deformity (DWV), non-pupated pale yellow larvae stretched on their backs with heads lifted (SBV), blackened cell walls of sealed queen cells (BQCV) (Table 1). Aside from these apparent symptoms that are normally accompanied by

individual mortality, recent research has revealed that these viruses can also cause "inapparent" sub-lethal effect interfering the normal behavior of bees (Li et al., 2013; Meeus et al., 2014).

Table 1 Overview of symptoms of eight most studied bee viruses in the honeybee (*Apis mellifera*)

Virus	Family	Symptoms[a] of overt infection	References
ABPV	Dicistroviridae	-Paralysis (body trembling) -Darkened cuticle pigment -Mortality (adult and immature bees)	(Bailey, 1963 #113; Chen and Siede 2007, de Miranda et al., 2010)
KBV	Dicistroviridae	-Mortality	(de Miranda et al., 2010)
IAPV	Dicistroviridae	-Paralysis (body trembling) -Impaired cognition and homing ability -mortality	(Cox-Forster et al., 2007; Maori et al., 2007; Li et al., 2013; de Miranda et al., 2010)
SBV	Iflaviridae	-Pale-yellowish, leathery cuticle of capped larvae Failure of larvae to pupate -Mortality (potential in adult and certainly in capped larvae) -Dead larvae become dark and little scale	(Chen and Siede 2007, McMenamin and Genersch 2015)
CBPV	?	-Paralysis (body and wings trembling) -Flight inability -Bloated abdomen -Hair loss	(Bailey et al., 1963; Bailey, 1974 #111); Chen and Siede 2007)
BQCV	Dicistroviridae	-Pale-yellowish, leathery cuticle of capped larva -Failure of larvae to pupate -Deceases larvae and walls of cells turn black -Larvae mortality	(Chen and Siede, 2007, McMenamin and Genersch, 2015)
SBPV	Iflaviridae	-Paralysis of anterior pair of legs -Adult mortality	(Bailey and Woods 1974)
DWV	Iflaviridae	-Deformed wings -Bloated abdomen -Discoloration in adult bees -Mortality (adult and immature bees)	(Bailey and Ball, 1991)(Chen and Siede 2007)

a, virus infected colonies normally undergo a covert infection pattern (i.e. not showing any symptoms), but can develop into an overt infection with typical symptoms.
"?" indicates undetermined family

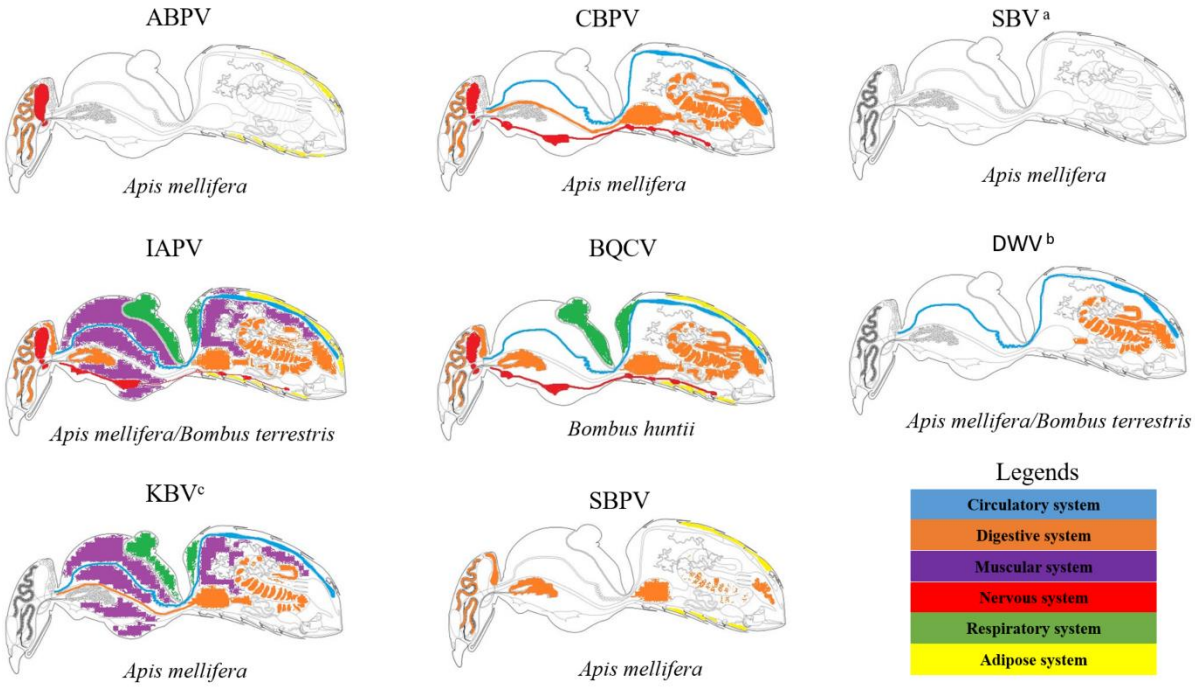

Figure 3. Internal tissue infection of eight common bee viruses in honeybee or bumblebee adult. Internal tissues are classified into six different system: circulatory system (hemolymph), digestive system (food glands and alimentary canal), muscular system, nervous system (brain, thoracic and abdominal ganglia), respiratory system (trachea and air sacs) and adipose system (fat body). Tissues reported to be infected with virus are filled in corresponding colors, those without infection or data insufficient remain colorless. Species names under each bee tissue profile indicates the species used for study in corresponding references. These results are based on a multitude of research techniques (e.g. PCR, FISH, electron microscopy) and infection methods ranging from natural infection towards artificial infections. Differences between the viruses could therefore be related to a differential experimental setup. Tissues infection data of each virus, are based on the following researches: ABPV (Bailey and Milne, 1969); CBPV (Lee and Furgala, 1965; Blanchard et al., 2006); SBV (Lee and Furgala, 1967; Park et al., 2016); IAPV (Chen et al., 2014; Chapter III); BQCV (Peng et al., 2010); DWV (Boncristiani et al., 2009; Fievet et al., 2006); KBV (Dall, 1987); SBPV (Denholm, 1999). See table S1 for infection tissues of each virus

[a], SBV is reported to infect many tissues in larvae but information of infection of adult tissues is scarce (See table S1 for tissue infection of SBV in larvae).

[b], DWV is reported to spread through all body parts (head, thorax and abdomen) while the tissue infection information is scarce.

[c], information comes from infection pupae.

The mechanism behind these symptomologies is not fully understood. One hypothesis is that the occurrence of symptoms is associated with specific virus tissues infection (Chen and Siede, 2007). For example, viruses associated with paralysis symptoms, such as ABPV, CBPV, SBPV and IAPV are reported to infect the bee nerve system including brain, thoracic ganglia and abdominal ganglia (Figure 3, Table S1). KBV, a

genetically related virus with ABPV and IAPV, does not induce paralysis symptoms and is not reported to infect the bee nerve system. (Chen et al., 2006; Dall, 1987). However, not all viruses infecting the nerve system can induce a paralysis symptom. For example, BQCV can infect the nerve system of *Bombus huntii*, but is not reported to cause any bee paralysis (Peng et al., 2011), indicating the occurrence of paralysis symptoms may not always be concluded as specific nerve tissue infection. It is also worth mentioning that viral detection in most of these studies rely on PCR (Table S1), thus lacking evidence of cellular infection. Herein figure 3 also illustrates the need for a uniform study of virus tissue tropism in different bees. Besides, tissues like brains have many functional regions like mushroom bodies, optical lobes and antennal lobes, which are closely related to the bee sensing ability (Figure 4). Thus, visualizing tissue viral infection in brain may provide more knowledge towards understanding the paralysis symptom.

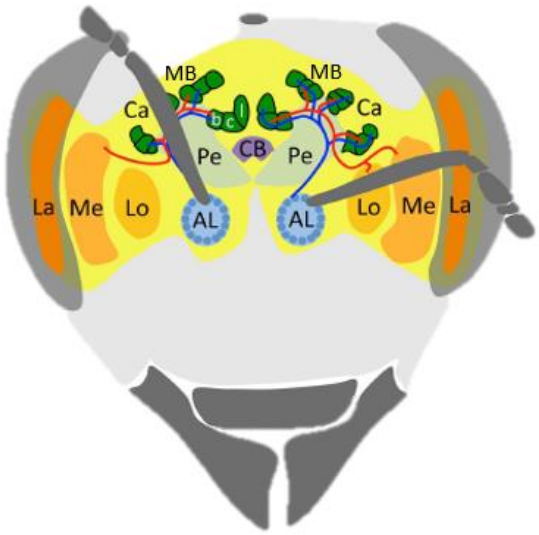

Figure 4. Schematic drawing of a honeybee worker brain (*Apis mellifera*). The visual lobes composed of the lamina (La), the medulla (Me) and the lobula (Lo), received the sensory inputs from the compound eyes. The antennal lobes (AL) receive the inputs from the olfactory sensory neurons of the antennae. The mushroom bodies (MB) are the central structures that process multimodal information and participate in learning and memory. These structures have a characteristic morphology consisting of a pedunculus (Pe) and two calyces (Ca). The central body (CB) has connections to all major parts of the brain and is involving in leg coordination and motor control. Figure adapted from (Lihoreau, Latty, and Chittka, 2012).

Recent detection of these viruses in non-*Apis* pollinators suggests a possible wider spread with broader impact (Levitt et al., 2013; Manley et al., 2015; Singh et al., 2010) (Figure 5). It is therefore vital to study the ecology and epidemiology of these viruses in the hymenopteran pollinator community as a whole (Singh et al., 2010).

Understanding the viral infection dynamics in bumblebee species is an important step in this direction.

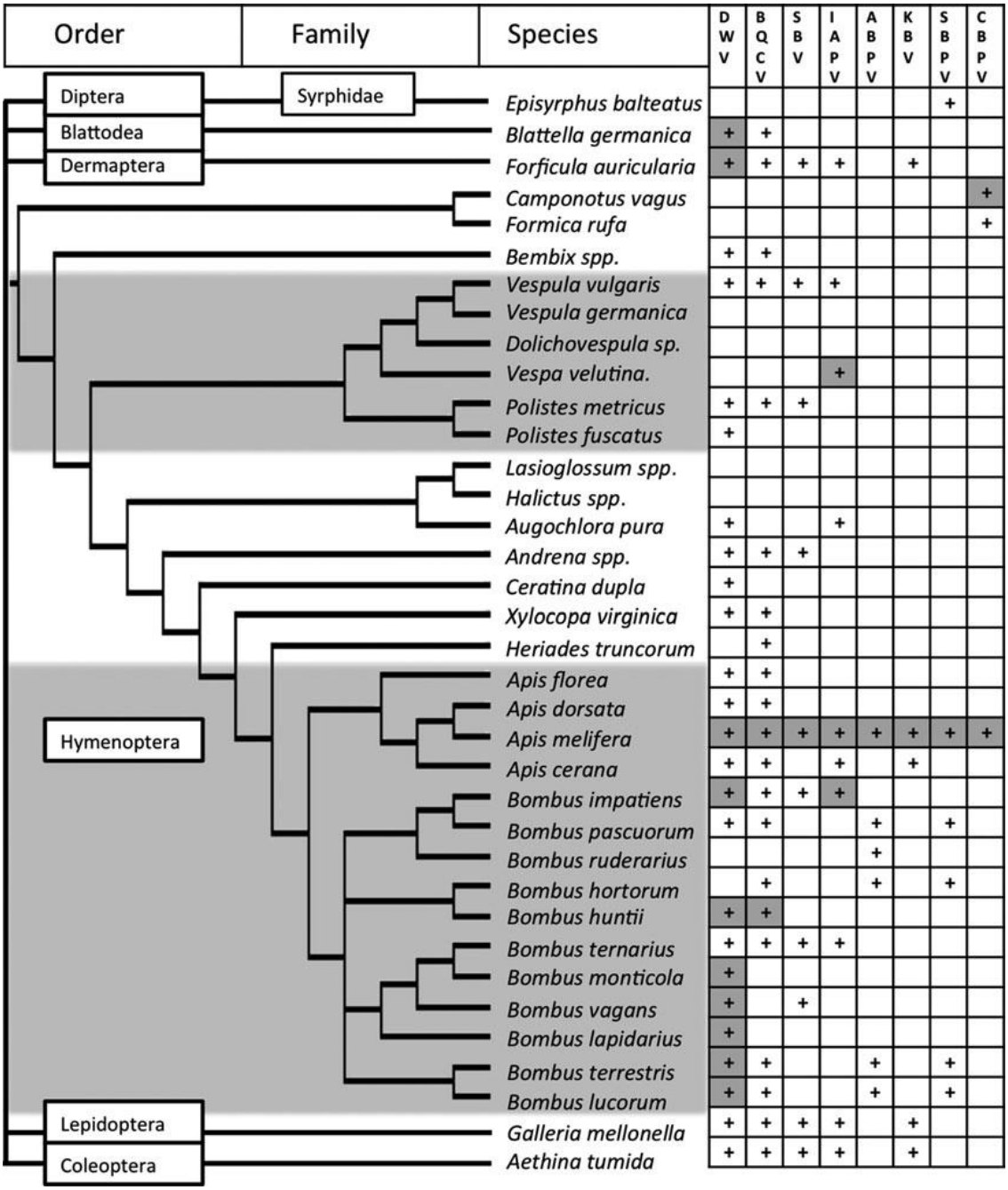

Figure 5. Phylogeny of pollinator species, and other insects associated with honeybee colonies, focusing on the Hymenoptera. Shaded species are social insects. "+" indicates that the species has been identified as positive for virus, "+" indicates virus replication has been demonstrated. Virus abbreviations, DWV, deformed wing virus; BQCV, black queen cell virus; SBV, sacbrood virus; IAPV, Israeli acute paralysis virus; ABPV, acute bee paralysis virus; KBV, Kashmir bee virus; SBPV, slow bee paralysis virus; CBPV, chronic bee paralysis virus. Figure adapted from (Manley, Boots, and Wilfert, 2015).

2.2 IAPV

IAPV is a positive single stranded RNA virus in the family of *Dicistroviridae*. It was originally purified in 2002 by propagating the extracts of dead bees from collapsing hives in Israel and its genome was characterized in 2007 (Maori et al., 2007). IAPV carries a 9487 nucleotides (nt) genome in positive orientation with two open reading frames separated by an intergenic region. Together with ABPV and KBV, these three viruses form a genetically and biologically related virus complex with a worldwide distribution (de Miranda et al., 2010a) (Figure 6).

Figure 6. ABPV-KBV-IAPV genomes. The identified functional domains are the helicase, 3C-protease and the RNA-depended RNA polymerase (RdRp) in the non-structural open reading frame, followed by an internal ribosome entry site (IRES) in the intergenic region, and the four capsid proteins (VP1-VP4) in the structural reading frame. Another IRES is also expected in the 5' untranslated region (5' UTR) Figure adapted from (de Miranda, Cordoni, and Budge, 2010a).

This viral complex is frequently implicated in honeybee colony losses, and IAPV has been mentioned to be related with the colony collapse disorder (CCD) mainly based on the first metagenomic study on the honeybees microbiome (Cox-Foster D.L. et al., 2007) without any following confirmations. Besides, IAPV was also detected in the samples that predates CCD, thus the role it plays in CCD is also weakened (Chen and J.D., 2007). A field study showed that IAPV can transmit from infected honeybee hive which suffer from CCD to the nearby bumblebee species (Singh et al., 2010), providing experimental evidence of inter genus transmission. Plus, this transmission route is likely bidirectional for the virus can move from infected honeybee to bumblebee and then from bumblebee to honeybee (Singh et al., 2010). However, little is known about the effect of IAPV infection in bumblebee colonies due to the lack of reliable monitoring systems in the wild. When performing virus infection experiments on reared bumblebees under laboratory conditions, IAPV can cause both lethal and sub-lethal

effects in *B. terrestris* workers (Meeus et al., 2014; Niu. et al., 2016a). This undoubtedly indicates that IAPV is an active infectious agent in bumblebee species. To better understand its infection dynamics in these non-*Apis* pollinator, more study is needed to focus the infection dynamics and epidemiology of IAPV in different bee species.

3. Insect antiviral defense

3.1 General overview (insect antiviral pathways)

Viruses, being obligate intracellular organism, need to hijack the host cell machinery to promote their own replication. Correspondingly, the host immune system is activated to control and clear the viral infection. Insects, lacking an adaptive immunity, mount on their innate immunity to confront the virus infection. The innate immunity of insect can be broadly divided into humoral and cellular defense (Strand, 2008). This innate immune system comprises several conserved pathways which activation is initiated with the binding of pathogen associated molecular patterns (PAMPs) to pattern recognition receptors (PRRs) (Kingsolver, Huang, and Hardy, 2013). This binding ultimately leads to the production of effector molecules and/or cellular processes capable of suppressing virus replication. The conserved small interfering RNA (siRNA) pathway and the Jak/Stat pathway has been described to play a role in the insect antiviral defense (Dostert et al., 2005; Wang et al., 2006). Other pathways like Toll and IMD are also associated with the host antiviral activity. However, aside from the siRNA pathway, the mechanism of how other pathways are involved in the antiviral responses remain unclear. Also, noting that the initial evidence of the involvement of these pathways in antiviral defense is from flies and mosquitos thus there is a possibility that the mechanism of these immune pathways may be different among insect species.

3.2 siRNA pathway

The most robust insect response upon virus infection is through the RNA interference (RNAi) pathway. It utilizes virus-derived double stranded RNA (dsRNA) to generate small interfering RNA (siRNA) which target the viral genome for specific degradation, thereby preventing virus replication (Ding, 2010; Kingsolver et al., 2013; Ronald and Beutler, 2010). There are currently three well characterized RNAi-related pathways: the siRNA pathway, micro RNA (miRNA) pathway and the piwi-interacting RNA (piwiRNA) pathways (Kim, Han, and Siomi, 2009). Among them, the siRNA pathway is predominantly responsible for the antiviral activity (Kingsolver et al., 2013). The siRNA pathway is activated after the recognition of virus-derived dsRNA by Dicer-2 (member of the RNase Ⅲ family of ribonuclease). The dsRNA can be part of the virus genome (e.g. dsRNA virus) and/or it can also be a replication intermediate produced by single stranded RNA (ssRNA) viruses. Then the virus-derived dsRNA is processed into 21-22 nucleotide (nt)-long siRNAs which are loaded onto the Argonaute-2 (Ago-2), forming a pre-RNA induced silencing complex (preRISC) (Figure 7). Then the passenger strand is degraded and the guide strand serves as a specific template for the degradation of viral genome. Inhibition of the siRNA pathway through silencing the key genes like

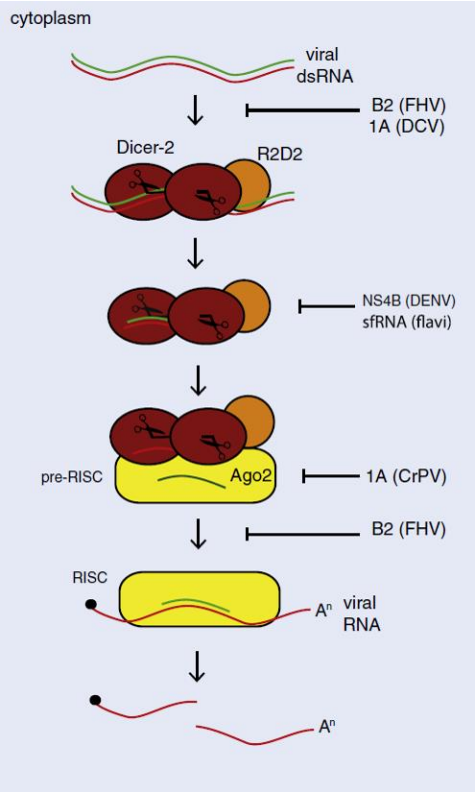

Figure 7. siRNA pathway. Virus derived dsRNA is recognized by Dicer-2 in the complex with R2D2. Dicer-2 cleaves the dsRNA into 21-nt siRNAs. The siRNA is loaded into the pre-RISC complex where duplex unwinding and selection of a guide strand occurs. The guide strand functions to direct RISC to the viral RNA target through base pairing. The Ago-2 protein in the RISC cleaves the viral RNA target inhibiting virus replication. Points in the pathway at which viral suppressors of RNAi function are shown. Figure adapted from (Kingsolver 2013).

Dicer-2, *Ago-2* can lead to increased virus accumulation in flies (Galiana-Arnoux et al., 2006; van Rij et al., 2006; Wang et al., 2006; Zambon et al., 2005) and other insects (Myles et al., 2008; Sanchez-Vargas et al., 2009; Siu et al., 2011), highlighting the importance of this pathway in the antiviral defense.

However, there is mounting evidence showing that this pathway can be suppressed by virus infection, including many bee viruses (Brutscher and Flenniken 2015). Sequence analysis revealed that the dicistroviruses IAPV, KBV and ABPV contain a DvExNPGP motif at the 5′ terminus of their genomes, suggesting these viruses may encode a virus-encoded suppressors of RNAi (VSR) protein (Chen et al., 2014). However, to date this links between DvExNPGP and the presence of VSR is not clear in IAPV. In other dicistroviruses, such as CrPV, the N-terminus of ORF1 encodes for a VSR and this can also be expected for IAPV. A recent study also showed that the key components of RNAi pathway (e.g. Dicer-2) are down-regulated in highly-infected honeybees (De Smet et al., 2017), providing additional data that virus infection may modulate the expression of RNAi related genes.

In bumblebees, key components for siRNA pathway such as, Dicer-2, Ago-2 and R2D2 have been identified (Niu et al., 2014b). However, the function of this pathway on viral infection in *B. terrestris* is not clear as silencing of *Dicer-2* did not alter the accumulation of Israeli acute paralysis virus (IAPV) nor slow bee paralysis virus (SBPV), although IAPV infection induced the production of predominant 22 nt-long virus-derived siRNA (vsiRNA) which contain a high proportion of anti-genomic IAPV sequences (Niu. et al., 2016a). Interestingly, IAPV infection seems to enhance the RNAi machinery in different tissues of bumblebee (Capelle et al., 2016). Besides, the key component of RNAi pathway, *Dicer-2* was upregulated after IAPV infection

(Capelle et al., 2016; Niu et al., 2016a). Whether IAPV infection can suppress the host immune system in bumblebee requires more studies.

3.3 Jak/Stat pathway

The Jak/Stat pathway also contributes to the insect antiviral response (Dostert et al., 2005; Hedges and Johnson, 2008; Souza-Neto, Sim, and Dimopoulos, 2009), although by which mechanism is not fully understood. Silencing signaling molecules and transcription factors of this pathway resulted in higher viral titers (Dostert et al., 2005). While an effector molecule, virus induced gene 1 (*vir-1*) (in Drosophila and mosquitos, not identified in other species) could not be linked with changing viral titers, thus mainly serve as readout for the Jak/Stat activation towards virus infection (Deddouche et al., 2008; Dostert et al., 2005).

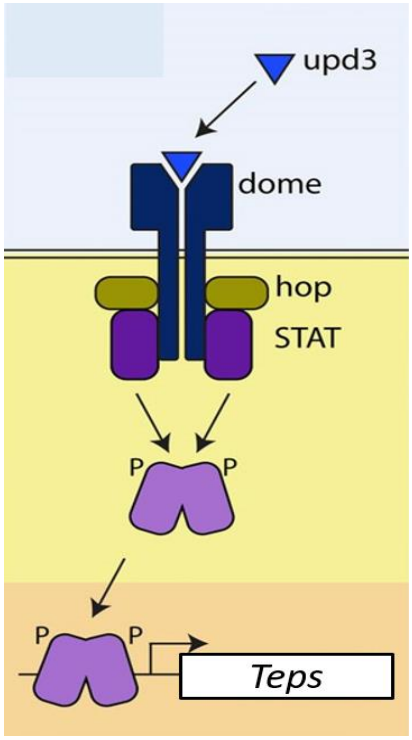

Figure 8. Jak/Stat pathway. The Upd3 ligand binds Domeless, leading to recruitment of hopscotch (Jak) and STAT. Phosphorylation of STAT allows nuclear translocation, promoter binding, and activation of transcription of effector molecules like Teps. Figure adapted from (Kingsolver 2013).

This pathway is well recognized as a response to septic injury. Here it is activated via the ligand unpaired (Upd) binding to the Domeless receptor (Xu et al.) which is a homolog of the vertebrate type I cytokine receptor. The *D. melanogaster* genome encodes three Upd-related ligands (Upd, Upd2 and Upd3), while in the bumblebee genome, there are no Upd-like proteins identified (Figure 8). This ligand binding allows the transphosphorylation of Hopscotch (Hop) kinases, leading to the phosphorylation and dimerization of signal transducer and activator of transcription (STAT). Then the activated STATs are translocated to the nucleus and transcriptionally regulate the

expression of downstream effector molecules like thioester-containing proteins (Teps) (Figure 8) which are defined as opsonin and can promotes phagocytosis of gram negative bacteria (Levashina et al., 2001). Jak/Stat pathway is also important in bees. A recent study in *B. terrestris* showed that silencing of *hop* can result in increased SBPV titers in whole abdomen of bees at 2 days post infection (dpi) but not at 3dpi. However silencing hop did not have an impact on the viral titers of IAPV (Niu, Meeus, and Smagghe, 2016b). In *A. mellifera*, key components of Jak/Stat signaling pathways are induced after IAPV infection, although the functional role of this pathway upon virus is still unclear (Chen et al., 2014). However, in bees, the effector molecule (e.g. *vir-1*) of Jak/Stat regarding to the virus infection is unknown. Within the genome of *Apis mellifera* and *Bombus terrestris* no orthologue of *vir-1* is found.

3.4 Interaction of siRNA and Jak/Stat through Vago

Despite the clear role that Dicer-2 plays inside RNAi pathways, increasing evidence indicates that Dicer-2 can also act as a virus sensing molecule triggering the activation of downstream signaling cascades like Jak/Stat upon virus infection through a recently identified ligand, namely Vago (Figure 9) (Paradkar et al., 2012). In *Drosophila*, *vago* was strongly induced after Drosophila C virus (DCV) and Sindbis virus (SINV) infection and weakly induced by the Flock House virus (FHV) (Deddouche et al., 2008). Besides, its expression is highly depended on the Dicer-2 but not by the other components in the siRNA pathways (e.g. Ago-2 and R2D2), indicating that the expression of vago is activated after the virus recognition (Deddouche et al., 2008). Paradkar *et al*. characterized vago as a secreted protein that can activate the Jak/Stat pathway upon West Nile virus (WNV) infection in *Culex quinquefasciatus* cells (Figure 9). Surprisingly the *Cq*Vago does not bind to the domeless receptor, indicating that the vago-mediated antiviral responses occur via an alternative receptor. Besides, silencing *vir-1*, the

effector molecule of Jak/Stat pathway in mosquito failed to alter the WNV titers, which also demonstrated that an alternative downstream STAT-activating effector may exist in this vago mediated antiviral defense activity. This Dicer-2 dependent, vago mediated activating of Jak/Stat against virus infection acts similarly to the mammalian interferon (IFN) system and vago therefore appeared to function as an IFN-like cytokine.

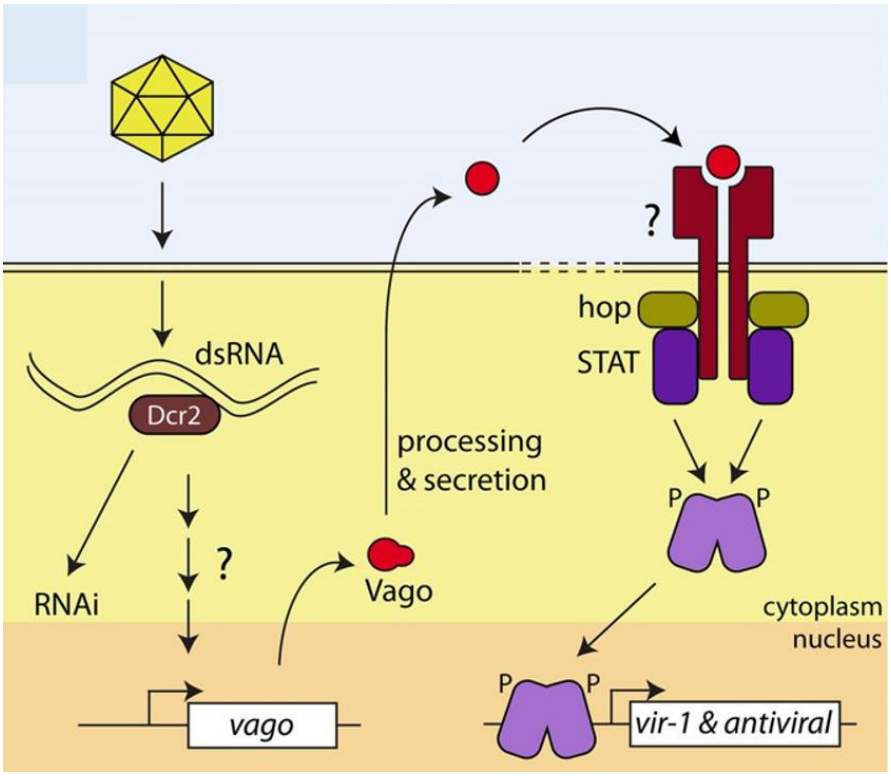

Figure 9. **Interactions between siRNA and Jak/Stat pathway**. Dicer-2–dependent activation of STAT transcription via Vago signaling. Dicer-2 binds viral dsRNA and, through an unknown mechanism, activates expression of Vago. Processed and secreted Vago binds to an unknown cellular receptor, resulting in Jak/Stat activation and expression of vir-1 and yet-uncharacterized antiviral genes. Figures adapted from (Kingsolver 2013)

3.5 The single domain von Willebrand factor type C protein family

Vago belongs to a group of short peptides called single-domain von-willebrand factor type C proteins (SVCs) which are initially identified in *D. melanogaster* (Sheldon et al., 2007). They are characterized by a single von Willebrand factor type C domain (SVWC

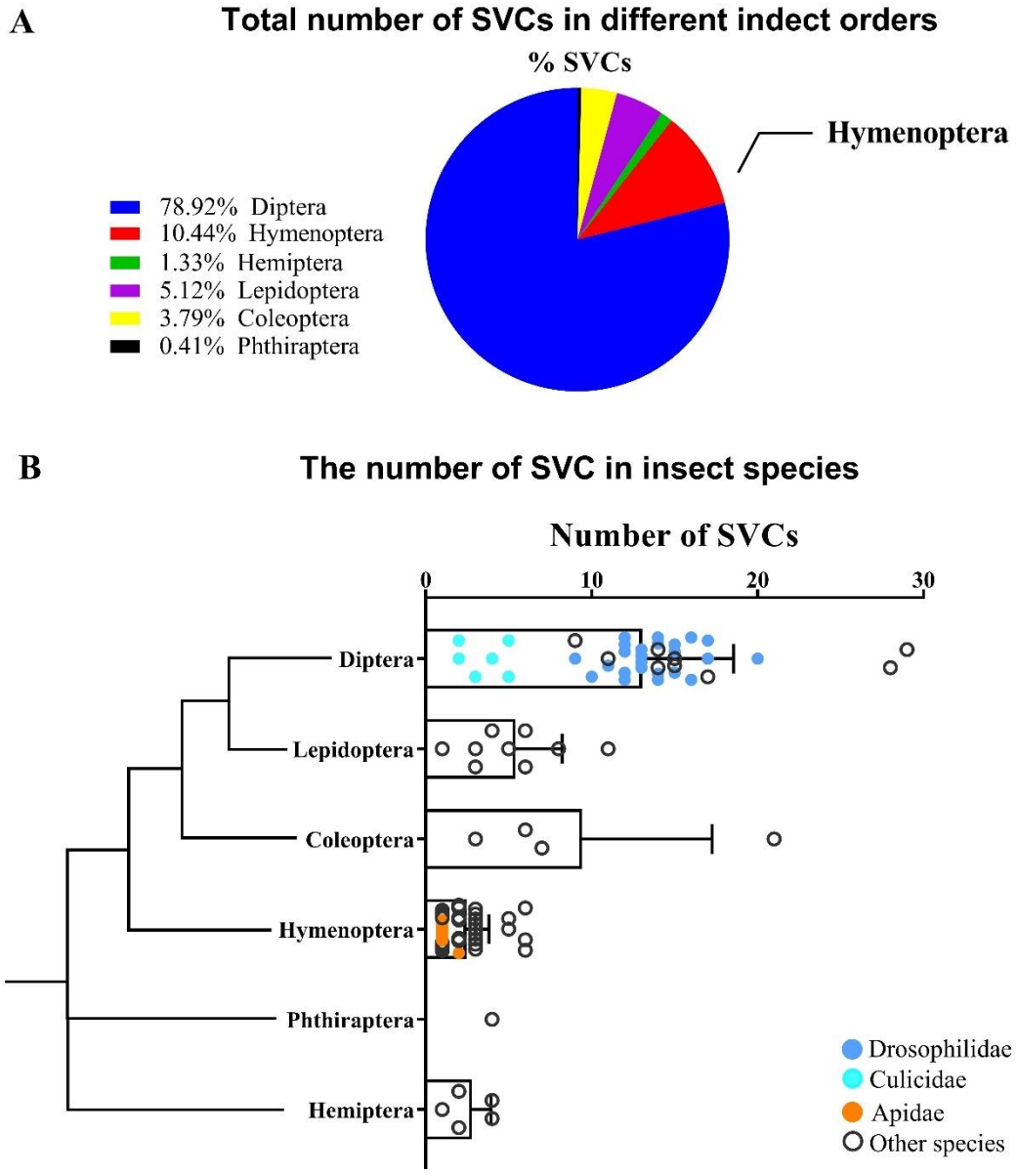

Figure 10. The number of SVCs in insect orders and species. SVC amino acid sequences were collected by searching the SVWC domain (pfam15430) related proteins. Note that all insect species listed here have their genome sequenced. See supplementary, Table S1 for all insect species with SVCs. **A**. Pie chart shows the percentage of SVCs taken by different insect orders. Hymenoptera species possess around 10% of the total SVCs, following Diptera which holds the highest number of SVCs (~80%). Other species hold around 10% of total SVCs. **B**. Phylogenetic tree (adapted from (Ishiwata et al., 2011)) shows the relationships amongst the insect orders. Branches do not indicate the phylogenetic distance. Bar chart which shows the average number of SVCs in each insect order (error bar represent standard deviation, SD). Scatter dot plot shows the SVCs in each insect species individually. Dots filled with light blue represent Drosophilidae species; dots filled with cyan represent Culicidae species; dots filled with orange represent Apidae species.

domain), having 8 of the 10 conserved cysteines of the canonical von Willebrand factor type C domain (VWC domain). When searching the SVWC domain in proteins of all species, we found that they are mainly restricted to arthropods (Figure 10A) and their numbers in insect species are diverse (Figure 10B).

Flies normally have more than 10 SVCs while the other insects tend to have less. Strikingly, there is only 1 SVC identified in most of the bee species. Aside from the antiviral role of vago and its orthologues (in mosquitos) in the host innate immunity, the function of other SVCs are less studied. In this section, we will focus on the limited functional studies of SVC in *D. melanogaster*, mosquitos, shrimps and bees.

3.5.1 SVC in Drosophila melanogaster

By searching SVWC-domain related proteins in different database, we found 12 SVC members in *Drosophila melanogaster* (Table 2), of which 8 were among the report of Sheldon et al., 2007. Another four SVCs members, CG32667, CG34215, CG34177 and CG34178 which also contain SVWC domain were not included in Sheldon's study (Table 2).

Table 2. SVCs in Drosophila melanogaster

NCBI	Uniprot	Interpro	pfam	SMART	Sheldon et al., 2007
CG2081	✓	✓	✓	✓	✓
CG31997	✓	✓	✓	✓	✓
CG14132	✓	✓	✓	✓	✓
CG32667	✓	✓	✓		
CG15199	✓	✓	✓	✓	✓
CG15202	✓	✓	✓	✓	✓
CG34460	✓	✓	✓	✓	✓
CG15203	✓	✓	✓	✓	✓
CG34215	✓	✓	✓	✓	
CG34177		✓	✓	✓	
CG2444	✓	✓	✓	✓	✓
CG34178	✓	✓	✓	✓	

Searching of several transcriptome-wide libraries (Christina et al., 2002; Tomancak et al., 2002) revealed that seven of these SVCs (CG2081, CG15202, CG34460, CG34215, CG34177, CG2444 and CG34178) have low or no expression in the embryo stages and appeared mainly to be expressed in the adult stages (Figure 11A). Besides, four *Dm*SVCs (CG2081(vago), CG2444, CG31997 and CG14132) are expressed in larval challenged with bacterial (Sheldon et al., 2007). Moreover, CG2081, CG31997, CG34215, CG32667, CG15203, CG34215 and CG2444 are also found to be highly induced by Sindibis virus (SINV) infection (Figure 11B). Furthermore, CG2081, CG15199 and CG14132 are also reported to be nutritionally regulated (Christina et al., 2002). Therefore, the *DmSVCs* are described as response genes towards pathogen infection or nutritional status.

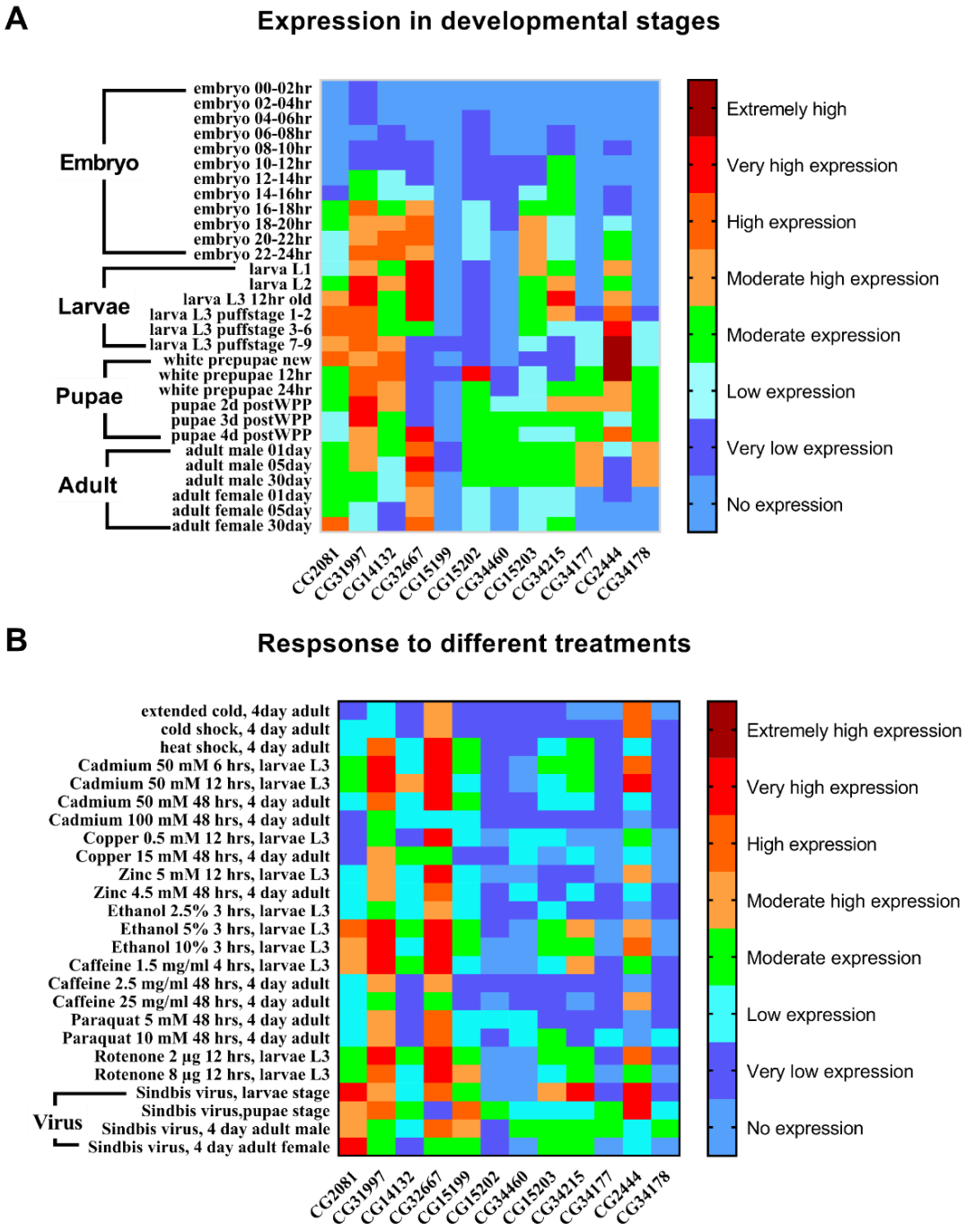

Figure 11. Heatmap of 12 *D. melanogaster* SVCs expression profiles. **A.** *D. melanogaster SVCs* expression in different developmental stages. **B.** Expression data are extracted from flybase, modENCODE RNA-Seq project (http://www.modencode.org/celniker/) and heatmaps were established by Prism v7 software.

3.5.2 SVC in mosquitos

Functional studies of SVCs in mosquitos are largely focused on the *Dm*vago orthologue in *Culex* quinquefasciatus, the salivary cysteine-rich secreted peptide (*Cq*vago) (XP_001842264) (Paradkar et al., 2014; Paradkar et al., 2012). Both qPCR and western blotting showed that *Cq*vago was upregulated upon West Nile virus (WNV) infection. However, there is a significantly lower increase in mRNA levels of *Cq*vago after WNV infection in *Dicer-2* silenced Hsu cells, indicating that Dicer-2 is also required for WNV-induced upregulation of *Cq*vago. Also, it is reported that the Rel2 and TRAF are both essential to the Dicer-2 dependent *Cq*vago antiviral function, which is similar to the interferon regulation in the vertebrate cells (Paradkar et al., 2014). Besides, overexpression of *Cq*vago in Hsu cells decreased WNV titers by ~40 fold and silencing of *Cq*vago increased the WNV titers by ~25 fold, indicating its involvement in the antiviral activity. Interestingly, overexpression of an *Aedes albopictus* SVC (*Aa*vago NCBI number XP_001658930) in *Cq*vago-silenced Hsu cells also decreased WNV titers, suggesting a conserved function of vago in both *Culex* and *Aedes* mosquitos.

3.5.3 SVC In shrimps

In Pacific white shrimp, *Litopenaeus vannamei*, there are five SVCs identified, namely *Lv*SVC1-5. An in *vitro* study showed that three of these *Lv*SVCs (1,4 and5) could be activated by both *LvDicer-2* and *DmDicer-2*. When challenged by viral infection, the induction of these three *LvSVC* together with *LvDicer-2* were also observed (Chen et al., 2011). Besides, an interferon regulator factors like (IRF-like) gene which could bind to the *LvSVC*4 promoter and regulate its transcription was identified (Li et al., 2015). An in *vitro* test on *Drosophila* S2 cells showed that the *Lv*IRF could significantly upregulate the expression of *LvSVC4* and *LvSVC*5 but not *LvSVC*1-3. An in *vivo*

functional study showed that suppression of either *Lv*SVC4 or *Lv*SVC5 significantly increased the mortality of shrimps caused by white spot syndrome virus (WSSV) infection and was related with higher viral copies in the shrimp tissues. Therefore, shrimp might possess an IRF-vago-Jak/Stat regulatory system which acts like the IRF-IFN-Jak/Stat in vertebrates. However, the downstream activation of Jak/Stat pathway to restrict virus by *Lv*SVC remains hypothetical as there is no study showing that Jak/Stat pathway is involved in the antiviral activity of shrimp and on its relation with *Lv*SVC.

3.5.4 SVCs in bees

In most bee species, there is only one SVC identified, which function is not clear. The amino acid sequences of SVC in honeybees (*Apis* spp.) and bumblebees (*Bombus* spp.) are shown in Figure 12. The aa sequences of these SVC share a high similarity (>90%), indicating a conserved function of SVC in honeybees and bumblebees. Study in *B. terrestris* revealed a surprising downregulation of *BtSVC* (XP_003399812) upon IAPV infection but not after SBPV infection. Further silencing this gene failed to alter IAPV titers in whole abdomen of bees (Niu et al., 2016b). It is also worth noting that

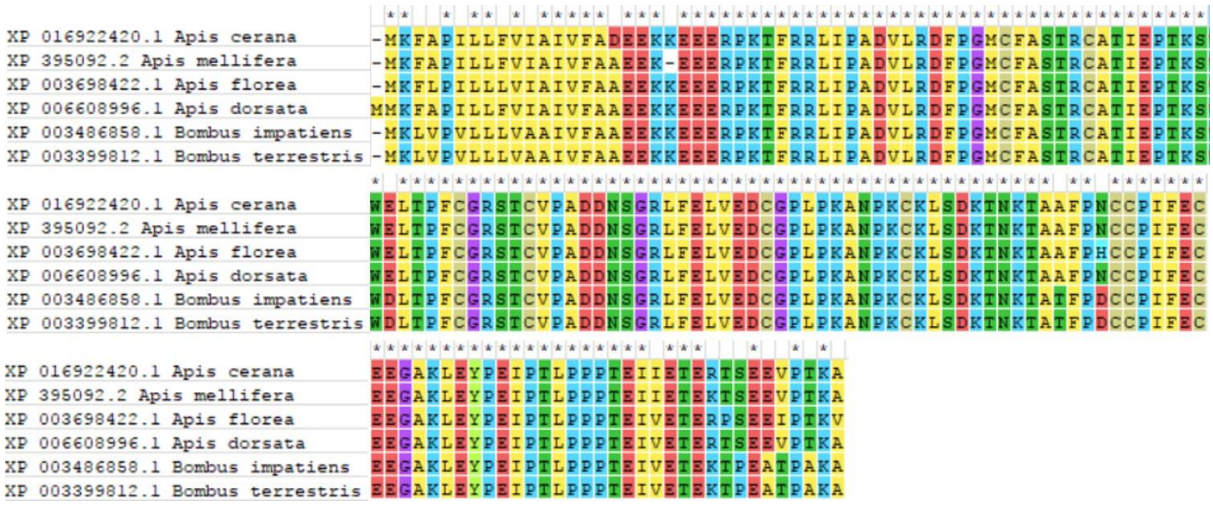

Figure 12. The alignment of amino acid sequences of SVC in *Apis* and *Bombus* species. Sequences are extracted from NCBI and alignment was done by ClustalW in the MEGA 7.0 software. The SVC sequence identities between these bee species are above 90%.

silencing *BtSVC* also resulted in lower expression of *hop*, indicating a potential link with the Jak/Stat pathway (Niu et al., 2016b). Interestingly, a protein blast inside the *D. melanogaster* genome using XP_003399812 as a query showed that the best hit is CG31997 but not CG2081 (vago), indicating that the function of *Bt*SVC may be different from vago of flies. Therefore, we explored the role this only SVC plays in the immunity of bumblebee *B. terrestris* especially regarding to the known antiviral function of vago in flies and mosquitos in the second part of this thesis.

3.6 The involvement of AMPs and NF-κB related immune pathways in antiviral defense

One hall mark of the *Drosophila* responses to bacterial/fungal infections is the secretion of a cocktail of antimicrobial peptides (AMPs) into the hemolymph (Ganesan et al., 2011). Two conserved immune pathways, Toll and Imd are responsible for the regulation of NF-κB transcription factors and the production of AMPs (Imler, 2014). However, the involvement of AMPs and these NF-κB related immune pathways in the antiviral responses is not fully understood. In this section, we will focus on the signaling cascades of these two pathways and their involvement in the antiviral activity.

3.6.1 Toll and Imd pathways

The Toll pathway can be activated through two detection methods (Figure 13A). The first method includes the pathogen recognition receptors (PRRs) (e.g., peptidoglycan receptor proteins (PGRPs) and Gram (-) binding proteins (GNBPs)), which recognize the components of the cell wall in bacteria and fungi (Gobert et al., 2003; Gottar et al., 2006; Takahasia et al., 2009). The second method involves the protease Persephone (Psh) that senses foreign proteolytic activity including proteases secreted by fungi (El

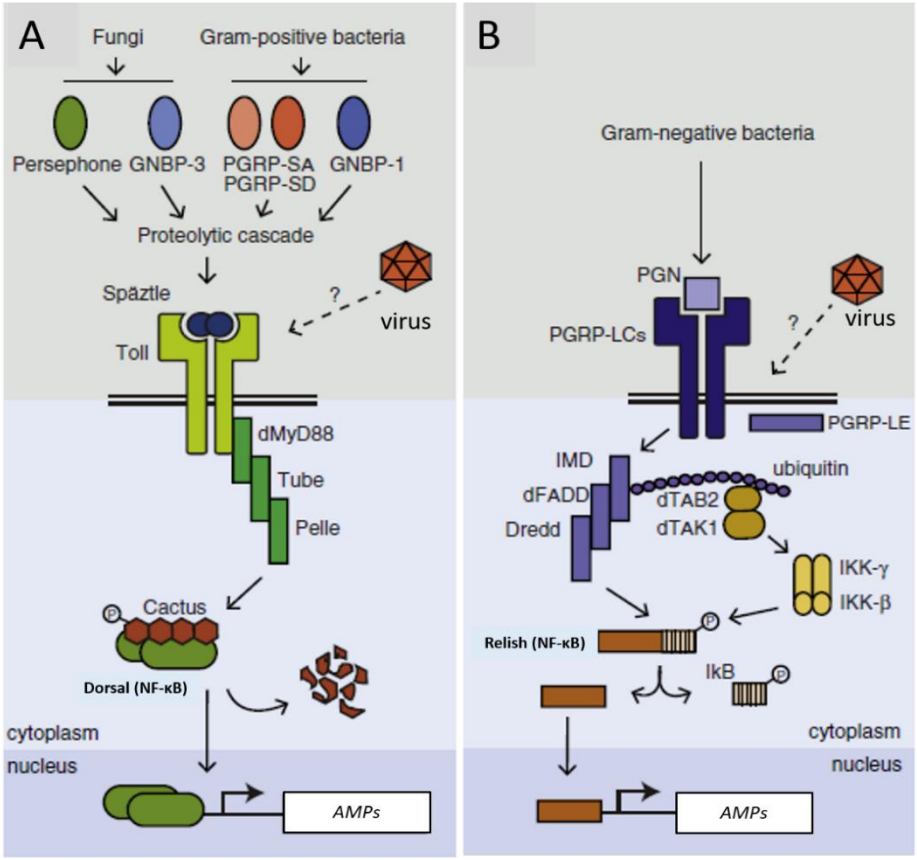

Figure 13. **Insect NF-κB related immune pathways for the production of AMPs**. **A**. The Toll pathway is activated by a family of pathogen recognition receptors (PRRs) (e.g., peptidoglycan receptor proteins (PGRP) and Gram (+) binding proteins (GNBP)) that bind fungal and bacterial PAMPs. The pathogen recognition can also through protease Persephone (Psh) that senses foreign proteolytic activity including proteases secreted by fungi. The activation of Toll upon virus infection is unclear. Following PAMP binding, a serine protease cascade results in cleavage of pro- Spaetzle into mature Spaetzle. Toll dimerization results in the recruitment of dMyD88, Tube, and Pelle. Pelle is likely involved in degradation of NF-kB inhibitors (Cactus), resulting in the release of transcription factors Dorsal/Dif. Nuclear translocation of Dorsal/Dif results in increased expression of antimicrobial peptides (AMPs). **B.** The Imd pathway is activated by Peptidoglycan recognition protein LC (PGRP-LC) binding to diaminopimelic-containing peptidoglycan of Gram (-) bacteria, followed by activation of the adaptor protein Immune deficiency (IMD), Relish phosphorylation by the IKK complex (IkB kinase), and cleavage of Relish by the caspase Dredd (Death-related ced-3/Nedd2). Relish transcriptionally regulates expression of AMPs. Figure adapted from (Kingsolver et al., 2013)

Chamy et al., 2008; Gottar et al., 2006). The signals from PRRs are integrated into the modular serine protease ModSP, which leads to the activation of another set of serine proteases (Buchona et al., 2009). Signals from the serine proteases and Psh can activate the Spätzle-processing enzyme. Toll dimerization results in the recruitment of dMyD88, Tube, and Pelle which is involved in the degradation of NF-kB inhibitors (Cactus), resulting in the release of NF-κB transcription factors Dorsal/Dif. Nuclear translocation of Dorsal/Dif results in increased expression of antimicrobial peptides (AMPs).

The IMD pathway is activated by Peptidoglycan recognition protein LC (PGRP-LC) binding to diaminopimelic-containing peptidoglycan of Gram (-) bacteria, followed by activation of the adaptor protein Immune deficiency (IMD), Relish phosphorylation by the IKK complex (IkB kinase), and cleavage of Relish by the caspase Dredd (Death-related ced-3/Nedd2) (Figure 13B). Relish transcriptionally regulates expression of AMPs.

3.6.2 Involvement in antiviral activity

Increasing evidence has suggested that the Toll and Imd may also be involved in the host antiviral immune defense, but by a mechanism which is unrelated with the ending products, AMPs. For example, AMPs are induced significantly in *D. melanogaster* against Drosophila X virus (DXV) but overexpression of them did not alter the virus titers (Zambon et al., 2005). Besides, the regulation of AMPs upon different virus infection can also be dynamic. For instance, the Toll pathway is also involved in the control of Dengue virus (DENV) in mosquito *Aedes aegypti*, while the AMPs regulation after DENV challenges are variable as both up and down regulations were observed (Ramirez and Dimopoulos, 2010; Xi, Ramirez, and Dimopoulos, 2008b). The IMD pathway is likely to be involved in the control of Cricket paralysis virus (CrPV) (Costa

et al., 2009) and Sindbis virus (SINV) (Avadhanula et al., 2009). AMPs are not induced in case of CrPV. While upon SINV virus, the IMD related AMPs (e.g. *Diptericin*) is induced but the Toll-related AMPs (e.g. *Drosomycin*) is not. In bees, functional study towards NF-kB related pathways upon virus infection are scarce. Limited information also indicates a diverse regulation of AMPs upon virus infection. Symptomatic young bees infected with IAPV through feeding showed increased expression of Toll pathway members (i.e., *toll-6*, *cactus*, and *hymenoptaecin*) (Galbraith et al., 2015), whereas transcriptional profiling of IAPV positive bees from naturally infected colonies did not indicate the involvement of either the Toll or Imd in antiviral defense (Chen et al., 2014). Besides, young bees infected with SINV via injection and harboring very low levels of other bee pathogens expressed less *apidaecin* and *hymenoptaecin* than non-infection mock controls (Flenniken and Andino, 2014). Similarly, neither ABPV challenges nor ABPV and *E. coli* co-challenge through injection resulted in AMP production (i.e., *defensin-1*, *abaecin*, and *hymenoptaecin*) in adults or larvae, indicating that ABPV may suppress bee immune responses (Azzami et al., 2012).

This indicated that the activation of either Toll or IMD upon virus infection may not lead to the production of AMPs. Besides, whether the induction of AMPs is due to the direct sensing of virus by Dicer-2 or through a secondary effect is not clear. Evidence seems to support that the indirect effect (e.g. inflammation induced by virus) plays a major role in the AMPs induction after virus challenges (Zomba 2005), while it still remains possible that alternative regulation mechanism may exist that can modulate AMPs expression after virus sensing (Figure 14).

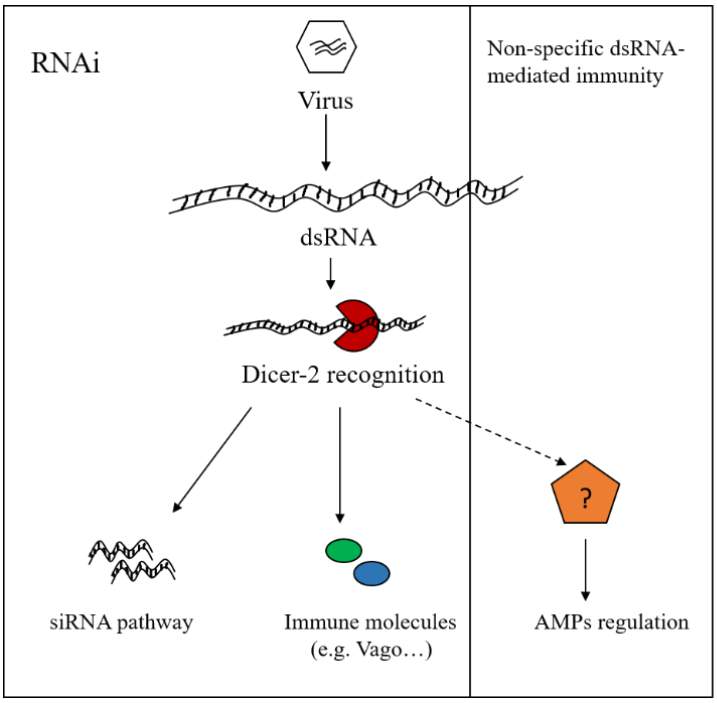

Figure 14. **RNAi and non-specific dsRNA mediated antiviral defense.** Viral derived dsRNA is recognized by Dicer-2 and activated siRNA pathway targeting virus replication. Besides, after viral sensing, other immune genes are also activated such as vago which can activate down-stream signaling immune pathway. Whether AMPs can be induced after virus sensing is not clear. Figure restyled from (Brutscher and Flenniken, 2015).

3.7 The cellular defense against virus infection

The insect cellular defense involves hemocyte mediated responses like phagocytosis and encapsulation (Irving et al., 2005; Strand, 2008). Noting that there is no clear border between these two defenses since many humoral factors can regulate hemocyte activity and hemocytes are important sources of many humoral defense molecules (Strand, 2008). To date the involvement of cellular immune defense in the antiviral responses is not well characterized.

3.7.1 Bee hemocytes classification

Hemocytes are the main components of cellular defense. In honeybee, few studies have focused on the classification of hemocytes (de Graaf et al., 2002; Van Steenkiste, Raes, and Jacobs, 1988). Van Steenkiste (1988) classified the honeybee hemocytes into five types, including plasmatocytes (PLs), prohemocytes (PRs), granular cells (GRs), oenocytes (OCs) and coagulocyts (CCs), depending on morphology and staining pattern (Table 3). The predominant cell type is PLs, representing 90% of the total circulating cells. Besides, PLs can be divided into four subgroups (P1-P4) (Table 3).

Table 2 Hemocytes identification in honeybee (*Apis mellifera*) (Van Steenkiste et al., 1988)

Cell type	Characterization
Plasmatocytes (PLs)-1	Round cells (diameter = 5–12 µm) with a dense, central nucleus
PLs-2	Atransitional stage between P1 and P3
PLs-3	Large oval, discoid cells (length = 8–20 µm, width = 8–12 µm)
PLs-4	Fusiform cells (length = 10–30 µm, width = 6–10 µm).
Prohemocytes (PRs)	Round cells (diameter = 6–10 µm), that attach rapidly and flatten thereafter, making them larger on haemolymph smears (length = 10–20 µm, width = 4–10 µm)
Granular cells (GCs)	Large (length = 10–25 µm, width = 8–20 µm) cells with various inclusions in their cytoplasm
Oenocytes (OCs)	Similar to GC
Coagulocyts (CCs)	Unstable and easily get burst during sampling

In contrast to this traditional differentiation method which is fully based on microscopy detection (light and electron microscopy), a recent study introduced new strategies towards studying honeybee hemocytes. By using flow cytometry with counter staining of propidium iodide (PI) and wheat germ agglutinin (WGA). Marringa *et al*. (2014) found four types of hemocytes: two kinds of permeabilized cells (Q1 and Q2 in Figure 15), unstained acellular objects (Q3 in Figure 15) and plasmatocytes (Q4 in Figure 15). Microscopy test after Wright staining showed that Q1 and Q2 have a dense nucleus

and may represent a continuum of permeabilized cell forms differing in the amount of associated plasma membrane and cytoplasm. These two cells are similar to the PLs-3 in Van Steenkiste's study (Table 3). The acellular objects are smaller than the two

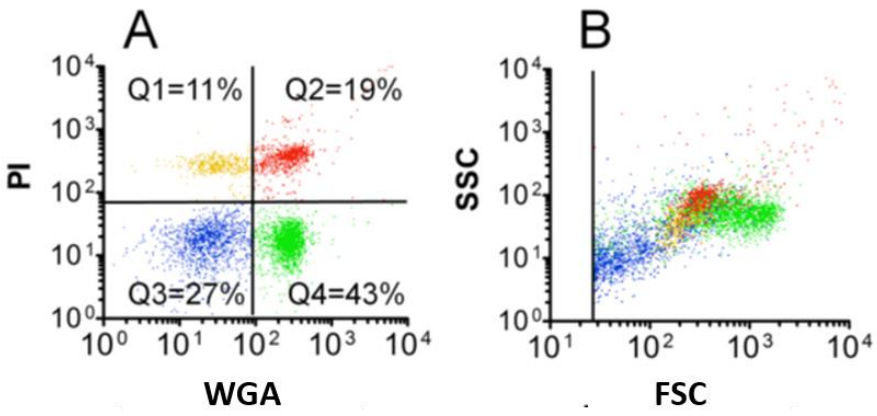

Figure 15. Honeybee hemolymph analysis by flow cytometry. A. PI vs WGA staining plot shows that there are four types of hemocytes identified based on their staining pattern. Two types of hemocytes are permeabilized to PI staining (Q1 and Q2). Plasmatocytes are stained with high WGA while acellular objects (Q3) are not stained with WGA. B. SSC vs FSC plot shows the corresponding events in A. Figure adapted from (Marringa et al., 2014)

pemerabilzied cells and show a smaller dense nucleus in the center and probably refer to the PL-1 or GCs in table 3. Q4 are large plasmatocyes that show similar characteristic as the PLs-4 in table 3. The authors also reported a high variety of hemocytes composition over individual bees. In some bees, Q1 and Q2 are found to be the dominant cells types (~80%), while in others, a dominant Q4 (>90%) was observed. This may be extra evidence that these cells (Q1, Q2 and Q4) are all plasmatocytes but in different developmental stages or in a response to environmental stresses. To date there is no study on hemocyte classficaition in bumblebees (*Bombus* spp.).

3.7.2 Apoptosis depended phagocytosis in antiviral defense

Phagocytosis is a well conserved cellular defense response in which binding its receptor induces the immune cell to form a phagosome. This results in engulfment of the target via actin polymerization-dependent mechanisms followed by maturation of

the phagosome into a phagolysosome by a series of fission and fusion events with endosomes and lysosomes (Stuart and Ezekowitz, 2005). Hemocytes phagocytose a diversity of targets including bacteria, yeast, apoptotic bodies, and abiotic particles like synthetic beads and India ink particles (Lanot et al., 2001; Lavine and Strand, 2002). Injection of latex beads, which can block/saturate the phagocytosis, is a common method utilized in insects to study the involvement of phagocytosis in the innate immunity towards pathogen infection (Savina et al., 2006).

A recent study in *Drosophila* revealed that phagocytosis can be involved in the antiviral activity in an apoptosis dependent manner (Lamiable et al., 2016; Nainu et al., 2015). Nainu *et al.*, found that DCV infection can induce apoptosis in infected S2 cell which can be phagocytosed by the hemocyte-derived l (2) mbn cells. To prove this mechanism *in vivo*, hemocytes were isolated from infected flies and found to contain DCV-infected cells. Then the authors blocked the phagocytosis by pre-injecting latex beads into the adult *D. melanogaster* flies prior to DCV infection, which resulted in an increased mortality (Nainu et al., 2015). This provided evidence that the mechanism is also present *in vivo*. Similarly, Lamiable et al. (2016) found that either injection of latex beads to block phagocytosis or genetic depletion of hemocytes resulted in decreased survival and increased viral titers following infection of CrPV, FHV and vesicular virus (VSV) in adult flies. Besides, CrPV and FHV can induce apoptosis in S2 cells which can be phagocytosed by the hemocytes (Lamiable et al., 2016). These studies presented a novel mechanism that cellular defense can involve in the host antiviral immunity. While it is noted that phagocytosis can also be involved in VSV infection where apoptosis is not induced, indicating that alternative targets triggering phagocytosis may also exist. It is unclear if apoptosis-dependent phagocytosis can be involved in the antiviral defense of bumblebees (*Bombus* spp.).

Table S1. Tissue infection of eight bee viruses in honeybee and bumblebee

Virus	Family	Tissues	Animal	Techniques	References
ABPV	Dicistroviridae	-Fat body -Brain -Hypopharyngeal glands	*A. mellifera* worker	Electron microscope	(Bailey and Milne, 1969)
KBV	Dicistroviridae	-Fore and hindgut -Alimentary canal -Musculature -Epidermis -Tracheal -Hemocytes -Eviscerated body	*A. mellifera* pupae queen	Electron microscope, PCR	(Dall 1987; Chen 2006)
IAPV	Dicistroviridae	-Hemolymph -Brains -Fat body, -Salivary glands -Hypopharyngeal glands -Gut -Nerve -Trachea Muscle -Hemolymph lowest and gut highest	*A. mellifera* & *B. terrestris* workers	PCR	(Chen et al., 2014)
SBV	Iflaviridae	-Fat body -Muscle -Tracheal -Hypopharyngeal glands of workers	*A. mellifera* larvae worker	Electron Microscope, ISH	(Chen et al., 2006; Lee and Furgala, 1967) (Park et al., 2016)
CBPV	?	-Particular tropism for nervous tissues Thoracic and abdominal ganglia does not appear in the fat body cell or muscle tissues -Hemolymph -Eviscerated body -Mandibular and hypopharyngeal glands -Brain -Alimentary canal	*A. mellifera* Queen adult	Electron Microscope PCR qPCR	(Lee and Furgala, 1965) (Chen, 2006) (Blanchard et al., 2007)

Virus	Family	Tissues	Animal	Techniques	References
BQCV	Dicistroviridae	-Wings -Legs -Antennae -Brain -Fat bodies -Salivary glands -Gut -Hemolymph, -nerves -Trachea -Food glands -Gut -Ovaries	*Bombus huntii*	PCR qPCR	(Peng et al., 2011) (Chen, 2006)
SBPV	Iflaviridae	-Head -Hypopharyngeal glands -Mandibular glands -Salivary glands -Fat body -Crop -Forelegs -less in the hind legs, midgut, rectum and thorax	*A. mellifera* workers	ELISA	(de Miranda et al., 2010b; Denholm, 1999)
DWV	Iflaviridae	-Throughout the whole body -Wings -Legs -Head -Thorax -Abdomen, -Ovaries (Queen) -Fat body (Queen) -Spermathecal (Queen) -Seminal vesicles (Drone)	*A. mellifera* queen, drone and woker *B terrestris* workers	PCR ISH	(Chen 2006) (Fievet et al., 2006)(lanzi et al., 2006)(Boncristiani et al., 2009)

Chapter Ⅱ: Systemic Israeli acute paralysis virus (IAPV) infection in bumblebee (*Bombus terrestris*) through feeding and injection

Parts of this chapter are submitted for publication:

Wang, H., Meeus, I., Piot, N. & Smagghe, G., 2017. Systemic Israeli acute paralysis virus (IAPV) in bumblebees (*Bombus terrestris*) through feeding and injection. *Journal of Invertebrate Pathology* (submitted)

1. Introduction

Viruses are obligate intracellular pathogens which hijack the host cell machinery to enable their own replication. A first requisite to establish initial replication is the success of cell entry which can lead towards systemic infection (Boulant, Stanifer, and Lozach, 2015). Different RNA viruses are able to infect bees and cause chronic (long term) or acute (short term) infections (Chen and Siede, 2007). An important horizontal route is oral infection: here viruses enter the gut lumen and infect the digestive tract from where they can disseminate to other body tissues and induce systemic infection. In this case, the host's local immune system in the digestive tract (e.g. the insect gut epithelium) forms the first line of defense against the viral invasion. Although evidence of gut local immune responses to bacterial infection has been well studied in the model *Drosophila melanogaster* and other insects, knowledge regarding the involvement of gut local immunity against viral infection is still limited (Bosco-Drayon et al., 2012; Buchon et al., 2009; Hakim, Baldwin, and Smagghe, 2010; Zaidman-Remy et al., 2006). Local antiviral immunity is important to understand viral infection dynamics, for example the midgut barriers in lepidopteran insects contribute to the developmental resistance of the host against baculovirus (Engelhard and Volkman, 1995). Furthermore, it is recognized that the Toll-Dorsal pathway seems to play an important role in the antiviral activity after oral infection (Ferreira et al., 2014; Xi, Ramirez, and Dimopoulos, 2008a).

Another route is through a vector, bypassing local immunity. The most well-known example of vectored virus transmission in bees is the ectoparasite *Varroa destructor* which is able to transmit different bee viruses towards honeybees, such as deformed wing virus (DWV) (Ryabov et al., 2014), Israeli acute paralysis virus (IAPV) (Di Prisco et al., 2011), Kashmir bee virus (KBV) and sacbrood virus (SBV) (Shen et al., 2005),

and of which DWV and IAPV can actively replicate in the vector. In this case, the mites puncture the honeybee pupae and adults and can thereby directly deliver viral particles into the host hemocoel (e.g. through the saliva (Shen et al., 2005)), circumventing the intestinal barrier. Consequently, multiple tissues are exposed to the virus and systemic infection is therefore induced. This infection route also bypasses the local immunity events (e.g. layered host-microbe interactions), leaving the host to fully rely on systemic immune responses to combat the virus. Other viral infection routes in insects such as through the respiratory system also exist, but it seems to be an alternative egress for the virus to escape the midgut epithelium after oral entry (Passarelli, 2011; Washburn, Kirkpatrick, and Volkman, 1995; Washburn et al., 1999).

IAPV has originally been isolated from infected honeybee (*Apis mellifera*) hives (Maori et al., 2007) and later on it was found to infect also other pollinators like bumblebees (Singh et al., 2010). In bumblebees, the natural cases of IAPV transmission by vectors have not been reported. However, there are several candidate vectors species, e.g. two species of phorid flies (*Apocephalus borealis* and *Megaselia scalaris*) which are known to attack bumblebees and they can carry DWV (Core et al., 2012; Menail et al., 2016). The replication of DWV has also been proved in *M. scalaris* larvae (Menail et al., 2016). Besides, the tracheal mite *Locustacarus buchneri,* shown to significantly reduce the lifespan of *B terrestris*, is also a potential vector species (Otterstatter and Whidden, 2004).

Under laboratory conditions, injection of IAPV resulted in an acute infection, inducing mortality in adult bumblebees even with a low virus dose (Niu et al., 2014a). Paralysis symptoms are observed, including immobilized/paralyzed front legs and severe body trembling after viral injection (see Chapter III). When IAPV was fed to adult bumblebees, high virus doses (2 x 10^7 and 1 x10^8 particles) were able to induce

obvious mortality in adults (Meeus et al., 2014; Piot et al., 2015) and typical trembling was observed shortly before death (Piot et al., 2015). Although both viral delivery method can cause bumblebee mortality, the viral infection dynamics are unknown. Additionally, a better understanding of the tissue tropism of dicistroviruses in bees may help us to understand the occurrence of the overt (systemic) infection of these viruses. Therefore, in this chapter, we tried to establish systemic infection of IAPV using reared *Bombus terrestris* workers in the lab through injection and feeding. We investigated the mortality and virus tissues infection after both delivery methods by qPCR and fluorescence *in situ* hybridization (FISH).

2. Materials and methods

2.1 Insect and IAPV infection

Newly emerged workers of *B. terrestris* were collected from different colonies (Biobest, Westerlo, Belgium). They were fed with sugar water and kept in plastic micro-colony containers (20 bees/container) for later experiments. All the micro-colonies were maintained in an incubator (Panasonic, Sakata, Japan) at 30 °C, 60 % relative humidity with continuous darkness.

IAPV injection stock ($IAPV^{inj\text{-}S}$) was kindly provided by Joachim de Miranda (Swedish University of Agricultural Sciences, Uppsala, Sweden). This virus stock was produced by propagating virus reference isolates (Allen and Ball, 1995) in 50 white-eyed honeybee pupae and preparing a chloroform-clarified extract in 10mM phosphate buffer (PH = 7.0)/0.02% diethyl dithiocarbamate as described previously (Niu et al., 2014a). The concentration of this stock was estimated with approximately 1×10^6 particles per microliter by transmission electron microscope. Besides, this IAPV stock had <0.1% contamination of other common honeybee viruses, such as ABPV, KBV, CBPV, DWV, SBPV, SBV and BQCV, as determined by RT-qPCR (Locke et al., 2012).

When injection was needed, $IAPV^{inj-S}$ was diluted 10,000 times by filter-sterilized phosphate buffer saline (PBS) to get a lower concentration of working solution, $IAPV^{inj-W}$ (1×10^2 particles/µl). Five microliters of either $IAPV^{inj-W}$ (500 viral particles) or PBS was injected into the bumblebee workers through the soft cuticle between the 1st and 2nd abdominal segmentsby a nano-injector (Eppendorf, Hamburg, Germany) (Niu et al., 2016a). Because $IAPV^{inj-S}$ did not contain enough viral particles to establish an infection after feeding, another IAPV stock for feeding was prepared (Piot et al., 2015). Specifically, 240 adult bumblebees were obtained from virus-free colonies (Biobest, Westerlo, Belgium). One hundred twenty bumblebees were injected with 2 µL of IAPV injection. The other 120 bumblebees were injected with nuclease free water and served as a control. After injection bumblebees were kept in micro-colonies of 10 workers at 30 ℃and 60% RH (MLR-352 incubator, Sanyo/Panasonic, Osaka, Japan) and *ad libitum* access to 50% sugar water. Four days after injection the bumblebees were stored at −80 ℃ until virus purification. Bumblebees were crushed in 0.01 M phosphate buffer (pH 7.0) 0.02% diethyl dithiocarbamate. The exoskeletons were discarded and the remaining liquid was centrifuged (20 min 800×g). Supernatant was collected and centrifuged at 40,000×g for 4h at 4 ℃. The pellet was suspended in nuclease free water and stored at −80℃. A quality control on both the viral stock and the control inoculum were performed. The virus titer was checked with transmission electron microscopy (CODA-CERVA) resulting in 1×10^8 virus particles/µL. We screened for possible contaminating viruses in both viral stock and control inoculum, we tested for slow bee paralysis virus, Kashmir bee virus, acute bee paralysis virus and DWV with PCR and all were negative. However, we have to mention that we cannot rule out the presence of the potential pathogens except for the common bee viruses.

Table 4. IAPV stock used in this chapter

Virus stock	Conc. (particles/µl)	Purpose	Production
[a]$IAPV^{inj-S}$	1×10^{6}	Storage	IAPV reference isolates (Allen and Ball 1995) was propagated in 50 white-eyed honeybees (*Apis mellifera*) pupae (Niu et al., 2014a).
$IAPV^{inj-W}$	1×10^{2}	Injection	$IAPV^{inj}$ storage stock was diluted by PBS.
[b]$IAPV^{fed}$	1×10^{8}	Feeding	2 µl of the $IAPV^{inj-W}$ (200 virus particles) was injected into 120 bumblebees (*Bombus terrestris*) workers (Piot et al., 2015).

[a] $IAPV^{inj-S}$, IAPV injection stock for storage was kindly provided by Joachim de Miranda (Swedish University of Agricultural Sciences, Uppsala, Sweden).
[b] $IAPV^{fed}$, IAPV feeding stock was produced by Niels Piot (Ghent University, Ghent, Belgium)

For oral infection, bees were starved for 5 h and subsequently fed with 20 µl of viral mixture (10 µl of sugar water + 10 µl of $IAPV^{fed}$) containing 1×10^{9} IAPV particles. Control groups were fed with a same volume of non-virus mixture where IAPV was replaced by the same volume of PBS. During feeding, each bee was kept in a petri dish with a cap of eppendorf tube containing either virus or non-virus mixture. The success of viral uptake of individual bee was confirmed by checking if the cap of the eppendorf tube was empty after about 10 -15 min. Once all Eppendorf tube caps were empty the bees were put back to the micro-colony container.

2.2 Mortality

To track the mortality induced by IAPV injection, five-days-old workers (n=14) were injected with 5 µl of IAPV working solution (estimated to contain 500 virus particles) and another group of bees (n=12) of the same age were injected with the same volume of filter-sterilized PBS (pH=7.4). To track the mortality after feeding, seven-days-old workers were fed with either 20 µl of virus mixture (containing 10^{9} virus particles) (n=22) or same volume of non-virus mixture (n=22). For both injection and feeding, each group of bees was kept in a micro-colony container with the same conditions mentioned above. Mortality was recorded on daily basis.

2.3 Tissue-specific IAPV relative normalized quantities (RNQs)

We chose 1 day post-injection (dpi) (n=5) and 3 dpi (n=5) to check the IAPV relative normalized quantities (RNQs) as an early and late infection stage, respectively. This because virus-injected bees started dying at the second or third day post-injection, and all infected bees normally died within five days post-injection. Similarly, workers fed with IAPV feeding stock were collected on both 5 days post-feeding (dpf) (n=5) when bees started to show mortality and 16 dpf (n=6) when the mortality was at the same pace with the control treatment. Another five bees fed with non-virus sugar water mixture at 16 dpf were employed as control. All the sampled bees were sacrificed immediately to remove their brain, midgut, ovary and fat body. Dissected tissues were either kept in RLT buffer for RNA extraction or fixative for sectioning.

2.4 RNA extraction, cDNA synthesis and qPCR

RNA was isolated using the RNeasy mini kit (Qiagen, Venlo, the Netherlands) according to the instructions. Briefly, bumblebee tissues were homogenized by an RZR 2102 auto homogenizer (Heidolph, Nuremburg, Germany) with a plastic pestle in 500 µl of RLT buffer (provided by the kit). After centrifuging for 5 min at max speed, the supernatant of each sample was collected and transferred to the filter columns (provided by the kits). The rest of the steps were performed according to the standard protocol of the kit. Genomic DNA was removed by TURBO DNA-free kit (Ambion, Foster, CA). The quantity and quality of the RNA samples were measured by 1% agarose gel electrophoresis and a Nanodrop spectrophotometer. All the RNA samples were stored at -80 °C. Five hundred nanograms RNA of each sample were used to synthesize the cDNA by the SuperScript II Reverse Transcriptase (Invitrogen, Waltham, MA) using oligo (dT) primers. qPCR was performed on a CFX Real-Time PCR Detection System using GoTaq qPCR master mix (Promega, Madison, WI). The

total volume of each reaction was 20 µl containing 8 µl of 100-times diluted cDNA, 1 µl (10 µM) of forward primer, 1 µl (10 µM) of reverse primer and 10 µl of master mix. Each reaction was performed in duplicate. In order to compare the viral titers among different tissues, two internal reference genes, peptidylprolyl isomerase A (*PPIA*) and 60S ribosomal protein L23 (*RPL23*), were introduced to normalize the qPCR data (Niu et al., 2014a).

Table 5. qPCR Primers

Target	Sequence (5'to 3')	Amplification factor
IAPV	TCGTAATGGAGTTGAGGAGTGA CTTGGCACATGAAGTTTGGAAT	1.927
PPIA	TCGTAATGGAGTTGAGGAGTGA CTTGGCACATGAAGTTTGGAAT	1.928
RPL23	GGGAAAACCTGAACTTAGGAAAA ACCCTTTCATTTCTCCCTTGTTA	1.932

Since the dicistrovirus may disturb the RNA content in the host cells, we checked the performance of reference genes in each experiment. This was evaluated by the calculated M and CV value under the qBase framework and for inter-tissues comparison, with M <1.0 and CV <0.5 (Hellemans et al., 2007). For virus-specific qPCR, we set a threshold for true amplification with Cq values lower than 35 with a single peaked melt curve. The tissues specific IAPV RNQs was calculated under qBase framework. Specifically, IAPV relative quantities in each sample were calculated by comparing the Cq of given samples with average Cq across all technical replicates. Then the relative quantities of IAPV were normalized by the relative quantities of two reference genes *PPIA* and *RPL23*.

2.5 FISH

We used fluorescence *in situ* hybridization (FISH) to localize IAPV in the midgut and brain tissue of *B. terrestris* workers after virus delivery. IAPV-fed bees were collected at 6 h (n=5) and 5 days (n=5) post-infection. Another five bees injected with IAPV were

also collected at 3 dpi. For each time point, five bees either fed or injected with PBS or PBS-sugar water mixture were collected as a non-virus control. Dissected brains or midguts were immediately fixed in freshly prepared 4 % formaldehyde (in PBS) at 4 °C overnight. After fixation, tissues were washed in PBS (pH = 7.9) (10 min, 3 times) and 75% ethanol (30 min, 3 times) and then stored in 100% ethanol at 4 °C until embedding. Prior to embedding, samples were firstly cleared in xylene (20 min, 3 times) and then soaked in liquid paraffin at 65 - 70 °C (40 min, 3 times). Next, samples were embedded into paraffin and 3 - 5 µm sections were then cut with an electronic rotary microtome (Microm HM340E, Walldorf, Germany) using sharp steel blades. Sections were then quickly straightened on warm sterile water (46 - 50 °C) and mounted on advanced adhesive StarFrost® slides (Knittel Glass, Braunschweig, Germany). All the slides were stored at 4 °C until hybridization.

Upon hybridization, slides were first incubated at 65 - 70 °C for 1 h and then deparaffinised in xylene (5 min, 3 times) and a series of ethanol (100 % for 5 min, 2 times; 90 % for 5 min, 70 % for 5 min; 50 % for 5 min) followed by brief dipping in sterile water for 2 min. To get the slides prepared for hybridization, pre-treatments were performed by incubating the sections in 2 - (N-morpholino) ethanesulfonic acid (MES) (Acros Organics, Geel, Belgium) at 95 - 99 °C for 10 min followed with proteinase K (200 µg/ml) treatment for 5 min at 37 °C. For hybridization, a 5'-Cy5-labelled oligonucleotide probe (antisense), IAPVbm-2 (5'-Cy5-CCTAGCCGATGAAGTATCCTGAGCC) (Eurofinsdna) was designed previously for specific detection of IAPV positive strand. Another probe, EUK 516 (5'-FITC-CCTAGCCGATGAAGTATCCTGAGCC) targeting 18S rRNA was used to visualize the cytoplasm (Amann et al., 1990; Yue et al., 2008). To make hybridization solution, 82.7 ng IAPVbm-2 and 52.7 ng EUK516 were diluted in 20 µl of hybridization buffer

[0.5µm IAPVbm-2, 0.5 µm EUK516, 20% (v/v) formamide, 0.9 M NaCl, 20 mM Tris-HCl (pH 7.9), 0.01% (g/v) SDS]. Each slide was applied with 20 µl hybridization solution. Hybridization was performed at 46 °C in a plastic humid chamber for overnight. After hybridization, slides were washed in PBS (137 mM NaCl, 2.7 mM KCl, 10 mM Na2HPO4, 1.8 mM KH2PO4) three times (5 min at RT, 5 min at 46℃ and 5 min at RT). Nuclei were then counter stained with 4', 6-diamidino-2-phenylindole (DAPI) and sections were mounted with Fluoroshield reagent (Sigma, St. Louis, MO). Fluorescence microscopy was performed by using a confocal laser scanning microscope (Nikon). FISH images were analyzed by NIS-Elements v 4.2 and ImageJ software.

2.6 Statistics

For both injection and feeding, one-way ANOVA was used to compare IAPV RNQs among tissues with built in “aov()” function in R environment (R Core Team, 2016). In case the ANOVA result was significant, Tukey-HSD multiple comparison was used to check the tissue preference. If no significant effect was observed by ANOVA, we introduced the random factor “Bees” to test the effect of the fixed factor “Tissues” on the IAPV levels with a linear mixed-effects models with lme4 package (Bates et al., 2015).

3. Result

3.1 Mortality in bumblebee workers by IAPV after injection and feeding

Injection of IAPV induced an acute mortality. Virus-infected *B. terrestris* workers started to die at 3 dpi and all bees were dead by 5 dpi (Figure 16A) which is identical to the previous data of Niu *et al*., (2016a). In the control group, only two bees injected with PBS were dead and the survival rate remained above 80% during the same period (Figure 16A). When bees were fed with high IAPV dose (1x 10^9 particles), both acute and chronic effects were observed. IAPV fed bees started to die at 5 dpf. After experiencing an acute drop at 6 dpf, the survival rate decreased gradually with the speed of 1 dead bee per day till the end of the recording (21 dpi) when all the infected bees were dead (Figure. 16B). This feeding data is in agreement with the previous data of Piot et al (2015) where multiple doses of virus are applied. In the control group,

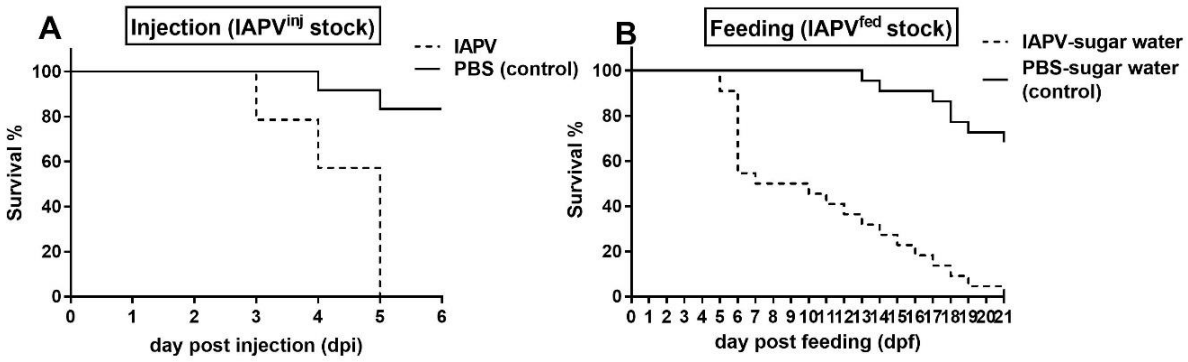

Figure 16. Mortality tracking of *B. terrestris* workers after IAPV injection and feeding. **A**, Mortality induced by IAPV injection. *B. terrestris* workers (n=14) injected with 5 µl of IAPV working solution (500 viral particles) started to show mortality at 3 days post-injection (dpi) and all bees infected with IAPV were dead by 5 dpi. Control bumblebees (n=12) were injected with 5 µl of PBS. **B**, Mortality induced by IAPV feeding. *B. terrestris* workers (n=22) fed with 20 µl of viral mixture (10 µl of sugar water + 10 µl of IAPV feeding stock) containing 1×10^9 IAPV particles started to show mortality on 5 days post-feeding (dpf) and a dramatic drop of survival rate was observed 1 day after. Oral infected bees were all dead by 21 dpf. Control bumblebees (n=22) were fed with the same volume of non-virus mixture where IAPV was replaced by PBS. Kaplan-Meier estimate was used to compare the significance of mortality between virus infection and non-virus infection bees (χ^2=16.14, P<0.0001 and χ^2=36.04, P<0.0001 for injection and feeding, respectively).

all bees survived until 12 dpf and then mortality was observed between 13 dpf and 21 dpf (Figure 16B); a final survival rate of 68% was observed at the end of the experiment.

3.2 Tissues-specific IAPV relative normalized quantities (RNQs) after injection and feeding

At 1 dpi, we did not detect viruses in all tissues and only one bee (bee#2) was systemically infected with high IAPV RNQs determined in its brain, midgut and fat body (Figure. 17A). At 3 dpi, all the tested tissues contained high amounts of viral RNQs and the tissue infection levels were comparable with that of bee#2 at 1 dpi. The highest viral RNQs was found in the fat body followed by brain, ovary and midgut (One-way ANOVA with post hoc Tukey-HSD comparisons, F=57.850, *P*<0.001) (Figure. 17B).

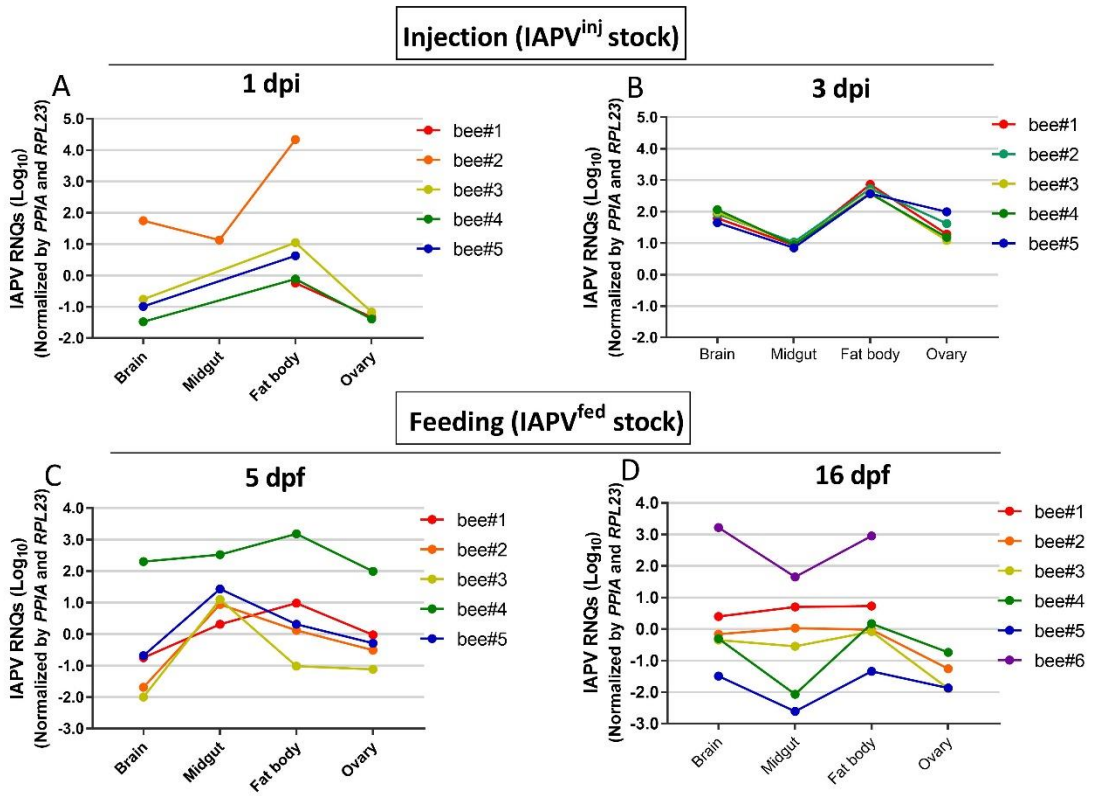

Figure 17. IAPV relative normalized quantities (RNQs) in *B. terrestris* brains, midguts, fat bodies and ovaries after viral delivery by injection and feeding. **A**, 1 day post-injection (dpi) (n=5). Brain samples of bee#1 and midguts samples of bee# 1, #3, #4 and #5 had Cq values higher than 35, and thus these were considered as non-infected and are not shown in the figure. **B**, 3 dpi (n=5). **C**, 5 days post-feeding (dpf) (n=5). **D**, 16 dpf (n=6). Ovary sample of bee#6 was not included due to poor RNA quality. Viral RNQs can be compared between figure A and B, and graph C can be compared to graph D.

We also detected a reduced standard deviation (SD) among the biological replicates at 3 dpi (Table 5). At the fifth day after feeding (5 dpf), we detected IAPV in all tissues and one bee (bee #4) was found to be highly infected with higher viral RNQs detected in its brain, midgut, fat body and ovary compared to others in this day (Figure 17C). Similar to the highly-infected bees at 3 dpi, the fat body of bee #4 at 5 dpf also harbored the highest viral RNQs. We did not observe a significant difference of IAPV RNQs among tissues (ANOVA (F=1.735, P=0.200)). However, when applying mixed models, integrating "bee" as a random factor, we noticed significant differences in IAPV RNQ between tissues (χ^2=17.886, P<0.001). Besides, a higher SD among the biological replicates was observed compared to that of 3 dpi (Table 6). A similar result was also found at 16 dpf where all tested bees exhibited a systemic infection and one bee (bee#6) was shown to have significantly higher viral RNQs than others in all tested tissues (Figure 17D). At this day, one-way ANOVA did not show a tissue preference in IAPV levels (F=1.595, *P*=0.226), while tissues still had impact on the viral titers when considering bee as random factor (χ^2=11.447, *P*=0.01).

Table 6. Standard deviation (SD) of IAPV RNQs in each tissue

	Injection		**Feeding**	
	SD (1 dpi)	**SD (3 dpi)**	**SD (5 dpf)**	**SD (16 dpf)**
Brain	1.45	**0.16**	1.70	1.59
Midgut		**0.06**	0.81	1.63
Fat body	1.87	**0.13**	1.56	1.42
Ovary	**0.11**	0.37	1.18	0.55

Boldface indicate the smallest SD observed in each tissue. SD of midgut from 1 dpi injection is not calculated for only one midgut sample is detected with IAPV.

3.3 Localization of IAPV in brain and midgut

FISH images confirmed the presence of IAPV particles inside the gut lumen at 6 h post-feeding (Figure 18A), indicating the bees had taken up the virus solution. At 5 dpf, no viral signal was found inside the midgut lumen anymore and strikingly also not in the columnar cells of the gut epithelium either. IAPV signal was only found at the basal side of the gut (Figure 18B).

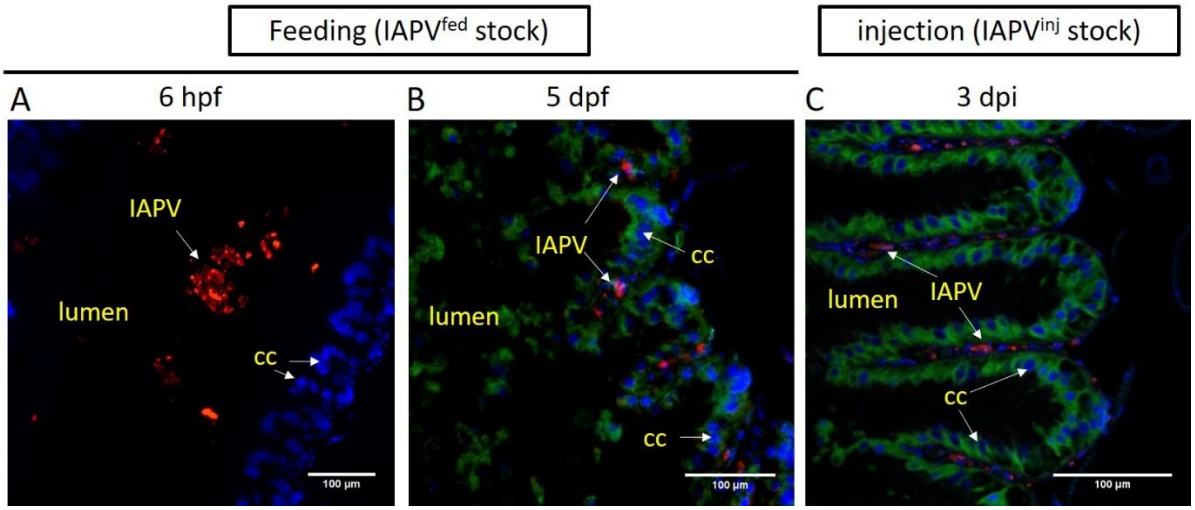

Figure 18. IAPV localized in the midgut of *B. terrestris* workers after feeding and injection. **A.** By oral infection, IAPV was localized inside the gut lumen at 6 h post-feeding (hpf). **B.** At 5 days post-feeding (dpf), IAPV was not found inside the lumen or in the columnar cells (cc) and it could only be found in the basal side of midguts. **C.** By injection, IAPV was also only observed in the basal side and no viral signal were detected inside the lumen or columnar cells. Bars indicate 100 µm.

We also checked the gut of bees after injection of the virus. Interestingly, IAPV was detected in the same regions, i.e. only at the basal side of the gut, as seen after the feeding of virus (Figure 18C). In the brain of IAPV-fed bees, the viral signal was mainly detected in the mushroom bodies, optic lobes and the protocerebrum at 5 dpf (Figure 19A). In mushroom bodies, the viral signal was observed in both class I Keyon cells and class II Keyon cells (Figure 19A). Kenyon cells are the intrinsic neurons of mushroom bodies and their numbers varies greatly in different insects. For example, there are about 2500 Kenyon cells in *Drosophila melanogaster* per mushroom body and 175000 in the cockroach (Farris and Sinakevitch, 2003; Heuer et al., 2012). A

strong IAPV signal was also detected in the neuron cells that connected the protocerebrum and the third optical lobe, lobula. After injection, we also observed similar infection patterns in brains (Figure 19B).

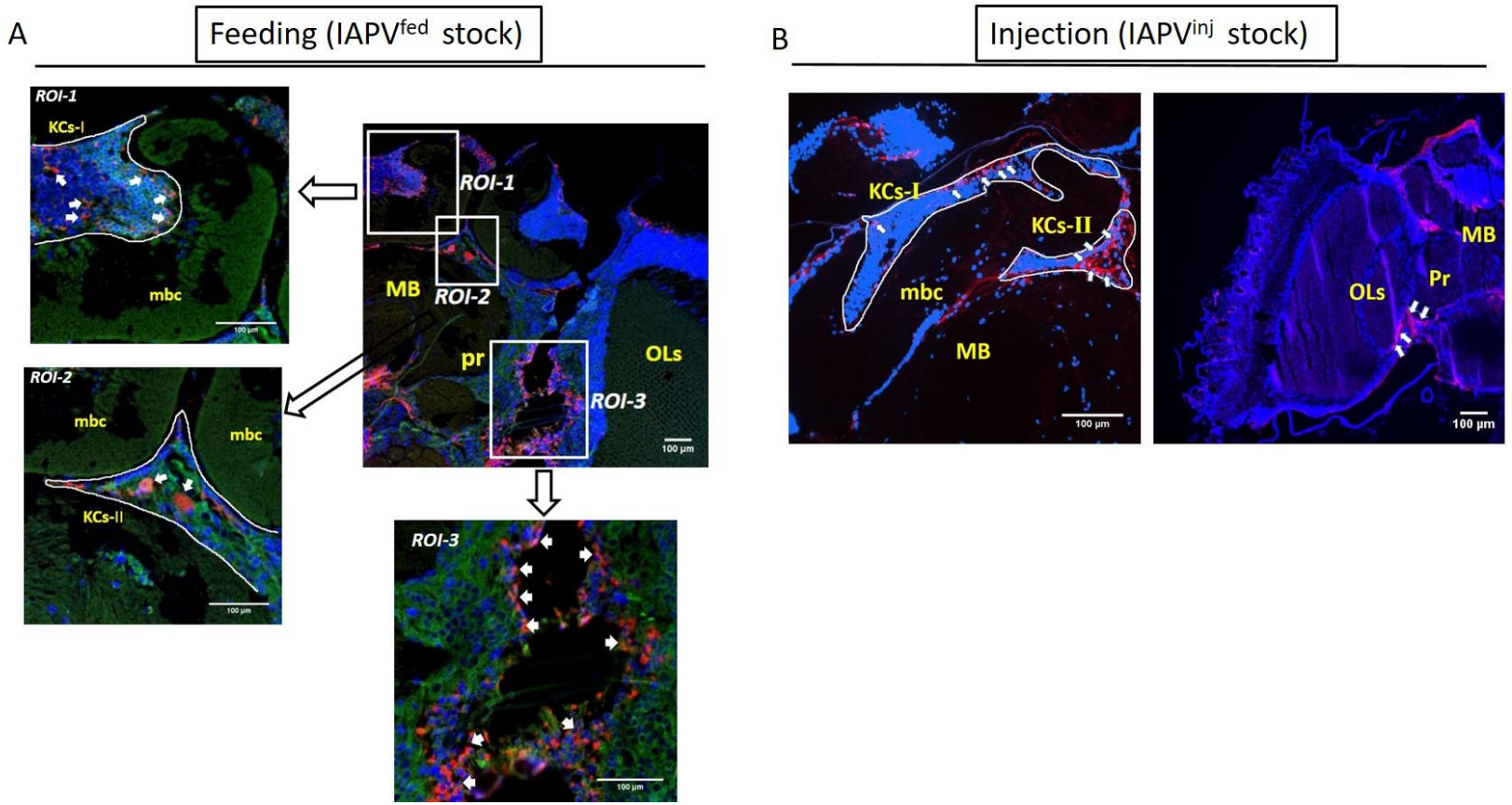

Figure 19. IAPV localized in the brain of *B. terrestris* workers. **A,** Brains samples after feeding with IAPV^{fed} stock. Regions of interest-*1*, IAPV localized in mushroom body Kenyon cells I. (White line outlines the area of Kenyon cells I were mainly localized). *ROI-2*, IAPV localized in mushroom body Kenyon cells II (white line outlines the area of Kenyon cells II were localized). *ROI-3*, IAPV localized in neuron cells that connected the protocerebrum (pr) and the third optical lobe, lobula (lo). B, Brains samples after injection with IAPV^{inj} stock. IAPV signal is detected in both Kenyon cells I and Kenyon cells II (left image). Also, IAPV signal can be found in the neuron cells that connected the protocerebrum (pr) and the optical lobes (OLs) (right images). IAPV signal is red (indicated by white arrows), nuclei are blue and cytoplasm is green. Bars indicate 100 µm.

4. Discussion

4.1 Systemic IAPV infection after feeding and injection

The IAPV stock used in our study for injection and feeding is from a different batch. The original IAPV stock ($IAPV^{inj}$), even at its highest concentration, was not able to result in systemic infection by feeding, indisputably showing that a higher viral titer is needed to establish an oral infection. In our setup, injection of $IAPV^{inj}$ induced a stable and acute infection where all infected bees were dead within 5 dpi with high IAPV titers determined in multiple tissues. Feeding with $IAPV^{fed}$ stock seemed to induce both acute and chronic infections. Bees with acute infection died within 7 dpf, while those with chronic infection tended to live longer and followed a mortality pattern along with the control treatment.

Our results also have certain implications for the choice of experimental design when studying host-virus interactions. Injection of $IAPV^{inj}$ allows to study how systemic infection impact host immunity, given its low variability of viral titers among biological replicates and therefore increases the power of an experiment and reduces potential differences on the host responses triggered by viral infection. Also, because the injected virus can reach multiple tissues through the circulatory system, virus injection clearly results in a systemic infection pattern. However, there are downsides to the injection method. For instance, when studying host immune gene or protein responses, injection itself can also be a physical stress (injury) which may trigger for instance the immune signaling pathways like Toll and IMD. Particularly for IAPV injection which leads rapidly towards bee mortality, thereby triggering potential indirect effects, early time-points need to be considered to study antiviral immune responses of IAPV in bumblebees.

While for oral delivery of IAPV^{fed} stock, the virus needs to pass the gut barrier to reach the host hemocoel and thus both the local (digestive tract) and systemic immune systems are challenged. Hence, we believe that different factors will/may influence the systemic infection success. For instance, the gut local immune activity and even the natural microbiota may interfere with the initial viral replication and following proliferation, thus resulting in a higher variability of infection levels among individual bees (Ferreira et al., 2014; Xi et al., 2008a). This variability lowers the power of an experiment. Yet the feeding methodology does provide means to study the immune barrier that viruses are facing, and also the local immune responses, to understand why higher amounts of IAPV are needed to be able to establish a systemic infection.

4.2 Tissue-specific infection patterns of IAPV

A previous report showed that IAPV attacks multiple tissues and causes systemic infection in honeybees and the gut was found to harbor the highest number of copies of viral RNA negative strand (Chen et al., 2014). In our oral feeding setup, we observed a difference in IAPV levels (positive strand) among tissues after including bee specimen as a random factor. Both midgut and fat body showed higher viral RNQs, especially opposed to the brain. Injection however led to a more consistent tissue infection pattern by a much lower viral dose. Besides, a clear tissue tropism was observed at 3 dpi where IAPV RNQs in the fat body were higher than that of other tissues. It is striking that this important immune tissue is mainly infected and the high virus accumulation may impair the systemic immune responses which is a major function of insect fat tissues. This immune impairment in turn would facilitate the viral replication and spreading, which may ultimately lead to host death. In addition, insect fat body is also a central storage depot for energy reserves (Arrese and Soulages, 2010). Insect adipocytes, the main fat body cells, can store a great amount of lipids

which are mobilized to the hemolymph in response to immune challenge (Cheon et al., 2006; Goldsworthy, Opoku-Ware, and Mullen, 2002). Thus, the infection of the fat tissues may also disrupt the host energy storage and utilization.

4.3 From local infection in the midgut towards systemic infection

In the current study, we found that by oral infection via the midgut IAPV can also infect similar brain regions like mushroom bodies and optical lobes. However, according to our FISH result, not all brains of the orally infected bees showed a viral signal (two out of five were detected with viral signal) at 5 dpf. We cannot guarantee that those bees with brains infection were also the ones that would die. But it at least indicates that for some orally infected bees, IAPV infection is constrained to the digestive tracts and very low in other tissues. It is also possible that these low infections can be detected by qPCR but they were beyond the detection limit of FISH. In honeybees, similar functional regions in the brain (e.g. mushroom body Kenyon cells and optical lobes) are reported to be infected with DWV (Shah et al., 2009). A recent study also showed that IAPV can be localized in the guts, ovaries and eggs of honeybee queen (Chen et al., 2014) Howeevr, wheter IAPV can be detected in the functional regions of honeybee brain is not clear.

By comparing midguts in 3 dpi and 5 dpf, we expected to see a dramatic impact of the delivery method or viral stock on the IAPV localization pattern, which surprisingly turned out to be quite the same. Here we chose 3 dpi and 5 dpf for comparison as both time-points result in systemic infection. Bees injected and fed with virus started to die on 3 dpi and 5 dpf, respectively. However, FISH could not detect IAPV in the columnar cells of the gut epithelium. Since there is a lack of data on how IAPV localize in the bee (both *Apis* and *Bombus* spp.) gut, thus we are not able to compare our data with other studies. However, a previous study showed that another bee virus DWV is

found to infect the gut epithelium cells of honeybee (Mockel et al., 2011). Whether there is a different infection mechanism behind these two viruses need more study. A possible explanation is that the accessed epithelium cells by feeding were lysed after the initial round of infection and missed in the time series of the experiment. Besides, virus particles are also likely to be blocked by the midgut basal lamina from accessing to the hemocoel and thus accumulated here resulting in a more clear detection by FISH (Passarelli, 2011). Similarly, virus accumulation can also occur in the midgut basal lamina when injection is applied. Therefore, both injection and oral feeding resulted in similar viral localizations. Whether an alternative infection route that does not involve the midgut, such as through the tracheal or respiratory system can result in IAPV systemic infection still needs more study (Passarelli, 2011; Washburn et al., 1995).

To sum up, our current study provides data on mortality and tissue infection pattern of IAPV infection after injection and feeding, which will serve the method selection to study virus-host interactions in bees. Plus, the similar viral localization in the midgut observed by FISH between injection and feeding may conceal the important role of this tissue in local viral immunity.

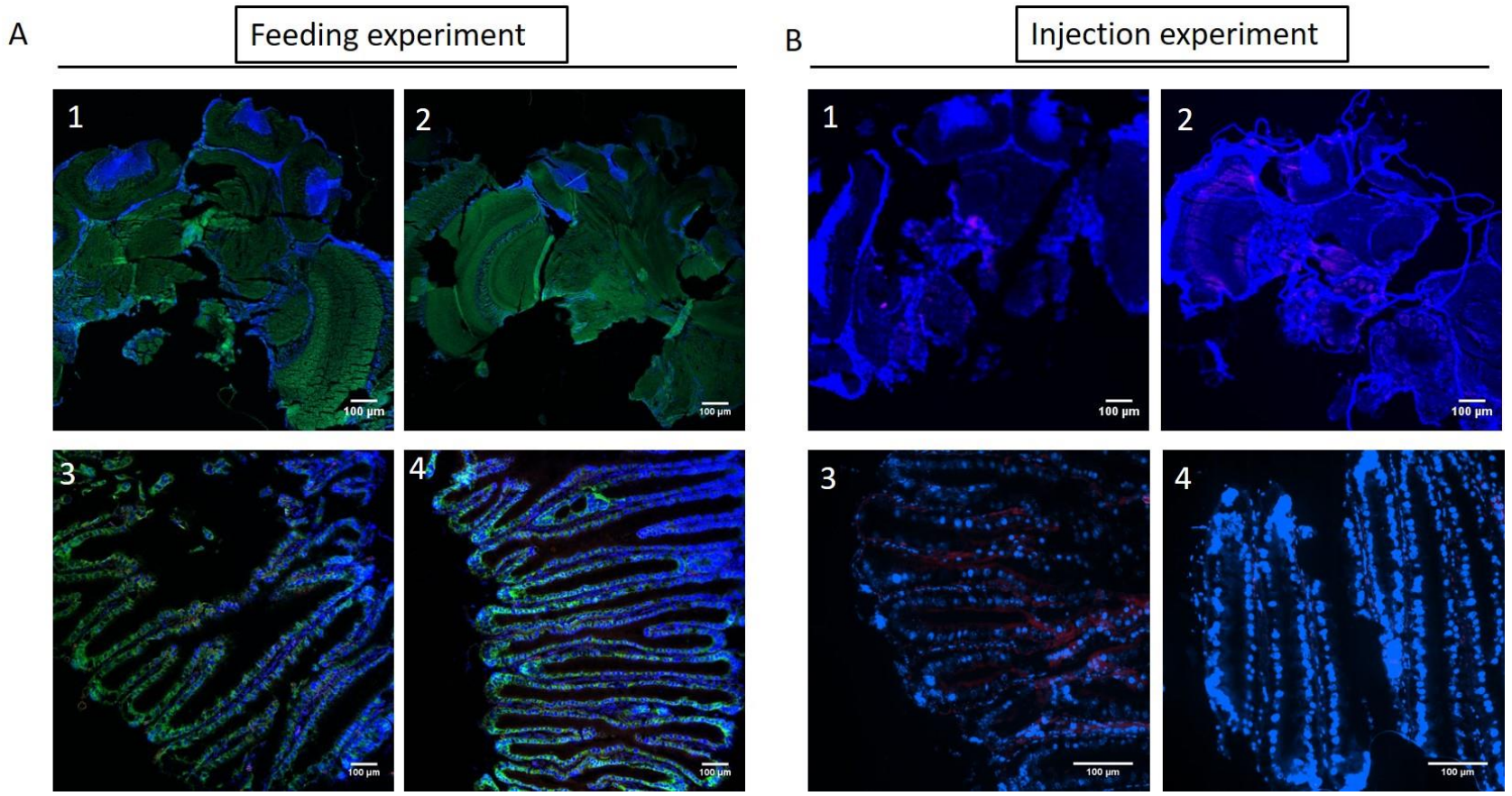

Figure S1. Negative samples of FISH experiments. **A.** Negative samples (IAPV-, Probe+) in the feeding experiments. Brains samples (A1 and A2) collected from two individual bees fed with PBS and sugar water. Guts samples (A3 and A4) collected from the two individual bees fed with PBS and sugar water. B. Negative samples (IAPV-, Probe+) in the injection experiments. Brains samples (B1 and B2) collected from two individual bees injected with PBS. Guts samples (A3 and A4) collected from two individual bees injected with PBS), nuclei are blue and cytoplasm is green. Bars indicate 100 µm.

Chapter Ⅲ: Israeli acute paralysis virus associated paralysis symptoms, viral tissue distribution and *Dicer-2* induction in bumblebee workers (*Bombus terrestris*)

Parts of this chapter are published in:

Wang, H., Meeus. I. & Smagghe, G., 2016. Israeli acute paralysis virus associated paralysis symptoms, viral tissue distribution and Dicer-2 induction in bumblebee workers (*Bombus terrestris*). *Journal of General Virology.* 97, 1981-1989

1. Introduction

Honeybees and bumblebees are the two most important bee species used in modern apiculture and agriculture. They host many viruses. When looking at the honeybee, there have been around 23 viruses reported and many of these viruses only persist as covert and asymptomatic infections which show no detectable impact on both individual and colony level (Cox-Foster D.L. et al., 2007; Fürst et al., 2014; Levitt et al., 2013; McMenamin and Genersch, 2015). However, under certain conditions, for example the presence of the ectoparasitic honeybee mite *Varroa destructor*, the covert infections of some viruses turn into overt ones with observable symptoms (Martin et al., 2012; McMahon et al., 2015; Singh et al., 2010). The symptoms of overt infections vary from virus to virus, including deformed wings, discoloration, hair losses, bloated abdomen, paralysis, decreased locomotion, impaired cognition and both brood and adult mortality (Lanzi et al., 2006; McMenamin and Genersch, 2015; Singh et al., 2010). Some symptoms can be easily recognized by the behaviour and appearance of the infected bees, while others can only be confirmed through meticulous and continuous observations or by molecular techniques.

In bumblebees (*Bombus spp.*) a subset of honeybee infecting viruses has been reported, such as deformed wing virus (DWV), Israeli acute paralysis virus (IAPV), acute bee paralysis virus (ABPV), Kashmir bee virus (KBV), slow bee paralysis virus (SBPV), sacbrood virus (SBV), black queen cell virus (BQCV) and Lake Sinai virus (LSV) (Genersch et al., 2006; Levitt et al., 2013; Parmentier et al., 2016; Peng et al., 2011). However, only DWV, KBV and IAPV have been reported to cause clinical symptoms (Genersch et al., 2006; Meeus et al., 2014). DWV caused crippled wings in bumblebee (*Bombus terrestris* and *Bombus pascuorum*) workers even without *Varroa* (Fürst et al., 2014; Genersch et al., 2006). Interestingly, viral tissue tropism was

different between DWV-infected (asymptomatic) and clinically diseased (symptomatic) honeybees and bumblebees, indicating that overt infection may also be associated with virus tissue spreading (Genersch et al., 2006).

IAPV is a positive single stranded RNA virus in the family of *Dicistroviridae* with a global distribution range (de Miranda et al., 2010a; Maori et al., 2007; Palacios et al., 2008). The nomenclature of this virus is largely based on its symptoms which are similar to ABPV. Both viruses can induce abnormal body trembling (Galbraith et al., 2015; Li et al., 2013; Maori et al., 2009). In bumblebees, injection of a low dose of IAPV particles into healthy workers could induce rapid mortality (Niu et al., 2014a). Orally delivered IAPV also increased mortality in adults, but a much higher starting dose is needed (Piot et al., 2015). Low oral viral doses did not induce mortality but had effects on reproduction of bumblebees (Meeus et al., 2014). Aside from the above mortality and sub-lethal effects, the symptoms associated with IAPV have not been well-characterized and thus hinder our ability to observe the progression of IAPV infection in these important pollinators, especially when considering that virus-induced paralysis symptoms are normally the signal of overt infection and death. Besides, the initial observation of IAPV symptoms are from honeybees, symptoms analysis in bumblebees would enhance our knowledge of this virus (de Miranda et al., 2010a; DeGrandi-Hoffman and Chen, 2015; Maori et al., 2007; Maori et al., 2009; Piot et al., 2015). Therefore, in this study, we report progressive viral symptoms in workers of *Bombus terrestris,* which is one of the most numerous bumblebee species in Europe (Velthuis and van Doorn, 2006). Furthermore, we investigated the relationships between IAPV symptoms and tissue tropism. Finally, a major insect immune response against viral infections, the siRNA pathway, was followed to infer if its impairment is correlated with viral symptoms. We aim to provide a better understanding of viral tissue

dynamics and host immune responses and the possible relationships with symptomatic infection in this important pollinator.

2. Material and methods

2.1 Insect and viruses

Callow workers were collected from virus-free colonies of *B. terrestris* (Biobest, Westerlo Belgium), and kept in micro-colonies supplied with sugar water at standardized conditions in an incubator (Panasonic, Japan) at 30 °C and 60 % relative humidity with continuous darkness (Mommaerts et al., 2010). The IAPV stock used in this study was the injection stock ($IAPV^{inj\text{-}S}$) in Chapter II. For injection, this IAPV stock was diluted to 1×10^2 particles/µl by phosphate-buffered saline (PBS, pH = 7.4).

2.2 Symptom observation and survival analysis

Five days old *B. terrestris* workers (N = 25) were injected with 5 µl (500 particles) of IAPV inoculum with a nanoinjector (Eppendorf, Hamburg, Germany) for mortality analysis. Workers of the same age and injected with 5 µl of PBS (PH = 7.4) were employed as control (N = 25). Besides, we included two extra controls: (i) i.e. physical injury (N = 10) where workers were injected with PBS by a blunted needle; and (ii) starvation (N = 10) where workers were kept without any nutrition. The controls allow us to record symptoms of a dying bee. We scored specific symptoms of paralysis and trembling, and when these appeared, those individuals were isolated. Besides, we scored for abnormalities in worker behaviour, such as foraging, feeding and the response of the workers by a gentle shaking (challenge) of the micro-colony where normal workers would fly up immediately (Mommaerts et al., 2010).

2.3 Sample selection and tissues dissection

To test the tissue tropism and infection level of IAPV, 60 workers (5 days old) were injected with the same amount of viral solution (5 µl, 500 particles) and subdivided into three micro-colonies (20 bees per colony). Workers that start showing IAPV-related symptoms were collected and labelled as SP+ bees. When detecting and selecting a SP+ bee, another bee infected with virus but without showing IAPV-related symptoms was also collected and labelled as SP- bees. SP+ and SP- from the same time point were collected from the same micro-colony. Twenty workers injected with 5 µl PBS (pH = 7.4) served as negative control. All sampled bees were sacrificed immediately after collecting. Dissections were performed in PBS (pH = 7.4) under a binocular microscope to remove the brain, midgut, fat body and ovary. Briefly, each worker was fixed on a wax dish by steel insect pins and the abdomen was opened by using a fine scissor. Then ovary, midgut and fat body were removed. To isolate the brain, the head was cut off from the body and fixed firmly in a wax dish with sterile PBS (pH = 7.4) to keep the structure of the tissues. Forceps and fine sharp needles were used to remove the antennae and open the front mask covering the compound eyes. Then brains were isolated carefully. Scissors, forceps, pins and other tools were cleaned during dissection by spraying of 70% ethanol and RNASE AWAY surface decontaminant (Molecular Bio Products, San Diego, CA) to prevent potential cross-contaminations. Freshly dissected tissues were transferred into either RLT buffer (Qiagen, Hilden, Germany) or fixative as a first step for RNA extraction or tissue fixation, respectively.

2.4 RNA isolation, cDNA synthesis and qPCR

Tissues were homogenized and lysed in RLT buffer (300 - 500 µl) and total RNA was extracted following the instructions of the RNeasy mini kit (Qiagen). The remaining genomic DNA was removed by TURBO DNA-free™ kit (Ambion, Foster, CA). The

integrity and quantity of the purified RNA were checked by 1% agarose gel electrophoresis and a Nanodrop spectrophotometer. Afterwards, 500 ng of total RNA from each sample was used to synthesize the cDNA by SuperScript® II Reverse Transcriptase (Invitrogen, Waltham, MA) using oligo (dT) primers. The qPCR was performed on a CFX™ Real-Time PCR Detection System using GoTaq® qPCR master mix (Promega, Madison, WI). The total volume of each reaction was 20 µl containing 8 µl of 100 - times diluted cDNA, 1 µl (10 µM) forward primer, 1 µl (10 µM) reverse primer and 10 µl master mix. Each reaction was performed in duplicate. In order to compare both the viral titers and *Dicer-2* expression among different tissues, the reference genes *PPIA* and *RPL23* were employed (Niu et al., 2014a). Quantification cycle values (Cq values) were transformed into normalized relative quantities (NRQs) taking the expression of the two reference genes into account (Hellemans et al., 2007). As the qPCR data was done on samples from different tissues the threshold for reference genes stability M value and CV value are set as 1.0 and 0.5 under the framework of qbase (Hellemans et al., 2007). Experiment specific M and CV values are provided in the legends of the figures and all passed this quality control. The amplification factor is calculated for each pair of qPCR primers from a 10-fold dilution series of a cDNA mixture of each used tissue. The qPCR primers used in this study and their amplification factors are shown in Table S1.

To check the IAPV relative normalized quantities (RNQs) in tissues, SP+ (N = 5), SP- (N = 5) and PBS-injected workers (N = 5) were collected at 3 dpi. The cDNA samples at 3 dpi used for IAPV RNQs analysis were also used for *Dicer-2* expression in this late infection stage. Besides, IAPV injected workers (N = 5) and PBS injected workers (N = 5) were also collected at 1 dpi to check the *Dicer-2* expression in this early infection stage.

2.5 FISH and microscopy

Fluorescence *in situ* hybridization (FISH) was performed as described previously with several modifications (Mockel, Gisder, and Genersch, 2011; Müller., Matthiesen., and Nielsen., 2009; Yue et al., 2008). SP+ (N = 10), SP- (N = 10) and PBS-injected (N = 6) bees were collected at 3 dpi from three micro-colonies. Dissected brains were immediately fixed in freshly prepared 4 % formaldehyde (in PBS) at 4 °C overnight. The following preparation steps for the tissue section were described in Chapter II. All the slides were stored at 4 °C until hybridization.

For the specific detection of IAPV RNA via FISH, a 5' - Cy5-labelled oligonucleotide (5'-Cy5-CCTAGCCGATGAAGTATCCTGAGCC) (Eurofinsdna) was used as probe (sequence designed according to Genbank accession No. EU 436423.1). The pre-hybridization preparation was followed the same procedure described in Chapter II. To make the hybridization solution, 100 ng of the probe was diluted in 20 µl hybridization buffer [0.5µm probe, 20% (v/v) formamide, 0.9 M NaCl, 20 mM Tris-HCl (pH 7.9), 0.01% (g/v) SDS]. Each slide was applied with 20 µl hybridization solution. Hybridization was performed at 46 °C in a plastic humid chamber overnight. Subsequently, sections were washed in PBS (pH 7.9) three times (5 min at room temperature, 5 min at 46 °C and 5 min at room temperature). Finally, nuclei were counter stained with 4', 6-diamidino-2-phenylindole (DAPI) and sections were mounted with Fluoroshield™ reagent (Sigma, St. Louis, MO). Fluorescence microscopy was performed using a confocal laser scanning microscope (Nikon). Images were analysed by NIS-Elements v 4.2 and ImageJ software.

2.6 Data analysis

Statistics of IAPV RNQs and immune gene expressions were processed by SPSS 23. Independent Student's *t*-test and two-way ANOVA with post-hoc Tukey HSD test were used for either two or multiple samples mean comparison.

3. Result

3.1 Symptoms and mortality associated with IAPV infections in bumblebees

IAPV injection (N = 25) caused a rapid mortality and all workers died within 5 days (Figure 20). In the control group of PBS injection (N = 25), all workers survived by the end of the recording which is 15 days post injection (dpi). We found some bees from the IAPV-injected group presented progressive symptoms and defined them as SP+ workers. The initial symptom as observed at 1 dpi, was crippled/immobilized forelegs and this resulted in impaired mobility (movie. S1). At this stage, bees moved slowly and did not fly or buzz when perturbed by gentle shaking of the micro-colony. Also, when compared with the workers injected with IAPV but did not show symptoms (SP-) and workers injected with PBS, SP+ bees visited the food source (sugar water feeder) less frequently and showed a "quiet" behaviour. They slowly passed the sugar water feeder and seemed to "ignore" it. An additional observation was that the normal

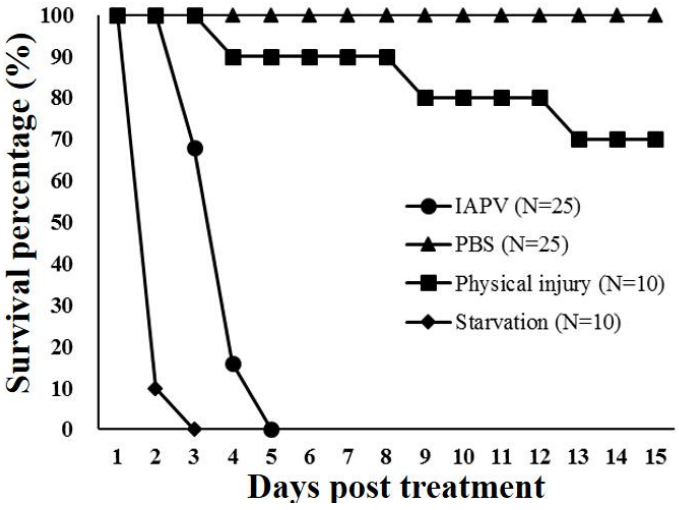

Figure 20 Survival percentage of *B. terrestris* workers after different treatment. Mortality of four treatment groups were recorded on daily basis. IAPV (N = 25): injection of 500 particles of IAPV (5µl); PBS (N = 25): injected of 5 µl PBS; Physical injury (N=10): injection of 5 µl PBS with blunted needle; starvation (N = 10): no nutrition supplied.

healthy workers expelled the workers with crippled/immobilized forelegs symptoms from the main group. When we isolated the workers with crippled/immobilized forelegs and kept them alone in a new micro-colony with nutrition, they exhibited intense abdomen shaking and bodies trembling within 12 to 24 hours. At that time, they were not capable of standing or walking anymore. Finally, they all died in the following 2 to 3 hours. To verify that the above reported symptoms before death are induced by IAPV, we included another two control groups, in which we induced stress by starvation (N = 10) and physical injury (N = 10) (bee injected PBS with a blunted needle) (Figure. 19). Results showed that the starved workers also died quickly and the survival rate dropped to only 10% by the 2nd day post treatment. However, no symptoms of crippled/immobilized forelegs, paralysis or trembling were observed from this group. Of the starved workers, which were also inactive and gathered around in group, none were expelled out by the others. Interestingly, bees seemed to handle physical injury better than starvation, as 70% of the bees survived after the injection of PBS with a blunt needle. Bees in this group showed no symptoms of crippled/immobilized forelegs, paralysis or trembling.

3.2 IAPV relative normalized quantities (RNQs) in tissues of SP+ and SP- workers

To explore the relationships between IAPV infection and paralysis symptoms, we determined the viral relative normalized quantities (RNQs) in 500 ng RNA of each

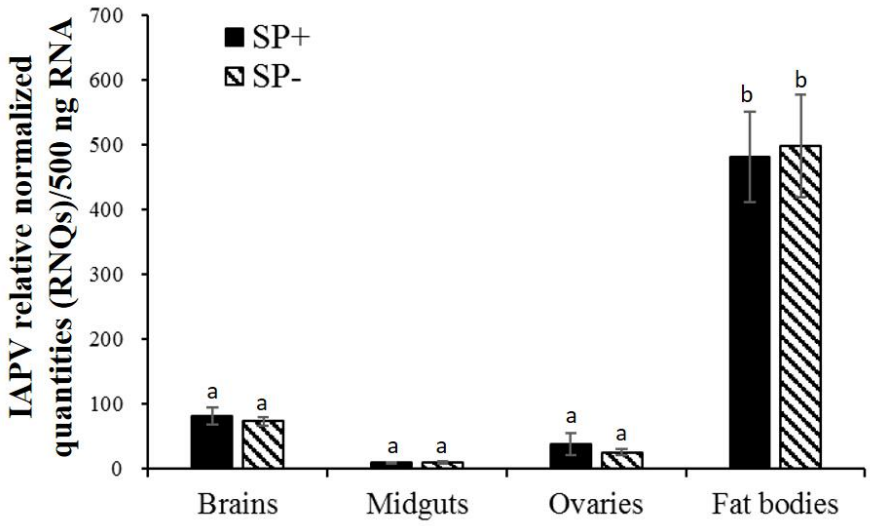

Figure 21 IAPV relative normalized quantities (RNQs) in different tissues of *B. terrestris* workers at 3 dpi. SP+ (N = 5): workers infected with IAPV and exhibited paralysis symptoms; SP- (N = 5): workers infected with same doses of IAPV but did not show any symptoms. SP+ and SP- workers were collected in pairs from three micro-colonies at 3 dpi. There was no significant difference in relative normalized quantities (RNQs) among samples designated with the same letter based on two-way ANOVA (F = 70.7830, $p<0.001$, p value was calculated with post-hoc Tukey HSD test (α=0.05)), SPSS 23. The average reference genes stability M = 0.482, CV = 0.168. Results are shown as means ± sem.

tissue sample and in association with two factors: tissue (brain, midgut, ovary and fat body) and symptom (SP+ and SP-) at 3 dpi. We used peptidylprolyl isomerase A (*PPIA*) and 60S ribosomal protein L23 (*RPL23*) as internal reference genes in the qPCR assay. The calculated reference genes stability M value and CV value by qbase were all under the threshold (M < 1.0 and CV < 0.5) for inter tissue comparison (Hellemans et al., 2007). Thus, the normalization among tissues was reliable. IAPV was detected in all examined tissues, but the viral RNQs varied (Figure 21). Specifically, the viral RNQs in the fat bodies was significantly higher (ANOVA: F = 70.7380, $p<0.001$, p value was calculated with post-hoc Tukey HSD test) than in the other tissues. Unfortunately, no effect of the factor symptom (SP+ versus SP-) on the viral RNQs

(ANOVA: F = 0.0012) or interaction between the factors tissue and symptom (ANOVA: F = 0.0604) could be reported.

3.3 IAPV localization in brains by FISH microscopy

Fluorescence *in situ* hybridization (FISH) was utilized to localize IAPV infected brain regions and retrieve differences between SP+ workers (N = 4) and SP- workers (N = 7). The summary of the FISH assay can be found in the Table S2. IAPV signal (Starkey et al.) could be detected in various brain regions including the somata in the mushroom bodies (MBs), antennal lobes (Danihlík et al.) and optic lobes

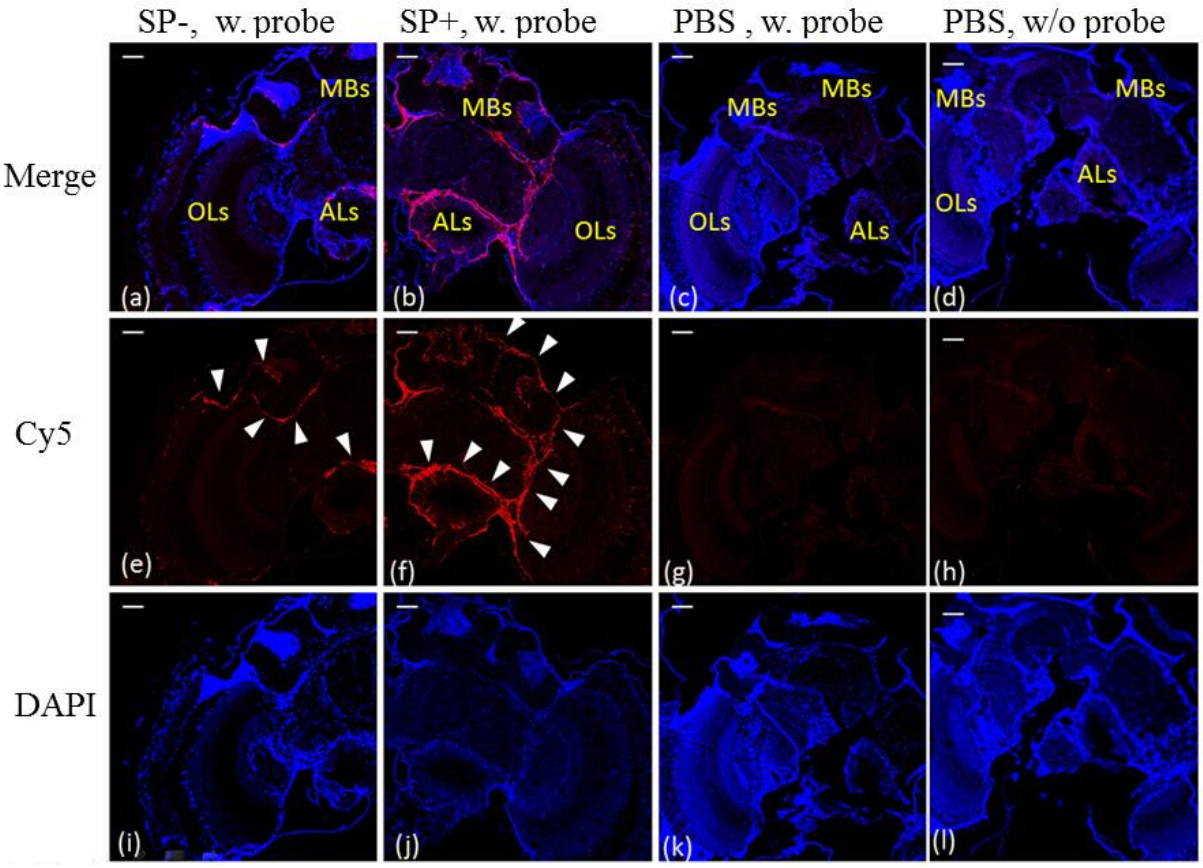

Figure 22 Localization of IAPV in the brains of *B. terrestris* workers with and without symptoms at 3 dpi. (a), (e) and (i): brain sections of viral infected workers without symptoms (SP-) stained with IAPV probe; (b), (f) and (j): brain sections of viral infected workers with symptom (SP+) stained with IAPV probe; (c), (g) and (k): brain sections of PBS-injected workers (PBS) stained with IAPV probe; (d), (h) and (l): brain sections of PBS-injected workers (PBS) stained without IAPV probe. Merge channel was shown in (a), (b), (c) and (d); Cy5 channel was shown in (e), (f), (g) and (h); DAPI channel was shown in (i), (j), (k) and (l). IAPV positive signal was in red and nuclei are in blue. Arrowheads indicate the position of the IAPV signal. Scale bars indicate 100 µm.

(OLs) (Figure 22a, b, e and f). While no IAPV signal could be detected in the no virus control samples (N = 5) stained with or without IAPV probes (Figure. 22c, d, g and h). We compared the viral distribution in MBs, ALs and OLs between SP+ and SP- samples. In MBs, the Kenyon cells (KCs) were found to be a main viral reservoir (Figure 23 a, b, c, d, e and f). KCs are classified into two types based on their localizations within the brains: KCs I are located inside of the mushroom body calyces (mbc) while the KCs II are mainly at the periphery of the calyces. For SP+ workers,

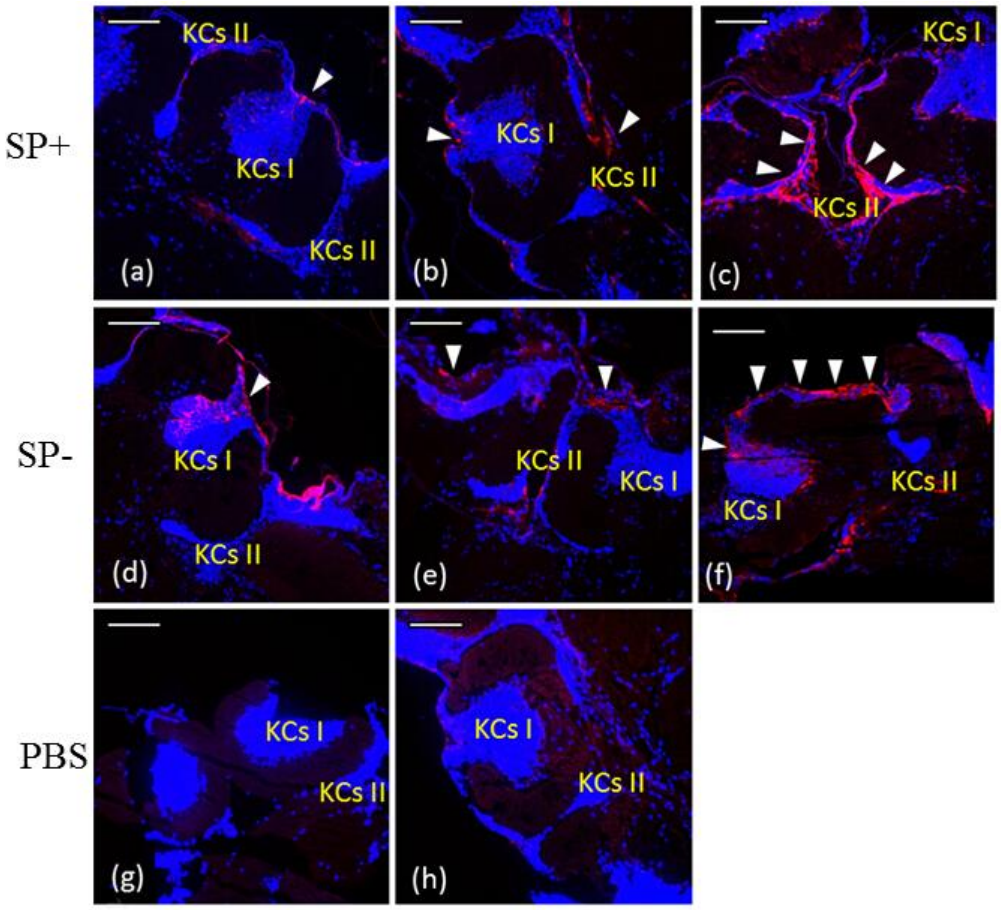

Figure 23 Localization of IAPV in mushroom bodies (MBs). (a), (b) and (c): mushroom bodies (MBs) of three IAPV infected workers with symptoms (SP+) stained with IAPV probe; (d), (e) and (f): MBs of three IAPV infected workers without symptoms (SP-) stained with IAPV probe; (g): MBs of PBS-injected workers stained without IAPV probe; (h): MBs of PBS injected workers stained with IAPV probe. IAPV signal (Starkey, Sargent, and Redman) was found in both types of Kenyon cells (KCs I and KCs II), nuclei were in blue. Abbreviation: KCs I, class I Kenyon cells; KCs II, class II Kenyon cells; mb-c, mushroom body calyces. Arrowheads indicate the position of the IAPV signal. Scale bars indicate 100 µm.

IAPV signals could be observed in both types of KCs in the MBs (Figure 23a, b and c). Similar viral distribution could also be found in the samples of SP- workers (Figure

23d, e and f). ALs are the main olfactory centre responsible for receiving and processing olfactory signals. We recorded a strong IAPV signal in the ALs of both SP- and SP+ workers (Figure 24a, b, c, d, e and f). Finally, we also localized the IAPV genome in the OLs, which are the main visual processing centre of bees. In both SP+ and SP- brains, the IAPV signal was mainly found in the lamina monopolar cells (Figure 25a, b, c, d, e and f) which are responsible for receiving visual signals from the retina (ret) and transferring them to the second optical lobe, the medulla (me).

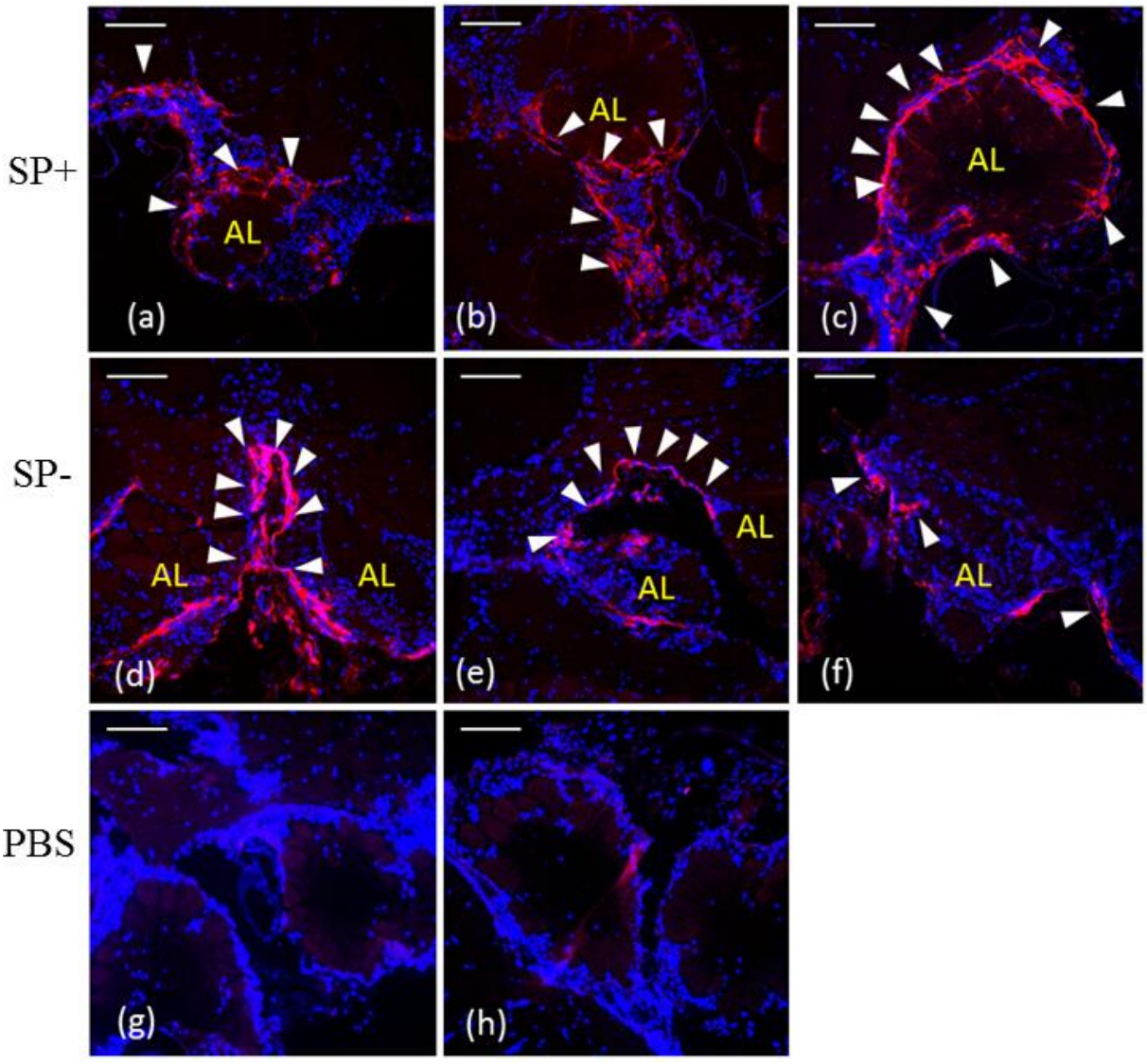

Figure 24 Localization of IAPV in antennal lobes (Danihlík, Aronstein, and Petřivalský). (a), (b) and (c): antennal lobes (Danihlík et al.) of three IAPV infected workers with symptoms (SP+) stained with IAPV probe; (d), (e) and (f): ALs of three brains from IAPV infected workers without symptoms (SP-) stained with IAPV probe; (g): ALs of PBS-injected workers stained without IAPV probe; (h): ALs of PBS injected workers stained with IAPV probe. IAPV signal are shown in red and nuclei were shown in blue. Arrowheads indicate the position of the IAPV signal. Scale bars indicate 100 µm.

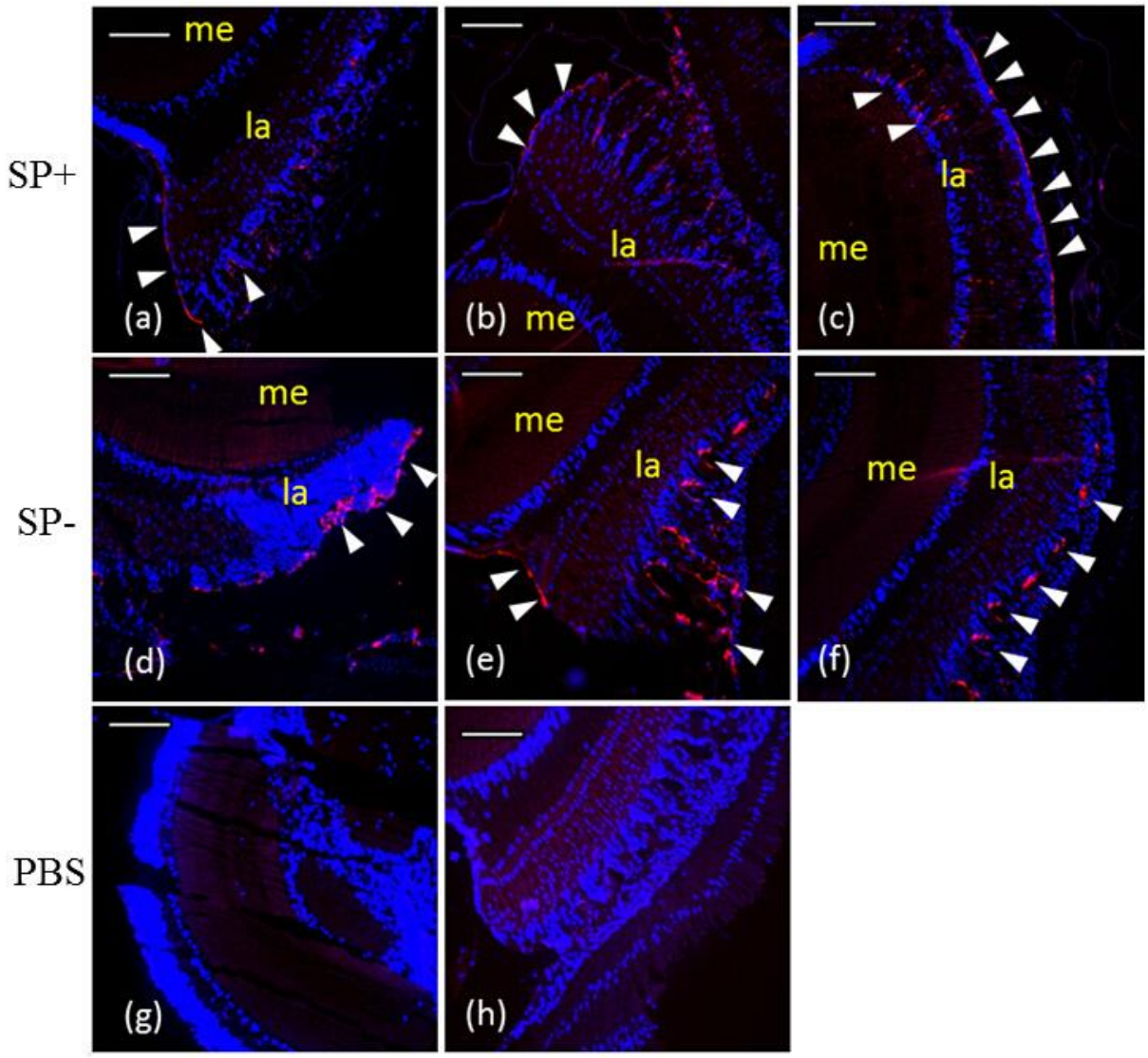

Figure 25 Localization of IAPV in optical lobes (OLs). (a), (b) and (c): optical lobes (OLs) of three IAPV infected workers with symptoms (SP+) stained with IAPV probe; (d), (e) and (f): OLs of two IAPV infected workers without symptoms (SP-) stained with IAPV probe, sections (e) and (f) are from same worker; (g): OLs of PBS-injected workers stained without IAPV probe; (h): OLs of PBS-injected workers stained with IAPV probe. IAPV signal was in red and nuclei were shown in blue. Arrowheads indicate the position of the IAPV signal. Scale bars indicate 100 µm.

3.4 Tissue-specific *Dicer-2* expression in SP+ and SP- workers

In order to get an insight into the molecular events of the host immune response upon IAPV infection, we determined the relative expression of *Dicer-2*, a core gene in the siRNA pathway, at two time points (1 dpi and 3 dpi). At 1 dpi, the *Dicer-2* induction was not significant in the four studied tissues (Figure 26a). At 3 dpi, a significant induction (t-test, $p<0.01$) of *Dicer-2* expression was observed in all four tested tissues (Figure 26b). However, we did not detect a difference between the SP+ and SP- samples (ANOVA: F = 2.229, $p = 0.1452$). The observed fold changes of *Dicer-2* in the ovaries (SP+, ~ 9 fold; SP-, ~11 fold) and midguts (SP+, ~8 fold; SP-, ~9 fold) were higher than those in brains (SP+: ~5 fold; SP-: ~5 fold) and fat bodies (SP+, ~2 fold; SP-, ~2 fold). These differences are mainly explained by the significant higher relative expression of *Dicer-2* in the infected midguts (SP+ and SP-) compared to other tested tissues (ANOVA: F = 12.327, $p < 0.001$, p value was calculated with post-hoc Tukey HSD test) and a higher *Dicer-2* basal level (*Dicer-2* relative expression in PBS control

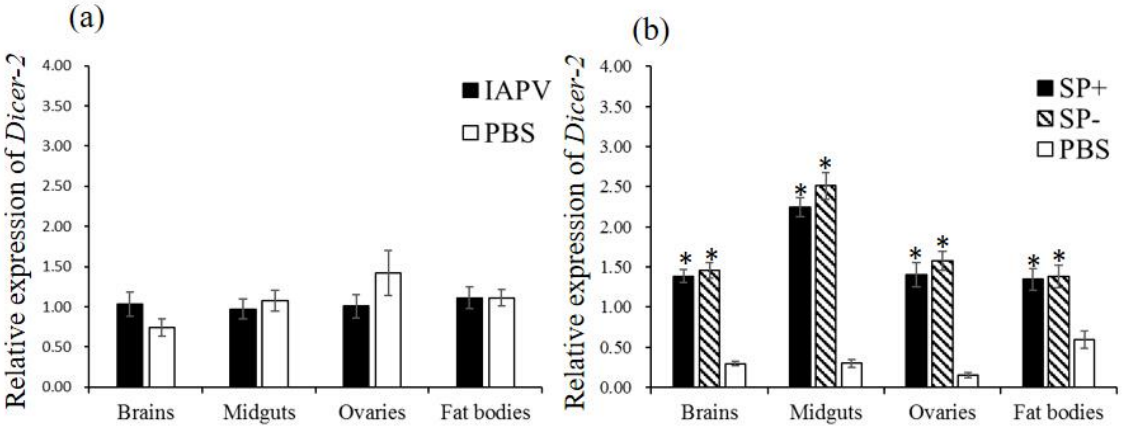

Figure 26 Tissue-specific relative expression of *Dicer-2* in *B. terrestris* workers post IAPV infection. (a): Tissue specific relative expression of *Dicer-2* at 1 dpi. IAPV (N = 5), PBS (N = 5). (b): Tissue specific relative expression of *Dicer-2* at 3 dpi. SP+ (IAPV injected bees with paralysis symptoms) (N = 5), SP- (IAPV injected bees without paralysis symptoms) (N = 5) and PBS controls (N = 5). Asterisks indicate significant *Dicer-2* induction compared between IAPV infected tissues (SP+ and SP-) and non-virus infected tissues (PBS) (student's t test, with * $p<0.01$). Results are shown as means ± sem. The average reference genes stability M = 0.482, CV = 0.168 for 3 dpi and M=0.817; CV=0.288 for 1 dpi.

groups) of fat bodies at 3 dpi (ANOVA: F = 8.622, $p < 0.01$, p value was calculated with post-hoc Tukey HSD test). In the fat body the increase of *Dicer-2* in the viral infected samples were only visible after reference genes correction (Figure. S1).

4. Discussion

4.1 Symptoms after infection with IAPV

IAPV symptoms reported in honeybees, such as body trembling, were also observed in the current study with *B. terrestris* workers. This symptom could be observed in the last couple of hours before death. Other symptoms described in the honeybee, such as discoloration and hair losses on thorax and abdomen, were not observed in our experiment setup. We observed a yet unreported symptom, namely crippled/immobilized forelegs in the IAPV-infected workers after 1 to 2 days of viral injection. Our result indicated that this early symptom was induced by IAPV and not by other stresses such as injury or starvation. Although confounding infection of other viruses cannot be guaranteed, the 10,000 times dilution of the IAPV purified stock significantly lowered the chance of confounding infection.

In 1976, Bailey and his colleague reported similar front legs symptom in honeybees infected with SBPV one or two days before death (Bailey and Woods, 1974). Unfortunately, we cannot compare the current front legs symptoms to the previous one in detail since no visual material of Bailey's observation was preserved. Interestingly, IAPV and SBPV are genetically unrelated and belong to different families. Another paralysis-related virus is ABPV which is genetically closely related to IAPV but not reported to be associated with the front legs symptoms. This evidence demonstrated that genetically unrelated viruses could be symptomatically related (IAPV and SBPV), while genetically related viruses could be symptomatically unrelated (IAPV/ABPV and KBV).

Another interesting observation is that we found the SP+ bees to be expelled from the main group by the others. A similar behaviour was noticed in ABPV and CBPV infected honeybees (Bailey et al., 1963). Although it remains to be determined if this behaviour is to avoid transmission of the virus through the entire colony, it is known that the contacts of networks are important for parasite transmission dynamics within bumblebee nests, with bee contact rate being a significant predictor of *Crithidia bombi* transmission (Otterstatter and Thomson, 2007). The forelegs are able to provide food-related information to the nerve system of worker bees and are important sensor organ. (de Brito Sanchez et al., 2014; Mommaerts, Wackers, and Smagghe, 2013). This could explain our observations that bees with crippled/immobilized forelegs seem to "ignore" the sugar water feeder.

We performed a paired sampling, meaning that workers showing obvious symptoms (SP+) and no symptoms (SP-) were sampled at exactly the same time after injection. This setup allowed us to see if dynamics in tissue tropism could explain the appearance of symptoms. According to our results, it was clear that IAPV accumulated in all four tissues tested (midgut, fat body, brain and ovary), and no significant differences in viral RNQs were observed between SP+ and SP- bees. Thus, the appearance of symptoms after IAPV infection cannot be explained by a specific viral tissue accumulation.

IAPV-infected honeybees have a decreased homing ability (Li et al., 2013). In the present study, the SP+ workers of *B. terrestris* also showed a decreased sensation and mobility, which could be explained by the viral presence in the brain, although the qPCR data did not reveal any differences between workers with and without symptoms (SP+ versus SP-). However, it still remains possible that brain regions, with various functions are differentially infected, which may lead to paralysis symptoms. Therefore,

we performed FISH to localize IAPV genomes in *B. terrestris* brains. FISH is a powerful method to determine DNA or RNA molecules in multiple types of samples. In honeybees, *in situ* hybridization has been applied to detect viruses as DWV, IAPV and Kakugo virus (KV) and bacterial diseases in both adult and larval tissues (Chen et al., 2014; Fujiyuki et al., 2009; Martinson, Moy, and Moran, 2012; Mockel et al., 2011; Shah, Evans, and Pizzorno, 2009; Yue et al., 2008). In the present study, we localized IAPV in different parts of the brains of *B. terrestris* workers using paraffin-embedded tissue sections. Our results clearly demonstrated the presence of IAPV in the MBs, antennal and optic neuropils. Therefore, it is reasonable to speculate that the sensory experience such as vision, taste and smell of the bees is affected. Unfortunately, we did not find any specific distribution of IAPV in SP+ brains other than in SP- ones, indicating that the viral accumulation in the functional regions of the brain does not definitely lead to clinical symptoms. However, we cannot draw a definitive conclusion on this, as in our setup the FISH can only determine presence and absence of the virus. For more detailed information on viral distribution in brains, further analysis for instance 3D optical imaging is needed.

4.2 Host immune response after IAPV infection

The innate immune response plays a major role in controlling and eliminating invading pathogens in insects (Kingsolver et al., 2013). It has been described that the insect host recruits the small interfering RNA (siRNA) pathway when challenged with virus (Deddouche et al., 2008; Niu. et al., 2016a). Here Dicer-2 produces virus-specific siRNAs that are then loaded into the RNA-induced silencing complex (RISC) which is capable of cutting multiple viral RNAs (Brutscher, Daughenbaugh, and Flenniken, 2015; DeGrandi-Hoffman and Chen, 2015; Niu et al., 2014b; Sabin, Hanna, and Cherry, 2010). In the present study, we checked the expression of *Dicer-2*, a key gene

in the siRNA pathway in different tissues of SP+ and SP- *B. terrestris* workers. Differences in *Dicer-2* expression within the same tissue could inform us how individual workers cope with the viral infection. Our results demonstrated that *Dicer-2* transcription increased after IAPV injection in all tested tissues, but there was no difference between *Dicer-2* expression in SP+ and SP- bees. The fact that the *Dicer-2* increase was not yet observed at 1 dpi of IAPV infected tissues indicate that the siRNA pathway is only activated when IAPV has reached to a certain amount or during the viral fast replicating period.

Interestingly, in the fat body where the highest viral RNQs were detected, the up regulation of *Dicer-2* was the lowest among the tested tissues and actually this increase was only visible after the normalization with two reference genes (see Fig. S1). It is known that IAPV can influence transcriptional homeostasis of several fundamental cellular functions (Boncristiani et al., 2013), hence the induction of *Dicer-2* in the fat body cells could be a qPCR artefact. The two reference genes we used here have been proven to be stable and reliable under IAPV infection in different body parts, i.e. whole abdomen, heads and remnants (Niu et al., 2014a). When using multiple reference genes, the stability of these reference targets is also an important quality control within each experiment (Vandesompele et al., 2002). Within the qBase framework, we can choose a minimal acceptable reference genes stability by defining a threshold value for two indicators: the geNorme expression stability value (M) and the coefficient of variation of the normalized reference genes relative quantities (CV). For inter-tissues comparison, we set M<1.0 and CV<0.5 (Hellemans et al., 2007). In this study, the specific M and CV values for the fat bodies are (M = 0.587, CV = 0.204), and thus above the within tissue criteria of M < 0.5 and CV < 0.2 (Hellemans et al.,

2007). For tissues with high IAPV titters the use of exogenous internal references is therefore needed to be conclusive.

In natural conditions, the insect midgut epithelium is the first barrier against viral invasion (Hakim et al., 2010). Thus, a sensitive immune response in midgut could be beneficial to the host. However, in our experimental setup, IAPV could infect multiple tissues because viral particles were injected into the hemocoel. Therefore, the differences of viral titters we observed between midgut and fat body can very probably be explained by the differences of tissue-specific immunity against viral infection and/or viral uptake. We should also keep in mind that the insect innate immune system comprises several other immune responses, such as Jak/STAT, Toll, Imd and autophagy. The function of these immune responses upon viral infection is not fully understood. Thus, further study focusing on multiple immune responses, especially on tissue level would be helpful to reveal more details of host-virus interactions.

Table S1. Summary of FISH on brains

Groups	No. samples for sectioning	No. samples for FISH	No. samples with IAPV signal
With symptoms (SP+)	10	9	7
Without symptoms (SP-)	10	7	4
PBS	5	5	0

Table S2. Primers and oligonucleotide probe used for qPCR and FISH.

Target	Sequence (5'to 3')	Purpose	Amplification factor
IAPV	TCGTAATGGAGTTGAGGAGTGA	qPCR	1.927
	CTTGGCACATGAAGTTTGGAAT		
Dicer-2	TGGTCAAAACATCAAGAACAACCA	qPCR	1.943
	GATCGGGGCCATACGAACAT		
PPIA	TCGTAATGGAGTTGAGGAGTGA	qPCR	1.928
	CTTGGCACATGAAGTTTGGAAT		
RPL23	GGGAAAACCTGAACTTAGGAAAA	qPCR	1.932
	ACCCTTTCATTTCTCCCTTGTTA		
IAPV	Cy5-CCTAGCCGATGAAGTATCCTGAGCC	FISH	

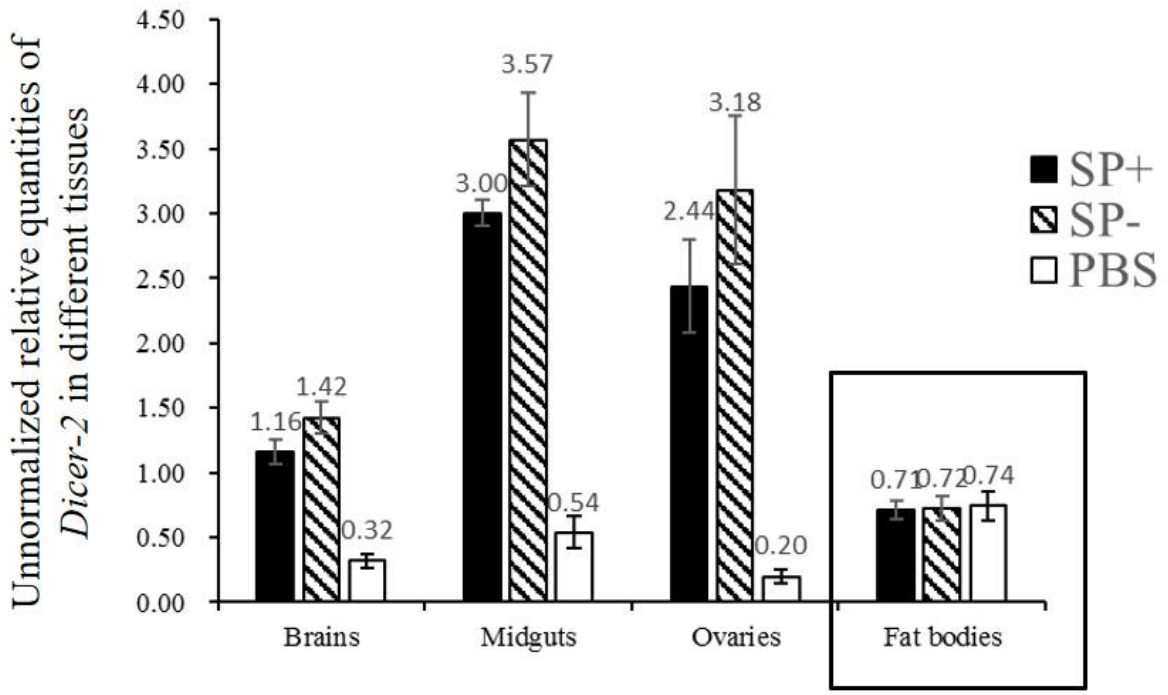

Figure S1 Unnormalized relative quantities (URQs) of *Dicer-2* at 3 dpi.

SP+ (IAPV injected bees with paralysis symptoms) (N = 5), SP- (IAPV injected bees without paralysis symptoms) (N = 5), PBS (bees injected with PBS) (N = 5). Results are shown as means ± sem. Numbers labelled above the error bars represent the mean of each sample.

Chapter Ⅳ: The role of von Willebrand factor C-domain protein (SVC) in bumblebee (*Bombus terrestris*) immunity is more than antiviral defense.

Parts of this chapter are submitted for publication,

Wang, H., Smagghe, G. & Meeus. I., 2017. The role of von Willebrand factor C-domain protein (SVC) in bumblebee (*Bombus terrestris*) immunity is more than antiviral defense. *Insect Biochemistry and Molecular Biology* (submitted)

1. Introduction

The single von Willebrand factor C-domain proteins (SVCs) are a recently discovered protein family mainly found in arthropods (Sheldon et al., 2007). They are characterized by a single von Willebrand factor type C domain (SVWC domain), having 8 of the 10 conserved cysteine residues in the canonical von Willebrand factor type C domain (VWC domain). In *Drosophila melanogaster*, 13 short proteins have been identified belonging to this novel family (Sheldon et al., 2007). Aside from some general expression profiling, most studies have focused on a member called Vago (*DmVago*, CG2081). *In vivo* studies have shown that *DmVago* is induced after Drosophila C virus (DCV) infection and is related with the viral loads in fat body of adult flies (Deddouche et al., 2008). Later *in vitro* studies in mosquito cell lines partially confirmed the flies' results. The orthologue of *Dm*Vago in *Culex quinquefasciatus* is induced after being challenged with West Nile virus (WNV) and *Cq*Vago is found to be a secreted peptide that can suppress the WNV infection by activating the Jak/Stat pathway in the neighboring cells (Paradkar et al., 2012). The mosquito data revealed similarities of *Cq*Vago with the mammalian interferons (IFNs), which led to the speculation that *Cq*Vago could be acting as an IFN-like circulating cytokine. This IFN-like theory is also supported by a recent study in Pacific white shrimp, *Litopenaeus vannamei* that *LvVago* is transcriptionally regulated by an interferon regulator factor (IRF)-like gene (Li et al., 2015). All together, these data highlight the role of Vago as being a potential antiviral immune modulator. In contrast, the functionality of other SVC members in *D. melanogaster* still remains unknown, with some being roughly described as responsive to different stresses, such as bacterial infection and nutritional status (Sheldon et al., 2007). In *Drosophila*, the innate immune pathways like Toll and IMD are activated upon bacterial infection and can increase the

production of several molecular effectors including antimicrobial peptides (AMPs) which are important in eliminating the invading bacteria (Lemaitre, 2004; Lemaitre and Hoffmann, 2007). However, whether *Dm*SVCs are involved in this process is not clear. When looking at different insects (with genome sequencing data) (see Figure 10 in Chapter I), we found that the number of SVCs is diverse. For instance, flies normally have more than 10 SVCs and mosquitos have 2 to 5 (Figure 10B). This number falls to one in multiple bee species belonging to different genera including *Apis*, *Bombus*, *Ceratina, Eufriesea* and *Melipona* (Figure 10B). Therefore, bees present an interesting case to study not only the functionality of this one SVC, specifically regarding the known antiviral role of Vago, but also its involvement in other immune related functions. A recent *in vivo* study in bumblebee *Bombus terrestris* has shown an unexpected downregulation of *BtSVC* upon Israeli acute paralysis virus (IAPV) infection in whole abdomen of bees (Niu et al., 2016b). This *BtSVC* gene was called *BtVago-like*, given its relation with virus and it influenced hopscotch (*Hop*) expression, the JAK kinase of the Jak/Stat pathway. In contrast to the results in flies and mosquitos silencing of this gene failed to alter the IAPV titers in the abdomen of bees (Niu et al., 2016b). We hypothesize that the effect on viral titers was masked because of looking at body part level. Indeed, the tissue tropism of IAPV in *B. terrestris* (Chapter III) and the tissue dependent silencing efficiency of genes (Cappelle et al., 2016) are limiting factors when detecting relations between gene expression and its influence on viral titers. Therefore, in this study, we first questioned if *BtSVC* silencing could influence IAPV infection in specific tissues (fat body and brain). Second, the differential expression of *DmSVC*s is related to a multitude of stressors, this suggests their potential involvement in different immune pathways (Sheldon et al., 2007). As most bee species have only one SVC protein it could be involved in multiple pathways of bee innate

immunity, also knowing its proposed function as an insect cytokine triggering the Jak/Stat pathway in mosquitos (Paradkar et al., 2012). To investigate the involvement of this unique *SVC* in bumblebees, we analyzed the expression of key genes of known immune pathways, comparing bumblebees in which *BtSVC* is silenced with non-silenced ones.

2. Material and methods

2.1 Phylogenetic analysis of *Bt*SVC with other SVCs from flies and mosquitos

To know the phylogenetic relations of *B. terrestris* SVC (XP_003399812) with other SVC members, especially regarding to *Drosophila melanogaster* Vago (NP_527680) and its orthologues in *Aedes aegypti* (XP_001658930) and *Culex quinquefasciatus* (XP_001842264). Then we performed a phylogenetic analysis based on the SVWC domain alignment. The amino acid sequences of SVCs were extracted from NCBI protein data base. Sequence alignment was down by using Clustalw algorithm in MEGA 7.0 version (http://www.megasoftware.net/). The conserved SVWC domain of each sequence was manually isolated after entire sequence alignment. Schematics of SVWC domain in *D. melanogaster* (Sheldon et al., 2007) was introduced as reference. Phylogenetic tree was constructed by MEGA 7.0 using maximum likelihood method with 1000 times bootstrap test. Phylogenetic tree branches corresponding to partitions reproduced in less than 50% bootstrap replicates are collapsed.

2.2 Insect, virus and injection

Callow workers of *B. terrestris* were collected from different colonies provided by Biobest (Westerlo, Belgium) and maintained in micro-colonies (25-30 bees/colony) by sugar water and pollen. All the micro-colonies were kept in an incubator (Panasonic, Sakata, Japan) at 30 °C, 60 % relative humidity with continuous darkness for later experiment.

The IAPV stock used in these experiments was originally purified from honeybee pupae, described in previous chapters (Niu et al., 2014a). The concentration of this IAPV stock was estimated to contain approximately 1×10^6 particles per microliter by transmission electron microscope. Besides, this IAPV stock had <0.1% contamination of other common honeybee viruses. The following viruses were screened by RT-qPCR (Locke et al., 2012): acute bee paralysis virus (ABPV), Kashmir bee virus (KBV), chronic bee paralysis virus (CBPV), deformed wing virus (DWV), slow bee paralysis virus (SBPV), sacbrood virus (SBV) and black queen cell virus (BQCV). A working stock was prepared, i.e. a 10.000-fold dilution of the virus stock in filter-sterilized phosphate buffer saline (PBS). This results in a working stock with approximately 1×10^2 particles/µl.

Viral infection was established by injecting five microliters of IAPV working stock (~500 viral particles per bee) into five to seven days old workers, after immobilized on wet ice for 10-15min. Five microliter PBS injection was employed as control treatment. Injections were performed by a nano-injector (Eppendorf, Hamburg, Germany).

2.3 *BtSVC* expression in tissues

A previous study showed that *Bt*SVC is down-regulated upon IAPV infection in whole abdomen of bees (Niu et al., 2016b). Here we investigated its expression in fat body, midgut and head after IAPV injection. Because injection of IAPV induces mortality within 5 days, we chose 1 day post injection (1dpi) and 3 dpi for the gene expression analysis. Bees injected with five microliters of IAPV (~500 particles per bee) (n=25) and same volume of PBS (n=25) were kept in two different micro-colonies supplied by sugar water and pollen. Another group of bees without any treatment were employed as mock control (n=25). All three micro-colonies were maintained under the same

condition mentioned above. Bees (n=8) sampled from each group were sacrificed for RNA extraction of head, midguts and fat bodies at both 1 dpi and 3 dpi, respectively.

2.4 Gene silencing

Gene silencing was conducted as previously described (Niu et al., 2016b). Specifically, a fragment of either *BtSVC* (XM_003399764) or *BtDicer-2* (XM_012307737) was amplified by PCR with sequence specific primers plus T7 promoters (Supp. Table S2) and purified by E.Z.N.A. Cycle-pure Kit (Omega, USA). The specificity of each template was checked by 1.5% gel electrophoresis and sequencing (LGC genomics, Germany). One microgram of each template was used to synthesize dsRNA according to the instruction of MEGA script RNA Kit (Invitrogen, USA). The quality and concentration of each dsRNA sample was measured by electrophoresis on a 1.5% agarose gel and a Nanodrop spectrophotometer. The same procedure was used to produce dsGFP. For silencing, bees were injected with 20 µl (~20 µg) of either ds*Bt*SVC or dsDicer-2. Injection with same amount of dsGFP was served as a control. The silencing efficiency of fat body and brain was tested two days after the dsRNA injection.

2.5 The effect of *BtSVC* silencing on IAPV load and innate immune responses

Bees were firstly injected with ds*Bt*SVC (n=22) and dsGFP (n=22). Eight bees per treatment were sacrificed to check silencing efficiency in both fat body and brains 2 days post dsRNA injection. We wanted to infer if *Bt*SVC silencing influences: (1) IAPV load (2) the crosstalk of Dicer-2 towards Jak/Stat, and (3) other immune genes.

(1) We injected bees with IAPV to check viral relative normalized quantities (RNQs) in *BtSVC* silenced bees compared to non-silenced ones. Two days after dsRNA treatment, the changes in *BtSVC* expression was checked by qPCR and bees were injected with 5 microliters of IAPV working stock (~500 particles per bee). To check

the effects on viral RNQs, qPCR was performed 2 days after the viral infection in both target-silenced (n=10) and control bees (n=10).

(2) To look at the *Bt*SVC effect on Dicer-2 and the Jak/Stat pathway, we compared the expression of *BtDicer-2*, *BtHop* and *BtTepa* in 1) *Bt*SVC silenced and non-silenced bees with or without IAPV infection.

(3) To look at the involvement of *BtSVC* in other immune pathways, we checked the expression of *BtPelle* (Toll pathway), *BtRelish* (Imd pathway), *BtBasket* (Jnk pathway) and four AMP genes, *BtAbaecin*, *BtApidaecin*, *BtDefensin* and *BtHymeonptaein* in dsRNA treated bees.

2.6 *BtDicer-2* silencing on *BtSVC* and IAPV load

Previous data from flies and mosquitos show that viral induced Vago regulation acted in Dicer-2 dependent manner. Thus, to see if *Bt*SVC also shares this character we performed a *BtDicer-2* silencing experiment. The set-up of *Bt*Dicer-2 silencing was the same as *Bt*SVC. Briefly, bees were first injected with dsDicer-2 (n=22) and dsGFP (n=22). Two days later IAPV (~500 particles) was introduced to these bees and viral RNQs and *BtSVC* expression was checked 2 days after viral infection.

2.7 RNA isolation, cDNA and qPCR

RNA was isolated using the RNeasy mini kit (Qiagen, Venlo, the Netherlands) according to the instructions. Five hundred microliters of RLT buffer (provided by the kit) was used to homogenize the bumblebee tissues by an auto homogenizer (Heidolph, Nuremburg, Germany) with a plastic pestle. After centrifuging for 5 min at max speed, the supernatant of each sample was collected and transferred to the kits-provided filter columns. The following steps were performed according to the standard protocol of the kit. Genomic DNA was removed using the TURBO DNA-free kit (Ambion, Foster, CA). The quantity and quality of the RNA samples were evaluated

by a Nanodrop spectrophotometer and 1% agarose gel electrophoresis. All the RNA samples were stored at -80 °C for future use. One microgram RNA was used to synthesize the cDNA by the SuperScript II Reverse Transcriptase (Invitrogen, Waltham, MA) using oligo (dT) primers. qPCR was performed on a CFX Real-Time PCR Detection System with GoTaq qPCR master mix (Promega, Madison, WI). The total volume of each reaction was 20 µl containing 8 µl of 100-times diluted cDNA, 1 µl (10 µM) of forward primer, 1 µl (10 µM) of reverse primer and 10 µl of master mix. Each reaction was performed in duplicate. Two internal reference genes, peptidylprolyl isomerase A (PPIA) and 60S ribosomal protein L23 (RPL23), were introduced to normalize the qPCR data (Niu et al., 2014a). The performance of these reference genes in each experiment was evaluated by the calculated M and CV value under the qBase frame work (Hellemans et al., 2007).

2.8 Statistics

The Shapiro-Wilk test was used to check the normality of each data sets. Then a student's t-test or Mann-Whitney *U* test was used to compare the means of two data sets depending on their normality. One-way ANOVA with Tukey's multiple comparison or Kruskal-Wallis test with Dunn's multiple comparison was used to compare the mean among three data sets. Statistics were done in Prism v 7.02 software.

3. Result

3.1 SVWC domain and phylogenetic analysis of *Bt*SVC

A sequence alignment of the SVWC domain from *B. terrestris*, *D. melanogaster*, *A. aegypti* and *C. quinquefasciatus* shows the conserved eight cysteines motif (Figure 267). The number of residues between each cysteine follows a consensus pattern reported by Sheldon *et al* (Sheldon et al., 2007). The schematics of this consensus pattern is shown in Figure 27A, where the digits in the grey box represent the range

of amino acids. Strikingly, we found that the number of residues between C3 and C4 do not always follow the reported pattern. Additional amino acids are present in *Bt*SVC (XP_003399812), *Cq*SVC (XP_001844380), *Aa*SVC (XP_001656438) and *Dm*SVC, CG31997 (NP_001284709) (highlighted in the box with black border in Figure. 27A).

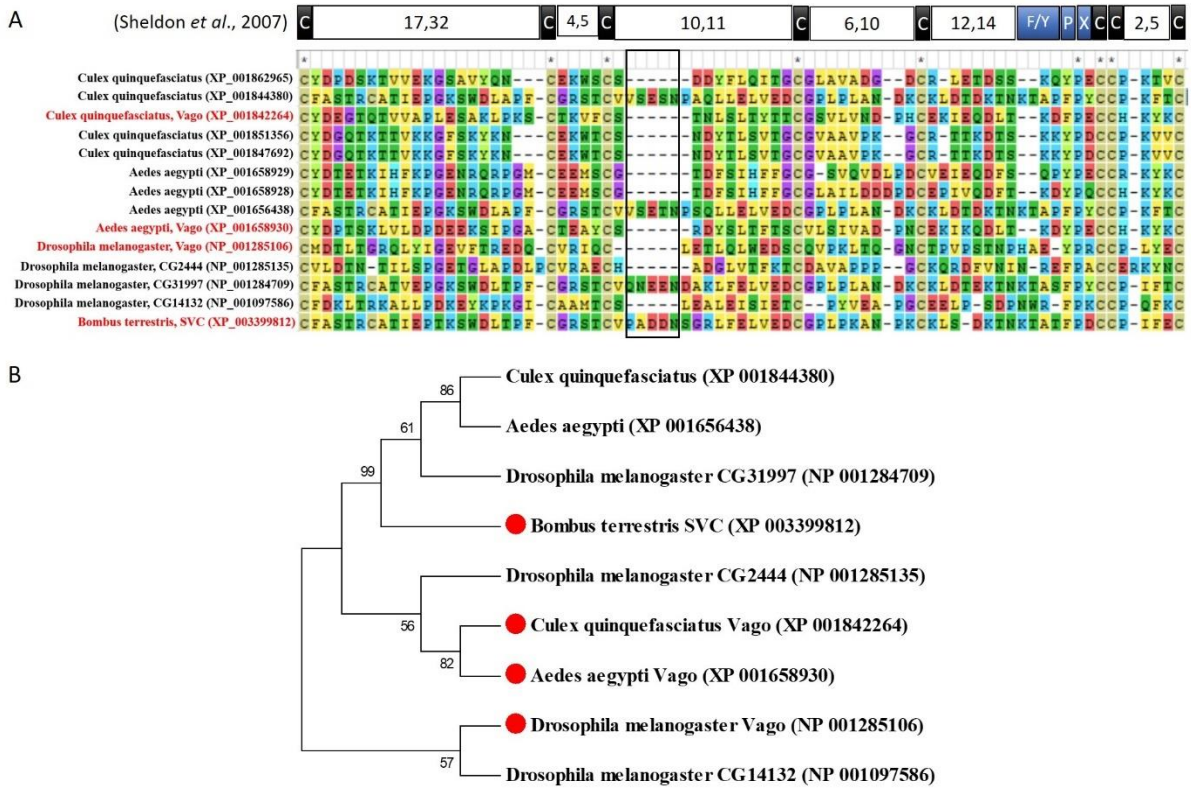

Figure 27. **A**. Schematics of consensus SVWC domain in Drosophila (adapted from Sheldon *et al*., 2007) and amino acid sequence alignment of SVCs from *D. melanogaster, Culex quinquefasciatus, Aedes aegypti* and *Bombus terrestris.* The eight-conserved cysteines of the consensus SVWC domain are represented by “c”. Grey and dark blue boxes represent the interval residues, where x, y represent between x and y residues inclusive. Accordingly, amino acid sequence alignment shows the similar pattern where the eight conserved cysteines are labeled by asterisks. Box with black borders shows a short fragment shared by four SVCs including the one in *B. terrestris*. *D. melanogaster* Vago, two reported *Dm*Vago orthologs in *C. quinquefasciatus* and *A. aegypti* mosquito and the only SVC in *B. terrestris* are highlighted in red. Alignment is carried out by Clustalw in MEGA 7.0 (http://www.megasoftware.net/). Sequences used for alignment are retrieved from NCBI protein database (https://www.ncbi.nlm.nih.gov/protein) and their accession numbers are given after the species names. **B.** A phylogenetic tree is established based on the above alignment of the SVWC domain to explore the relations of *Bt*SVC with other SVCs, including *Dm*Vago, its two reported orthologs in mosquitos and the four SVCs with extra interval residues between C3 and C4. Besides, two *Dm*SVCs (CG2444 and CG14132) that were reported to respond to bacterial infection are also included. The evolutionary history was inferred by using the Maximum Likelihood method based on the JTT matrix-based model. The bootstrap consensus tree was inferred from 1000 replicates. Branches corresponding to partitions reproduced in less than 50% bootstrap replicates are collapsed. Phylogenetic analyses were conducted in MEGA 7.0 (http://www.megasoftware.net/).

Phylogenetic analysis shows that *Bt*SVC is highly related with the other three SVCs containing the extra residues (Figure 27B). Besides, the reported *Dm*Vago orthologues in *Culex* and *Aedes* mosquitos, are more related to another *Dm*SVC (CG2444) but not *Dm*Vago (CG2081) (Figure 26B).

3.2 *BtSVC* is down-regulated in three tissues upon IAPV infection

At 1 day post injection (dpi), there is no obvious difference in *BtSVC* expression among three treatment groups, Mock (n=8), PBS (n=8) and IAPV (n=8) (Figure 28A, C and E). At 3 dpi, we saw clear downregulation of *BtSVC* in IAPV infected head (Figure 28B) (Kruskal-Wallis test with Dunn's multiple comparison, χ^2=15.405, *P*<0.001) and midgut

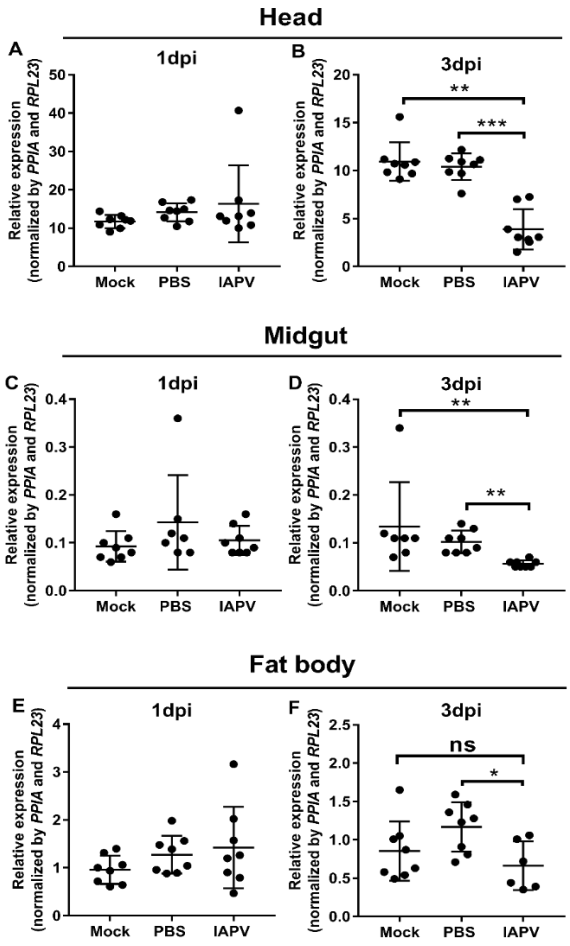

Figure 28. Relative expression of *BtSVC* upon IAPV infection in tissues of head, midgut and fat body. Five days old *Bombus terrestris* workers injected with IAPV (~500 particles) (n=8), PBS (n=8) and non-treatment control Mock (n=8) were kept in three different micro-colonies and maintained with sugar water and pollen bread. RNA samples of head, midgut and fat body were isolated at 1dpi and 3dpi. (**A, C** and **E**), At 1dpi, there is no obvious difference in relative expression of *BtSVC* among all three groups. (**B, D** and **F**), at 3 dpi, *BtSVC* is downregulated in all three tissues compared to PBS and Mock, except in fat body where significant downregulation was only observed between PBS and IAPV. Significance of the mean of each group was calculated by either one-way ANOVA or Kruskal-Wallis test with Dunn's multiple comparison depending on the normality of the data sets. Asterisk (*), (**) and (***) represent significant difference with *p* value < 0.05, 0.01 and 0.001.

(Kruskal-Wallis test with Dunn's multiple comparison, χ^2=15.116, *P*<0.001) (Figure 28D). The same downregulation of *BtSVC* was also observed in IAPV infected fat body (Figure 28F) (ANOVA, F (2, 19) =3.885,

p=0.0385). These results showed that *BtSVC* is downregulated upon viral infection in tissues.

3.3 Silencing of *BtSVC* altered IAPV levels in fat body

To investigate the function of *BtSVC* in viral immunity, we suppressed its expression by injecting sequence specific dsRNA before introducing virus. A clear silencing effect was observed in the fat body (t-test, t=3.7241, df=14, *p*=0.0023) (Figure 29A) but not in the brain (t-test, t=-0.8157, df=14) (Figure 29B) two days after the dsRNA injection. In these *BtSVC* silenced bees we injected IAPV viral particles and relative viral normalized quantities (RNQs) were checked two days later. IAPV RNQs was significantly higher in the BtSVC silenced fat body samples compared to the non-silenced (dsGFP) controls (t-test, t=-2.4374, df=18, p=0.0254) (Figure 29C).

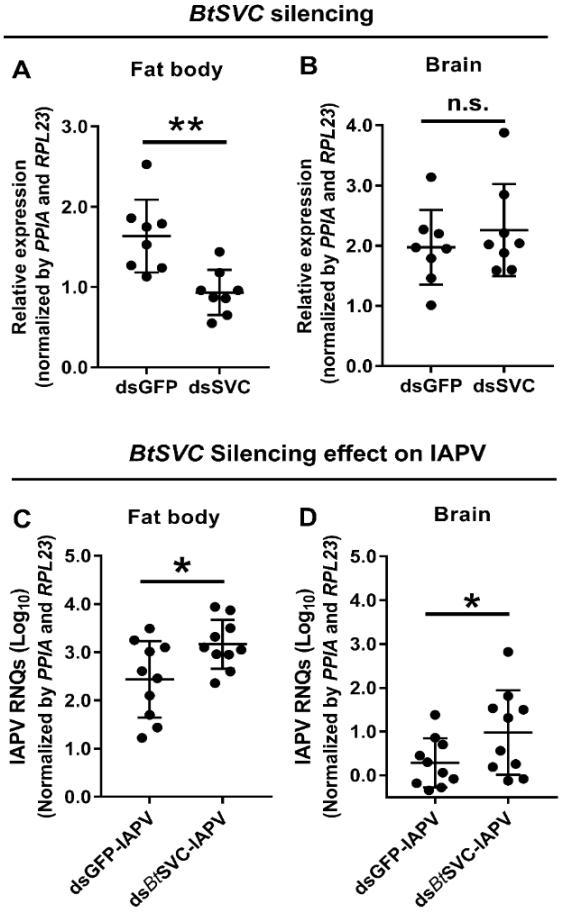

Figure 29. *BtSVC* silencing and effect on IAPV in tissues of fat body and brain. Five days old *B. terrestris* workers were injected with either 20 µl of ds*Bt*SVC (20 µg) or same volume of dsGFP (20 µg). Silencing efficiency was tested 2 days after dsRNA injection. **(A)** *BtSVC* is silenced in fat body (n=8). **(B)** *BtSVC* is not silenced in brain (n=8). Then bees after dsRNA injection were injected with IAPV, viral relative normalized quantities (RNQs) was checked 2 days after the viral infection. (**C**) *BtSVC* silencing lead to a higher IAPV RNQs in fat body (n=10). (**D**) Although *BtSVC* is not silenced in brain, IAPv RNQs is still higher in the ds*Bt*SVC injection bees (n=10). Significance of the mean of each group was calculated by either Student's t test or Mann-whiteny u test. The asterisk (*) and (**) represent significant difference with p value < 0.05 and 0.01, respectively, n.s. means no significant difference observed.

Interestingly, there is also a higher viral RNQs in head of ds*Bt*SVC injected bees than the control ones (t-test, t=1.955, df=18, *p*=0.0332) (Figure 29D). These results indicate that the *Bt*SVC is involved in the anti-IAPV activity in fat body and can have effect on the viral infection of brain.

3.4 The expression of *BtSVC* is *Bt*Dicer-2 dependent

In flies and mosquitos, the antiviral activity of Vago is reported to be mediated by Dicer-2, a key player of the small interfering RNA (siRNA) pathway and also a sensor of the viral-derived double stranded RNA (Wilson and Doudna, 2013). However, other components of the siRNA pathway, like Ago-2 and R2D2 have no effect on viral

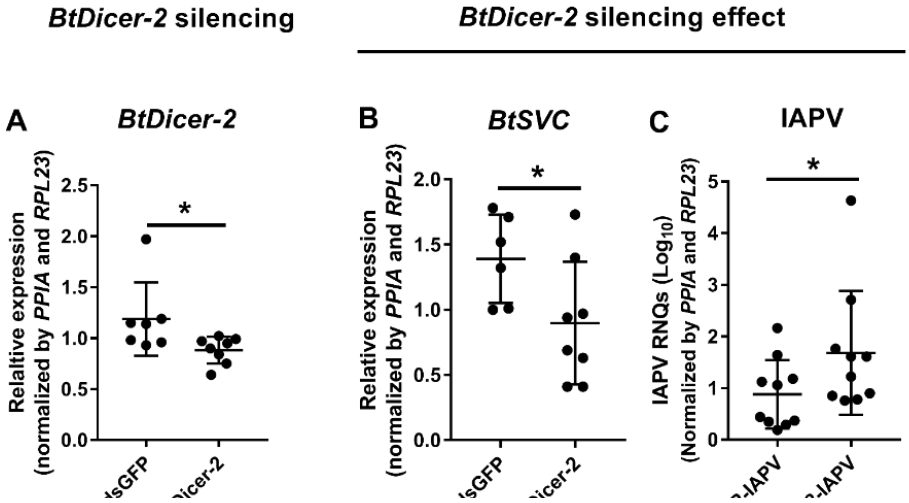

Figure 30. ***BtDicer-2* silencing in fat body**. Five days old *B. terrestris* workers were injected with either 20 µl of dsDicer-2 (20 µg) or same volume of dsGFP (20 µg). IAPV was injected two days after the dsRNA injection. (A) *BtDicer-2* silencing efficiency was tested two days after dsRNA injection. (B) *BtDicer-2* silencing effect on relative expression of *BtSVC*. (C) *BtDicer-2* silencing effect on IAPV RNQs. Either t-test or Mann-Whitney *U* test was used to calculate the significance of the mean between two groups. * represent significant difference with p value <0.05.

induced Vago regulation, indicating that Vago activity is not mediated by the siRNA pathway but very probably initiated after the virus is sensed by Dicer-2 (Deddouche et al., 2008; Paradkar et al., 2012). These data highlighted the importance of Dicer-2 on Vago mediated antiviral activity. To explore this on *B. terrestris*, we silenced *BtDicer-2* to see its effect on both *BtSVC* expression and IAPV infection. When we checked *BtDicer-2* silencing at 2 dpi (Mann-Whitney *U* test, *U*=9, *p*=0.0145) (Figure 30A), we

also observed a downregulation of *BtSVC* (t-test, t=2.172, df=12, *p*=0.0253) (Figure 30B). Then we introduced IAPV to *BtDicer-2* silenced bees and checked the viral RNQs two days later. We found that IAPV RNQs were also higher in the *BtDicer-2* silenced fat body compared to the non-silenced controls (Mann-Whitney *U* test, *U*=27, *p*=0.0427) (Fig 30C). These results indicate that *Bt*SVC is regulated by *Bt*Dicer-2. The effect on IAPV levels can be a direct effect of the siRNA pathway or indirect by silencing *BtSVC*.

3.5 Silencing of *BtSVC* has no effect on the induction of *BtDicer-2* and *BtHop* upon IAPV infection

Viral infection is known to trigger important antiviral-defense pathways, like siRNA (Galiana-Arnoux et al., 2006; van Rij et al., 2006) and Jak/Stat (Dostert et al., 2005; Souza-Neto et al., 2009). Besides, *Bt*SVC has been reported to work as a cross-talk molecule in the *Culex* mosquitos. Previous experiments have shown the upregulation of *BtDicer-2* in different tissues of *B. terrestris* after IAPV infections (Cappelle et al., 2016; Wang, Meeus, and Smagghe, 2016) and genes from Jak/Stat pathway (Hop) can also be influenced (Niu et al., 2016b). In this study, we confirmed that *Dicer-2* and *Hop* are upregulated in *B. terrestris* tissues upon IAPV infection (see supplementary, figure S1 and S2).

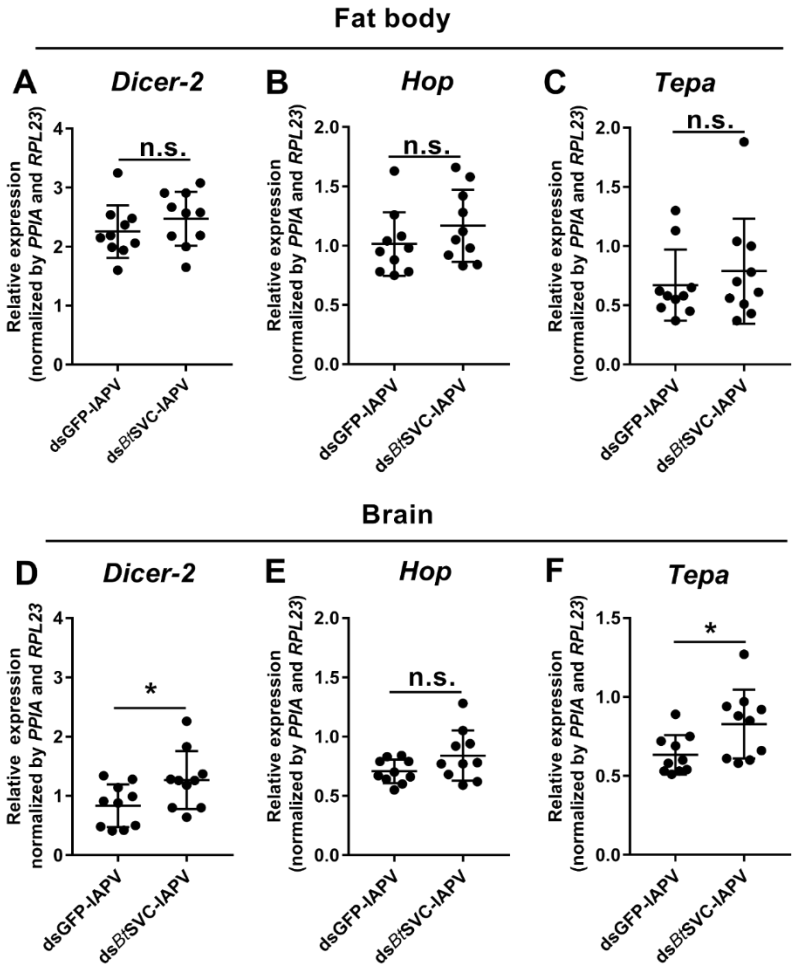

Figure 31. **Relative expression of *BtDicer-2, BtHop* and *BtTepa* in fat body and brain after dsRNA injection and IAPV infection**. **(A-C),** In fat body, no obvious difference of expression was observed in all three genes between ds*Bt*SVC-IAPV and dsGFP-IAPV. **(D-F)**, In brain, relative expression of *BtDicer-2* and *BtTepa* were higher in the ds*Bt*SVC-IAPV group. The asterisk (*) represent significant difference with p value < 0.05, n.s. means no significant difference observed.

Here we evaluated if this induction can be impaired in the *BtSVC* silenced bees. Aside from *BtDicer-2* and *BtHop*, we also followed *BtTepa*, the only reported end-product of the Jak/Stat pathway in bumblebee, mainly induced in wounding healing and improving opsonication (Barribeau.et al., 2015; Levashina et al., 2001) In fat body, no influence on any gene induction could be detected (Figure 31A, B and C). Thereby we are not able to prove the involvement of *BtSVC* as a cross talk molecule, towards Jak/stat. In the brain, we do see an effect on *BtDicer-2* but *BtSVC* is not silenced in

this tissue thus we are probably seeing the secondary effect that *BtSVC* treated brain has higher viral loads and thereby higher *Dicer-2* induction (Figure 31D). The higher expression of *BtTepa* in *BtSVC* silenced bees upon IAPV infection (Figure 31F) is more peculiar, as IAPV infection did not induce *BtTepa* expression (Fig S1 and S2).

3.6 The involvement of *BtSVC* in the expression of antimicrobial peptides (AMPs)

AMPs are important effector molecules to protect insects from a multitude of microorganisms. Their constitutive expression in specific tissues forms a first line of defense. We therefore checked the expression of AMP genes, but also of some other key immune genes from different pathways in the *BtSVC* silenced fat body. Surprisingly, the expression of four AMPs genes, *BtAbaecin*, *BtApidaecin*, *BtDefensin* and *BtHymenoptaecin* were all significantly downregulated in the *BtSVC* silenced fat body (Figure 32A). We did not see difference in expression level of *BtDicer-2* (siRNA pathway), *BtHop* (Jak/Stat pathway), *BtTepa* (Jak/Stat pathway), *BtRelish* (Imd pathway) and *BtBasket* (Jnk pathway) after *BtSVC* was silenced (Figure 32B). But we observed a down-regulation trend for *BtPelle* from the Toll pathway (multiple t-test, p=0.0589) (Figure 32B). These results indicate that *BtSVC* is involved in the basal expression of AMP genes in fat body.

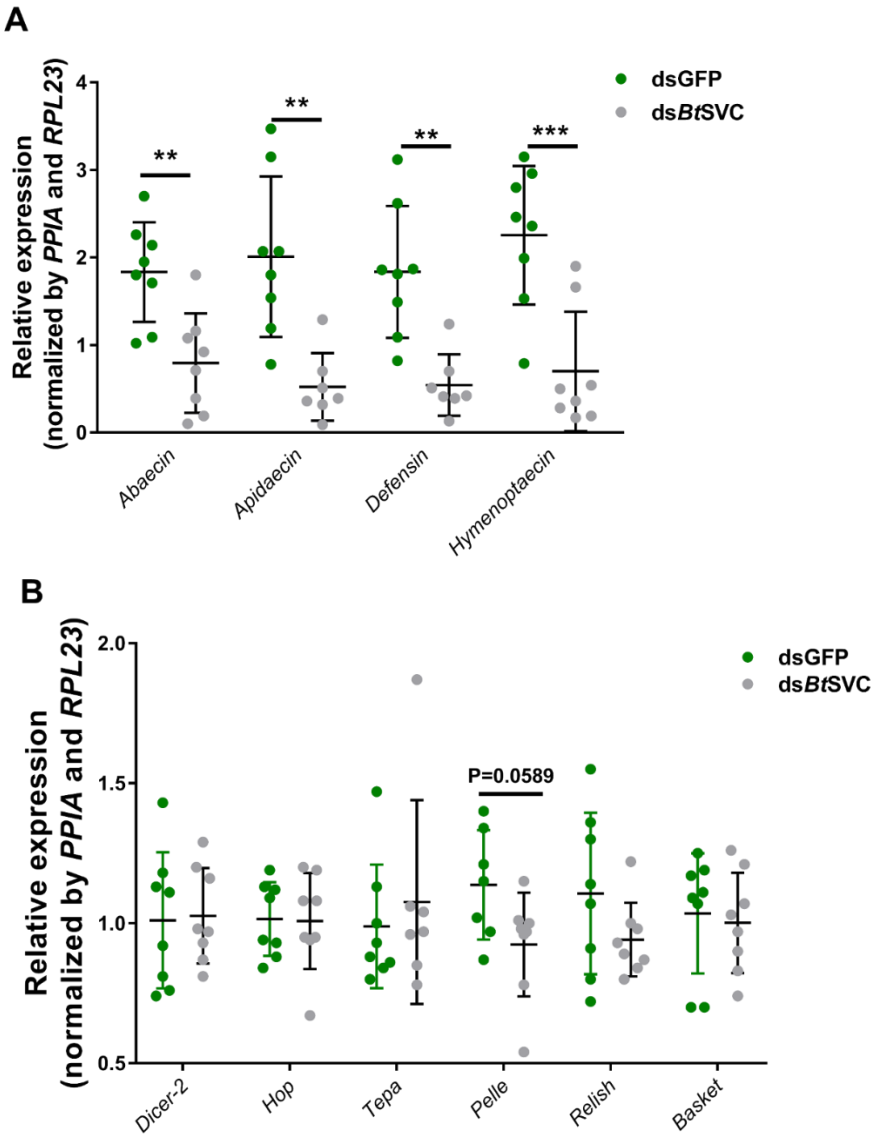

Figure 32 *BtSVC* silencing lower the expression of AMPs genes in fat body. (**A**) Relative expression of *BtAbaecin*, *BtApidaecin*, *BtDefensin* and *BtHymenoptaecin* are all significantly lower in the *BtSVC* silenced fat body than in the non-silenced ones. (B) There is no significant difference in relative expression of *BtDicer-2*, *BtHop*, *BtTepa*, *BtRelish* and *BtBasket* in ds*Bt*SVC and dsGFP injected fat body, except *BtPelle* which shows a down regulation trend. Multiple t-test was sued to compared the gene expression between dsGFP and ds*Bt*SVC groups. The asterisks (**) and (***) represent significant difference with p value < 0.01 and 0.001, respectively.

4. Discussion

4.1 *Bt*SVC is important in antiviral immunity of *B. terrestris*

To date, the SVC protein family is mainly studied on gene level and *Vago* is among the originally identified and best studied *SVC* genes in *D. melanogaster.* Many members of this family show induction after stress challenge, and *DmVago* particularly, is upregulated after viral infection on a *Dicer-2* dependent manner (Deddouche et al., 2008; Sheldon et al., 2007). This raises the question of the presence of Vago orthologues in the other species. In bumblebees and other bee species, there has been only one *SVC* gene identified, and is provisionally named *BtVago-like* (Niu et al., 2016b). Here we provided evidence that two core features of *Vago* are shared by the *SVC* gene in *B. terrestris* and therefore we conclude it has a similar antiviral functionality as described in the fruit fly (Deddouche et al., 2008). First, silencing of *BtSVC* in the fat body of *B. terrestris* results in increased IAPV levels. Second, a common feature shared by the Vago in flies, mosquitos and shrimps is the Dicer-2 dependent induction manner. Dicer-2 belongs to the same DExD/H-box helicase family as do the RIG-I-like receptors, which can sense and mediate interferon induction in mammals (Deddouche et al., 2008). Our results have shown that silencing *BtDicer-2* can lower the expression of *BtSVC* and increase the IAPV titers in fat body of *B. terrestris*. This indicates that next to the RNAi machinery, Dicer-2 also activates a series of immune molecules, including SVC, to confront viral infection.

Another feature of "*Cqvago*" reported in the mosquito *C. quinquefasciatus* mosquitos is the antiviral defense related with the Jak/Stat pathway. This part we could not confirm, however, in bees we lack the clear end-point molecule which could function as a marker of this pathway upon viral infection. We screened two known key components, *BtHop* and *BtTep* of the Jak/Stat pathway. Hop is a signaling molecule

and Tepa is an effector molecule but rather for injury and bacterial infection (Levashina et al., 2001). Therefore, we cannot provide evidence that link *BtSVC* to the Jak/Stat pathway in case of IAPV infection. This is in contrast to Niu *et al.,* (2016), where silencing *BtSVC* results in a lower expression of *BtHop* in whole abdomen of bees without viral infection (Niu et al., 2016b). This may be due to the different gene silencing effect between tissue level and body part level. Besides, checking gene expression on whole abdomen may also mask the information of those tissues that contribute less to the total RNA composition.

4.2 *Bt*SVC on the expression of AMPs

AMPs are important effector molecules and involved in a wide range of innate immune activities and their expression can be either constitutive in a basal level or induced after bacterial challenge (Li et al., 2012). The induction of AMPs is often associated with the Toll and Imd pathway, while the regulation of basal expression of these immune molecules is less studied. In *Drosophila*, the homeobox gene *caudal* can negatively regulate the expression of *drosomycin* and *ceropin* in the epithelia tissues (Ryu et al., 2008; Ryu et al., 2003). A recent study showed that a microRNA mir-8 can also negatively regulate the basal levels of *drosomycin* and *diptericin* in the fat body of unchallenged flies (Choi and Hyun, 2012). Besides, *D. melanogaster rbf-1* and *dCap-D3* genes can positively regulate the transcription of AMP genes in adult fat body (Longworth et al., 2012). Here we found that silencing *BtSVC* results in a lower expression of *BtAbaecin*, *BtApidaecin*, *BtDefensin* and *BtHymenoptaecin* in the fat body of *B. terrestris* and conclude that BtSCV is involved in the constitutive expression of AMPs.

Constitutive immunity is mainly linked with local immunity and less reported as to be linked with systemic infections where Toll and Imd have strong AMP inducible powers

after pathogen associated molecular patterns recognition. For instance, gut epithelium has to constitutively express AMPs to cope with the commensal bacteria immunity (Ryu et al., 2008). Besides it is also reported that the symbiotic bacteria can also pass the intestinal barrier and gain access to the insect hemocoel (Sanchez-Contreras and Vlisidou, 2008), hence constitutive expression of AMPs may also be important for the bacteria tolerance inside the body cavity. While for systemic infection, the synthesis and secretion of AMPs by the fat body cells into hemolymph is a well-known immune response in insects and a pivotal defense mechanism against invading microorganism (Lemaitre and Hoffmann, 2007). Whether *BtSVC* is involved in the induction of AMPs is unclear and need more study.

After silencing *BtSVC*, we also saw a trend in the downregulation of *BtPelle*. Pelle is a signaling molecule inside the innate immune cascade of Toll, which is mainly activated upon challenge by gram-positive bacteria and results in AMP production (Valanne, Wang, and Ramet, 2011). We therefore consider the Toll pathway as a potential candidate to be influenced by *BtSVC*. Although Toll pathway is often associated with bacterial challenges, it can also be involved in the antiviral activity (Ramirez and Dimopoulos, 2010; Xi et al., 2008a; Zambon et al., 2005). However the mechanism of how it involves in the antiviral immunity is still unclear since enhancing a single AMP failed to alter viral titers (Zambon et al., 2005).

4.3 Functional divergence of SVC proteins

Our results have shown that the *Bt*SVC can be involved in both antiviral activity and expression of AMPs. In flies, there are multiple SVC members (including *Dm*Vago) and most of them are proposed to be responsive to different stresses. This could result from a functional divergence of the genes, with each protein being able to adapt to a specific stressor. This specialization is not present in bees with only one SVC identified.

In this study, we showed that *Bt*SVC can encompass multiple functions within the innate immune system, indicating that it may still exhibit the ancestral functionality that is involved in multiple immune activities. When we compared the amino acid sequence of different SVCs from multiple insect species, no clear orthology can be inferred. However, we detected a closer sequence similarity of *Bt*SVC with *Dm*SVC (CG31997) than with *Dm*Vago (CG2081). Although, sequence similarity is the first basic means to infer relatedness, without detailed information on evolutionary pathways and its influence on divergence of biological functions, it is difficult to decide if genes are indeed orthologs within a specific family (Jensen, 2001). This difficulty is particularly present for SVC members which are classified based on their Cys-motif and without apparent sequence similarity to each other (Kleinjung et al., 2004). In *B. terrestris* we can prove the involvement of *Bt*SVC in the antiviral immunity, which is linked with *Bt*Dicer-2, like shown for *Dm*Vago, nevertheless but we still recommend to use the family name SVC, particularly because the exact function of CG31997 (the most similar sequence in the fruit fly) is yet to be elucidated. Besides, CG31997 does show high amino acid sequence similarity with homologs of different insect species of multiple orders (NCBI blastp, e-value <0.001). While *Dm*Vago (CG2081) only shows high similarity within Diptera species. This indicates that the function of CG31997 is conserved in multiple insect species while that of *Dm*Vago (CG2081) is specific to flies. This functional divergence of SVC immune genes could contribute to an enhanced immune repertoire and thereby differentiate the defense armory of flies. On the contrary, the absence of similar functional divergence in bees lead to a reduced immune repertoire, which is agreement with other immune genes, reported to be less diverse in bees.

Supplementary

Table S1. The number of SVC-related protein across different insect species in NCBI

Orders	Families	Species	SVCs	Orders	Families	Species	SVCs
Diptera	Drosophilidae	*Drosophila melanogaster*[a]	12	Hymenoptera	Formicidae	*Solenopsis invicta*	6
		Drosophila pseudoobscura	20			*Monomorium pharaonis*	6
		Drosophila simulans	14			*Vollenhovia emeryi*	3
		Drosophila ananassae	17			*Cerapachys biroi*	2
		Drosophila mojavensis	15			*Camponotus floridanus*	2
		Drosophila busckii[b]	15			*Acromyrmex echinatior*	3
		Drosophila virillis	15			*Pogonomyrmex barbatus*	3
		Drosophila willistoni	14			*Wasmannia auropunctata*	3
		Drosophila yakuba	12			*Dinoponera quadriceps*	3
		Drosophila erecta	12			*Harpegnathos saltator*	3
		Drosophila grimshawi	12			*Linepithema humile*	3
		Drosophila sechellia	10			*Trachymyrmex zeteki*	1
		Drosophila miranda	17			*Trachymyrmex cornetzi*	1
		Drosophila takahashii	16			*Trachymyrmex septentrionalis*	1
		Drosophila persimilis	9			*Atta cephalotes*	1
		Drosophila arizonae	16			*Atta colomica*	1
		Drosophila suzukii	14			*Cyphomyrmex costatus*	1
		Drosophila ficusphila	14			*Lasius niger*	1
		Drosophila kikkawai	13		Apidae	*Habropoda laboriosa*	2
		Drosophila bipectinata	13			*Eufriesea mexicana*	1
		Drosophila eugracilis	12			*Melipona quadrifasciata*	1
		Drosophila biarmipes	13			*Bombus terrestris*[b]	1
		Drosophila rhopaloa	11			*Bombus impatiens*	1
		Drosophila elegans	12			*Apis florea*	1
		Drosophila navojoa	9			*Apis mellifera*	1
	Tephritidae	*Bactrocera cucurbitae*	15			*Apis cerana*	1
		Bactrocera oleae	15			*Apis dorsata*	1
		Rhagoletis zephyria	14			*Ceratina calcarata*	1
		Bactrocera dorsalis	14		Halictidae	*Dufourea novaeangliae*	2
		Ceratitis capitata	11		Megachilidae	*Megachile rotundata*	2
	Muscidae	*Stomoxys calcitrans*	29		Braconidae	*Microplitis demolitor*	3

Orders	Families	Species	SVCs	Orders	Families	Species	SVCs
		Musca domestica	28			*Fopius arisanus*	2
	Culicidae	*Aedes aegypti*[b]	5			*Diachasma allooeum*	2
		Culex quinquefasciatus[b]	5		Trichogrammatidae	*Trichogramma pretiosum*	6
		Anopheles gambiae str. PEST	3		Vespidae	*Polistes dominula*	5
		Anopheles sinensis	4		Pteromalidae	*Nasonia vitripennis*	5
		Aedes albopictus	2		Encyrtidae	*Copidosoma floridanum*	3
		Anopheles darlingi	2		Agonidae	*Ceratosolen solmsi marchali*	1
	Calliphoridae	*Lucilia cuprina*	17				
Hemiptera	Cicadellidae[c]	*Cuerna arida*	30	Lepidoptera	Papilionidae	*Papilio xuthus*	11
		Homalodis liturata	25			*Papilio machaon*	8
		Graphocephala atropunctata	19			*Papilio polytes*	4
	Clastopteridae[c]	*Clastoptera arizonana*	5		Nymphalidae	*Dananus plexippus*	5
	Cimicidae	*Cimex lectularius*	4		Pyralidae	*Amyelois transitella*	6
	Pentatomidae	*Halyomorpha halys*	4		Plutellidae	*Plutella xylostella*	6
	Aphidoidae	*Acyrthosiphon pisum*	2		Bombycidae	*Bombyx mori*	6
		Diuraphis noxia	1		Geometridae	*Operophtera brumata*	3
	Psyllidae	*Diaphorina citri*	2		Sphingdae	*Manduca sexta*	1
Coleoptera	Tenebrionidae	*Tribolium castaneum*	21	Phthiraptera	Pediculidae	*Pediculus humanus corporis*	4
	Curculionidae	*Dendroctonus ponderosae*	7	Entognatera	Entomobryidae	*Orchesella cincta*	3
	Silphidae	*Nicrophorus vespilloides*	6				
	Scarabaeidae	*Oryctes borbonicus*	3				

[a] A SVC protein in *D. melanogaster*, also named Vago is found to have antiviral function
[b] Represent species that have SVC protein that have similar function with *Dm*Vago
[c] Species that do not have their genome sequenced.

Table S2 Primers used in this study

Targets	Forward primers	Reverse primers	Accession number	References	Amplification factor
IAPV (qPCR)	CCATGCCTGGCGATTCAC	CTGAATAATACTGTGCGTATC	EU436443.1	Niu et al, 2016a	1.884
BtSVC (qPCR)	TGTTACCCTTCAACGCAATTC	ACAGATTCCGAAACGCTGAT	XP_003399812.1	Niu et al, 2016b	1.957
BtSVC (dsRNA)	TAATACGACTCACTATAGGG AGACCTAGTCCCGGAAGTCG AGA	TAATACGACTCACTATAGGG AGAGTACGTACGAATTACAA GATCAACT	XP_003399812.1	Niu et al, 2016b	
Dicer-2 (qPCR)	TGGTCAAAACATCAAGAACA ACCA	GATCGGGGCCATACGAACAT	XM_012307737.1	Niu et al, 2016a	1.943
Dicer-2 (dsRNA)	TAATACGACTCACTATAGGG AGAGCGAAGGTGTCACCAAA TGT	TAATACGACTCACTATAGGG AGAGGGTGTGTAAAGGCCTG CAA	XM_012307737.1	Niu et al, 2016a	
Hop (qPCR)	TGGCACAATGTGTCTCATCTT	GAGGTACACAACGAGGTCCA G	XM_003401903.2	Niu et al, 2016b	1.942
Tepa (qPCR)	GGAACCAATCGTCACCAAGC	TCTTGCGATCAGGCATCCAT	XM_003399699.2	This study	1.884
Pelle (qPCR)	TAAATCGACCTATGCAAGCC	GGGTATAGCTGCTTCTGCTG	XM_003399470	This study	1.925
Relish (qPCR)	CAGCAGTAAAAATCCCCGAC	CAGCACGAATAAGTGAACAT A	XM_003399472	This study	1.916
Basket (qPCR)	GGAACAAGATAATCGAGCAA CTG	CTGGCTTTCAATCGGTTGTG	XM_003402794	This study	1.873
Abaecin (qPCR)	CCAGGGTTTGGTAATGGGTA TGGC	ACGACCGGGACAATCTAAAC CG	XM_003394653	This study	1.973
Apidaecin (qPCR)	CCCGACTAATGTACCTGCCA	GAAGGTGCGAATGTGTTGGA	XM_003402966	Barribeau et al., 2015	1.946
Defensin (qPCR)	GTCTGCCTTTGTCGCAAGAC	GACATTAGTCGCGTCTTCTTC G	XM_001280909	Barribeau et al., 2015	1.874
Hymenoptaecin (qPCR)	TTCATCGTACTGGCTCTCTTC TG	AGCCGTAGTATTCTTCCACA GC	EU411043.1	Barribeau et al., 2015	1.882
PPIA (qPCR)	TCGTAATGGAGTTGAGGAGT GA	CTTGGCACATGAAGTTTGGA AT	XM_003402218.2	Niu et al, 2016	1.921

Targets	Forward primers	Reverse primers	Accession number	References	Amplification factor
RPL23 (qPCR)	GGGAAAACCTGAACTTAGGAAAA	ACCCTTTCATTTCTCCCTTGTTA	XM_003400707.2	Niu et al, 2016	1.913

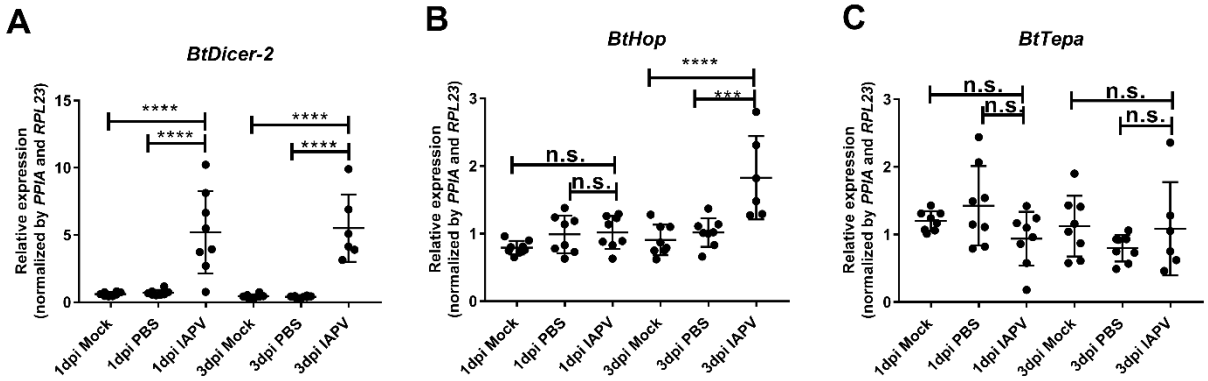

Figure S1. Immune genes expression in fat boy after IAPV infection. *BtDicer-2* (A), *BtHop* (B) and *BtTepa* (C) expression were represented in dots plot with mean±SD. Significance among treatment groups (Mock, PBS and IAPV) in both 1 dpi and 3 dpi are calculated by ANOVA with post hoc Tukey test. Asterisks**** and *** indicate significant difference with P<0.0001 and P<0.001, respectively. n.s. indicates no significance.

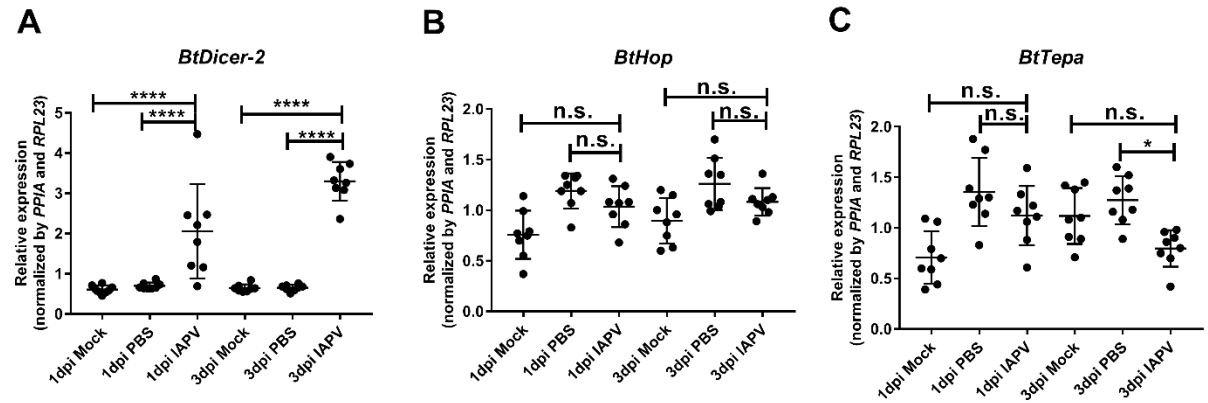

Figure S1 Immune genes expression in brain after IAPV infection. *BtDicer-2* (A), *BtHop* (B) and *BtTepa* (C) expression were represented in dots plot with mean±SD. Significance among treatment groups (Mock, PBS and IAPV) in both 1 dpi and 3 dpi are calculated by ANOVA with post hoc Tukey test. Asterisks**** and * indicate significant difference with P<0.0001 and P<0.05, respectively. n.s. indicates no significance is observed.

Chapter Ⅴ: Differential expression of antimicrobial peptides in *Bombus terrestris* workers upon Israeli acute paralysis virus (IAPV)

Parts of this chapter are submitted for publication:

Wang, H., Smagghe, G. & Meeus. I., 2017. Differential expression of antimicrobial peptides in *Bombus terrestris* workers upon Israeli acute paralysis virus (IAPV). *Developmental and Comparative Immunology* (submitted)

.

1. Introduction

Antiviral immunity in insects has very different features compared to mammals. A key defense pathway against RNA viruses in insects is the RNA interference (RNAi) pathway (Wang et al., 2006), with recent data highlighting its signal amplification potential to prime pre-infected tissues (Tassetto, Kunitomi, and Andino, 2017). Besides, the recruitment of Jak-Stat pathway is also well recognized as an antiviral defense (Dostert et al., 2005). The involvement of other pathways, like Toll and Imd, essential in antimicrobial peptide (AMP) regulation is more controversial. Silencing Toll and/or Imd resulted in altered viral titers. Although the mechanism behind it is poorly understood, no direct effect of AMPs on viruses are expected (Costa et al., 2009; Pan et al., 2012; Ramirez and Dimopoulos, 2010; Xi et al., 2008b; Zambon et al., 2005). A major unknown factor, regarding the activation of these pathways, is the recognition of the viruses, especially non-enveloped ones. Currently, no viral pathogen-associated molecular patterns (PAMPs) activating these two pathways have been identified. Besides, no conserved immune elicitor has been identified in the variable viral capsid proteins (Zambon et al., 2005). Therefore, changes in expression of AMPs in relation to viruses have often been attributed to indirect effects.

Double stranded RNA intermediates of the viral genome are known to activate the RNAi pathway. Aside from dicing long dsRNA, Dicer-2 also acts as a virus sensor molecule triggering other antiviral defense pathways, like the Jak-Stat, through Vago, an immune molecule belonging to the single von Willebrand factor C-domain proteins (SVCs) (Paradkar et al., 2012). Furthermore, random dsRNA has been described as potential PAMPs, reducing viral loads in honeybees and bumblebees although the mechanism remains unclear (Flenniken and Andino, 2014; Piot et al., 2015). Thus, the viral sensing action of Dicer-2 could potentially regulate other immune pathways,

directly in relation to combat the virus or to mitigate associated damages caused by viral infection. We hypothesize that this Dicer-2 sensing could also trigger AMP signaling. Especially because we recently identified that in bumblebees there is only one SVC protein, it is involved in antiviral activity and expression of 4 different AMPs (see chapter 4) (Wang et al. submitted). To the best of our knowledge, the relations between AMPs and viral infection in bumblebees is totally blank. Bringing us to the first question of this study: does viral infection induce AMP expression in *B. terrestris*? Second, we ask if there is a link between the *vago*-like gene *BtSVC* and AMP expression upon virus invasion? To serve this, we infected *B. terrestris* workers with two different viruses, Israeli acute paralysis virus (IAPV) and slow bee paralysis virus (SBPV) and tested the expression of four AMPs genes upon infection. The induction of AMPs upon viral infection in BtSVC silenced bees was followed to infer if immune crosstalk gene is responsible.

2. Material and methods

2.1 Insect and virus

B. terrestris callow workers were collected from different colonies and provided by Biobest (Westerlo, Belgium). Upon arrival in the lab, they were randomly transferred into plastic micro-colony (20 bees/colony) and maintained with sugar water and pollen. Plastic micro-colonies were kept in an incubator (Panasonic, Sakata, Japan) at 30 °C and 60 % relative humidity with continuous darkness.

The IAPV stock used in this experiment was $IAPV^{inj\text{-}S}$ (chapter Ⅱ). The SBPV stock was kindly provided by Joachim de Miranda (Swedish University of Agricultural Sciences, Uppsala, Sweden). Both viruses stocks were estimated to contain 1×10^6 particles per microliter by transmission electron microscope. To establish a systemic infection, the virus was injected into the hemocoel of bees with a nano-injector. Upon

injection, $IAPV^{inj-S}$ was diluted by 10,000 times and SBPV stock was diluted 50 times in filter-sterilized phosphate buffer saline (PBS). Bees were firstly immobilized on ice then, 5 µl of IAPV (~ 500 virus particles) and 5 µl SBPV (~ 1×10^5 virus particles) were delivered through the cuticle between 1st and 2nd segment in the abdomen.

2.2 Experimental design

Detection of AMP gene expression upon IAPV.

To investigate if AMPs can be induced by IAPV infection and exclude the possible induction by physical injury, we included two control group, PBS as infection control and mock as injection control. Bees injected with IAPV (n=25) and PBS (n=20) were kept in two new plastic micro-colonies. Another group of bees (n=20) without any treatment (mock) were also transferred into a new colony. All three colonies were maintained with the same condition as mentioned above. For IAPV, the viral titers are low at 1 dpi and can reach to the peak at 2 or 3 dpi (Niu. et al., 2016a). Thus, we chose two time points, 1dpi and 3 dpi representing as initial viral infection stage and systemic viral infection stage, respectively. Bees (n=8) randomly collected from each colony at both time points were sacrificed for RNA extraction.

Detection of AMP gene expression upon SBPV and dsRNA.

Another two independent tests with similar set-up were used to check if AMPs are induced upon SBPV (SBPV (n=12), PBS (n=10) and mock (n=10)) infection and dsRNA injection (dsGFP (n=10), PBS (n=10) and mock (n=10)) at 1 dpi. Bees (n=8) randomly collocated from each colony were sacrificed for RNA extraction.

Detection of the interaction between BtSVC and hymenoptaecin upon IAPV infection

To investigate if the *BtSVC* gene is involved in the AMP induction upon IAPV infection, we first silenced the *BtSVC* with dsRNA injection. The silencing experiment was done

as previously described (Niu et al., 2016b). Bees were injected with ds*Bt*SVC (n=22) and dsGFP (n=22) for silencing. Eight bees per treatment were sacrificed to check silencing efficiency and AMPs expression in fat body 2 days post dsRNA injection. The remaining bees were infected with IAPV. AMPs genes expression were checked 2 days after IAPV infection (4 days post dsRNA injection).

2.3 RNA extraction, cDNA synthesis and qPCR

Bees were firstly immobilized on wet ice and then dissected to collect fat tissues individually. RNA of fat tissues was extracted using the RNeasy mini kit (Qiagen, Venlo, the Netherlands). Five hundred µl of RLT buffer was used to lyse the fat body cells in a tissues lyser with metal beads for 3 min. After centrifuging for 5 min at max speed, the supernatant was extracted accordingly to manufacturer's instructions. Genomic DNA was removed using the TURBO DNA-free kit (Ambion, Foster, CA). cDNA was synthesized with one microgram of RNA by the SuperScript II Reverse Transcriptase (Invitrogen, Waltham, MA) using oligo (dT) primers. qPCR was performed on a CFX Real-Time PCR detection system using GoTaq master mix (Promega, Madison, WI). The total reaction volume of 20 µl contains 8 µl of 100-times diluted cDNA, 1 µl (10 µM) of forward and reverse primer, and 10 µl of master mix. Each reaction was performed in duplicate. Two internal reference genes, peptidylprolyl isomerase A (PPIA) and 60S ribosomal protein L23 (RPL23), were introduced to normalize the qPCR data (Niu et al., 2014a). The performance of reference genes in each experiment was evaluated by the calculated M and CV value under the qBase frame work (Hellemans et al., 2007).

2.4 Data analysis

The qPCR data transformation and normalization was performed by qBase (Hellemans et al., 2007). Specifically, relative quantities for each gene were calculated

by comparing the Cq value of given sample with the average Cq value across all samples from the same gene. The relative quantities of the target gene were normalized by the relative quantities of two reference genes PPIA and RPL23. Finally, the relative expression of each gene was rescaled to the average expression across all samples. The log10 transformed data were used for statistics. Normality of all data were checked by Shapiro-Wilk test. The mean of each group of data was separated by one-way ANOVA with Tukey's multiple comparison. Statistics were done by Prism 7 software.

3. Results and Discussion

Our result showed that at 1 dpi, *abaecin* was significantly induced by both PBS and IAPV compared to non-treatment mock (Figure 3 (One-way ANOVA with Tukey's multiple comparison, $F_{2,21}$=150.30, P<0.0001). This induction is due to the injection and physical injury. PBS treatment also induced *hymenoptaecin* (1 dpi), but injecting IAPV resulted in an additional trigger, boosting *hymenoptaecin* expression at this day (Figure 33C). This induction is still visible as a trend at 3 dpi (Figure 33D). For *abaecin*, we also see a significant difference between IAPV and PBS after 3 dpi (Figure 33B) (One-way ANOVA with Tukey's multiple comparison, $F_{2,20}$=8.107, P=0.0026). Rather than being directly induced by the virus it is more likely that *abaecin* increase is caused by physical injury and its expression is less attenuated in virus infected bees. Another two AMP genes *defensin* and *apidaecin* were not inducible by IAPV infection and only responded to injection at 1dpi (see supportive info Figure S1). Abaecin is in the class of proline-rich antimicrobial peptides, and hymenoptaecin is a glycine-rich antimicrobial peptide (Danihlík et al., 2016). In bumblebees, both AMPs were previously reported to be induced by bacterial infection and injury (Choi et al., 2008;

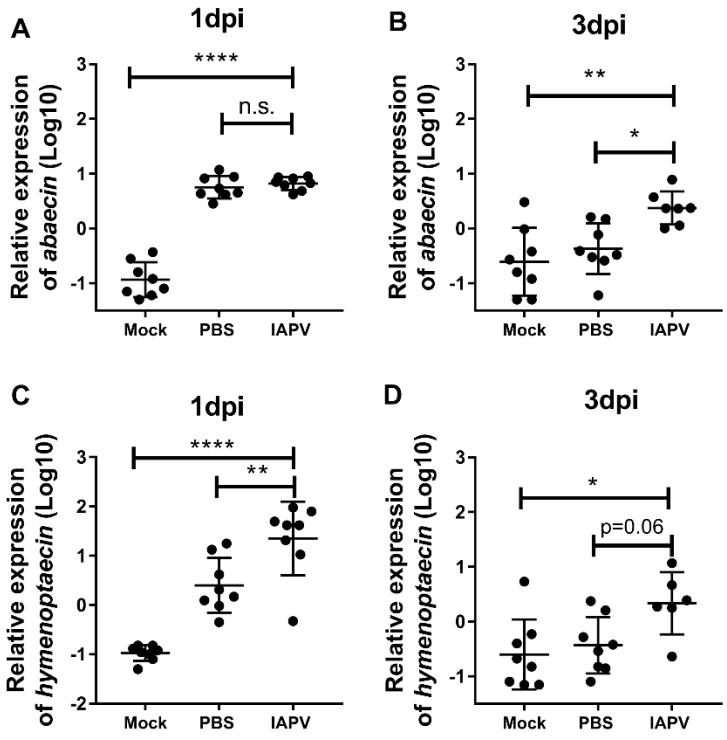

Figure 33. Induction of *abaecin* and *hymenoptaecin* upon IAPV Infection. A. *Abaecin* is significantly induced by both PBS and IAPV injection at 1dpi. **B**. at 3dpi, *abaecin* is still inducible by IAPV. The induction by PBS is gone. **C**. *Hymenoptaecin* is induced by IAPV at 1dpi. **D**. *Hymenoptaecin* is marginally induced by IAPV at 3dpi. The mean of each group was compared by one-way ANOVA with Tukey's multiple comparison. ****, ** and * represent significant difference between two groups with p <0.0001, <0.01 and <0.05. n.s. indicates there is no significant difference between two groups

Erler, Popp, and Lattorff, 2011). However, the regulation of these AMPs are not fully understood, although they are generally considered to be controlled by Toll and IMD pathways.

The higher expression of *hymenoptaecin* is virus-specific, because neither another RNA virus SBPV isolate nor non-virus specific dsGFP was found to induce *hymenoptaecin* at 1dpi (Figure 34A and B). Increased AMP expression after virus infection is often described as a secondary effect (Merkling and van Rij, 2013), of which the mechanism is not fully understood. IAPV injection can have severe impact on bee health, with mortality starting at 3 dpi and resulting at 100% mortality at 5~8

dpi (Niu. et al., 2016a; Wang et al., 2016). Thus, it is possible that the AMPs are upregulated because of general inflammation induced by IAPV infection.

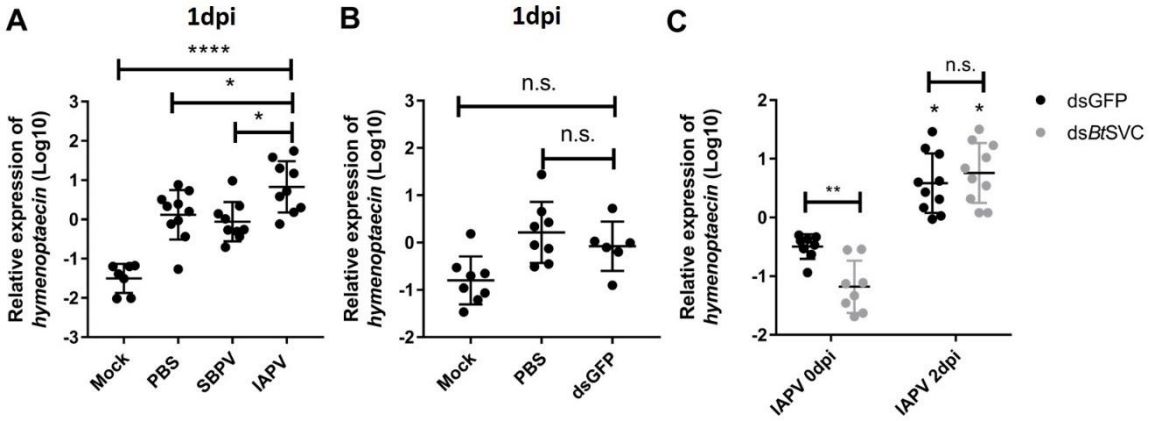

Figure 34. The induction of hymenoptaecin is virus specific and not affected after *BtSVC* silencing. **A**. *Hymenoptaecin* is not induced by SBPV infection. **B**. *Hymenoptaecin* is not induced by dsGFP. **C**. *BtSVC* did not interact with *hymenoptaecin* induction upon IAPV infection. Asterisk above the dots represent the significant induction is observed between non-IAPV and IAPV groups. The mean of each groups was compared by one-way ANOVA with Tukey's multiple comparison. ****, ** and * represent significant difference between two groups with p <0.0001 and <0.01 and <0.05. n.s. indicates there is no significant difference between two groups.

However, it is also possible that the AMPs are induced as a result of SVC involved in immune regulation. To test this, we first did a pretreatment and silenced *BtSVC* (silencing efficiency see chapter IV). Silencing *BtSVC* lowered basal *hymenoptaecin* expression. Then we evaluated the induction of *hymenoptaecin* at 2 dpi of IAPV. We found that in both *BtSVC* silenced and non-silenced groups *hymenoptaecin* had the same expression upon IAPV infection (Figure 34C). This indicated that *BtSVC* may not interact with AMP induction in the case of IAPV. Furthermore, one could question that the induction pattern observed for *hymenoptaecin* at 1 dpi follows the same dynamics as *abaecin* but with earlier dynamics.

To conclude, our results showed that two AMP genes, *abaecin* and *hymenoptaecin* express differentially upon IAPV infection in *Bombus terrestris*. Besides, we do not have proof of a direct induction of *hymenoptaecin* upon IAPV regulated by *BtSVC*.

Table S1 Primers used in this chapter

Targets (purpose)	Forward primers	Reverse primers	Amplification factor
BtSVC (qPCR)	TGTTACCCTTCAACGCAATTC	ACAGATTCCGAAACGCTGAT	1.957
BtSVC (dsRNA)	TAATACGACTCACTATAGGGAGACCTAGTCCCGGAAGTCGAGA	TAATACGACTCACTATAGGGAGAGTACGTACGAATTACAAGATCAACT	
Abaecin (qPCR)	CCAGGGTTTGGTAATGGGTATGGC	ACGACCGGGACAATCTAAACCG	1.973
Apidaecin (qPCR)	CCCGACTAATGTACCTGCCA	GAAGGTGCGAATGTGTTGGA	1.946
Defensin (qPCR)	GTCTGCCTTTGTCGCAAGAC	GACATTAGTCGCGTCTTCTTCG	1.874
Hymenoptaecin(qPCR)	TTCATCGTACTGGCTCTCTTCTG	AGCCGTAGTATTCTTCCACAGC	1.882
PPIA (qPCR)	TCGTAATGGAGTTGAGGAGTGA	CTTGGCACATGAAGTTTGGAAT	1.921
RPL23 (qPCR)	GGGAAAACCTGAACTTAGGAAAA	ACCCTTTCATTTCTCCCTTGTTA	1.913

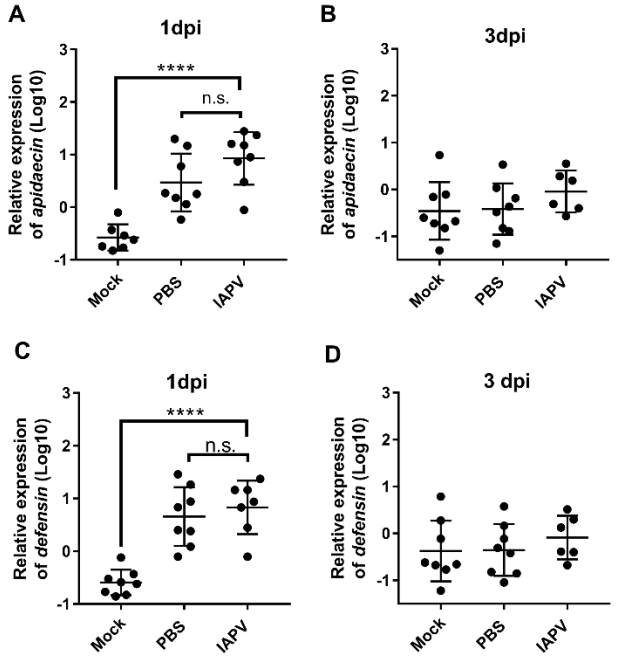

Figure S1. Expression of *apidaecin* and *defensin* upon IAPV infection. Induction of these two AMPs genes are only observed at 1dpi and due to physical injury but not virus infection.

Chapter VI: Exploration of interaction between virus and host cellular immune defense in bumblebee (*Bombus terrestris*)

1. Introduction

Hemocytes, known as the circulating cells inside the hemocoel, are the main component of insect cellular immunity and can respond immediately to invading microbes like bacteria, fungi and parasites (Lavine and Strand, 2002; Strand, 2008). When recognizing a surface as foreign hemocytes start to spread, which ultimately result in phagocytosis (Eleftherianos et al., 2009). Although recent studies in *Drosophila melanogaster* highlighted the importance of hemocyte mediated phagocytosis in the host antiviral defense (Lamiable et al., 2016; Nainu et al., 2015; Ye and Zhang, 2013; Zhu and Zhang, 2013), the mechanism is not fully understood. Here it is important to understand that cellular immunity, or even immunity as a whole, among different insect orders can be very different.

Aside from differences purely based on nomenclature[2], clear differences in hemocyte composition have been reported (Lavine and Strand, 2002; Ribeiro and Brehelin, 2006). Furthermore, addressing a basic function of hemocytes, like for example phagocytosis, to a specific cell type is difficult. Indeed, granulocytes are often reported to perform phagocytosis, while this function can also shift to other cell types like, plasmatocytes (PLs), spherulocytes (SPs) and adipohemocytes (ADs) (Gupta, 1985). Involvement of these cell types in viral immunity cannot be inferred from their morphology.

Bumblebees are frequently associated with different viruses (Manley et al., 2015; Singh et al., 2010), but knowledge of hemocytes composition and population dynamics

[2] For instance, hemocytes of *Drosophila* are often called lamellocytes, plasmatocytes and crystal cells. While this nomenclature really deviates from efforts to get systematics herein based on morphology. With Drosophila lamellocytes being (a type of) plasmatocytes, *Drosophila* plasmatocytes actually being named granulocytes in other insect, and finally crystal cells being oenocytes. (Lavine and Strand, 2002; Ribeiro and Brehelin, 2006).

upon virus infection is absent. Within chapter V we have shown the induction of AMPs, but this may not typically have a direct association with virus infection. General inflammation and recruitment of hemocytes to clean-up viral damage and apoptotic bodies could explain why other immune pathways, e.g. AMPs are activated after systemic virus infection. In chapter II we established an acute infection model in the bumblebee, *Bombus terrestri*s, by injection with IAPV leading towards high mortality within 5 days. Work of Niu et al. (2016) showed that injection with SBPV rather resulted in a chronic infection pattern with no mortality linked with the virus (Niu. et al., 2016a). These two infection models allow us to study the relation between hemocytes composition in bumblebees and different systemic virus infections patterns. We hypothesize that virus infection can have an impact on bumblebee hemocytes composition. We use changes in hemocytes profiles as a proxy for the impact of viruses on cellular immunity during virus systemic infections. Therefore, we compared the hemocytes profiles between virus infected bees and non-virus infected ones by flow cytometry analysis, which is recently used for hemocytes differentiation in another social insect, honeybee (*Apis mellifera*) (Marringa et al., 2014). Second, we try to infer if phagocytosis is involved in controlling virus infection. Hereto we blocked the phagocytosis mechanism by injection of latex beads (Elrod-Erickson, Mishra, and Schneider, 2000; Nehme et al., 2011) studied its effect on IAPV induced mortality and viral accumulation in tissues. As discussed in Chapter I, that latex beads injection is a common approach to test involvement of phagocytosis *in vivo* in insects.

2. Material and Methods

2.1 Insect and virus

B. terrestris callow workers were sampled from different colonies and provided by Biobest (Westerlo, Belgium). Upon arrival in the lab, they were randomly transferred

into plastic micro-colony (25 bees/colony) and maintained with sugar water and pollen. Plastic micro-colonies were kept in an incubator (Panasonic, Sakata, Japan) at 30 °C and 60 % relative humidity with continuous darkness.

The IAPV and SBPV stock used for infection were previously purified from white-eye honeybee pupae (Niu et al., 2014a). Both viruses stocks were estimated to contain 1×10^6 particles per microliter by transmission electron microscope. The contamination of other common viruses such as (ABPV), Kashmir bee virus (KBV), chronic bee paralysis virus (CBPV), deformed wing virus (DWV), slow bee paralysis virus (SBPV), sacbrood virus (SBV) and black queen cell virus (BQCV) were determined by RT-qPCR (Locke et al., 2012). Viruses were delivered into *B. terrestris* workers by a nano-injector. Upon injection, IAPV and SBPV stock were diluted by 10,000 and 50 times with filtered-sterilized phosphate buffer saline (PBS), respectively. Then 5 µl of either IAPV (~500 particles) or SBPV (~1×10^5 virus particles) was delivered into the hemocoel through abdomen.

2.2 Hemolymph collection

B. terrestris workers were starved for minimally 2 hours prior to hemolymph collection to exclude filled crops contaminating hemolymph collection. Upon collection, bees were first immobilized on wet ice for 10-15min. Then the thorax was punctured by a fine steel needle to break the dorsal sinus and bees were placed in a 0.65ml centrifuge tube (with a whole open in the bottom) with their abdomen removed. This 0.65 tube was placed in a 1.5 ml centrifuge tube containing 2µl phenylthiourea (PTU). After that the 1.5ml tubes complex was centrifuged at 3000g for 3 min at 4℃to collect 7~10µl hemolymph (including PTU).

2.3 Wheat germ agglutinin (WGA) and Propidium iodide (PI) staining

Lectin wheat germ agglutinin (WGA) and Propidium iodide (PI) have been used to differentiate hemocytes profiles in honeybees (de Graaf et al., 2002; Marringa et al., 2014). In this study, we used WGA and PI counterstaining to monitor bumblebee hemocytes. We injected *B. terrestris* workers (7 days old) with either IAPV (n=15) or SBPV (n=15) as described above. Here we introduce SBPV as a comparison to IAPV as SBPV can induce chronic infection and lower mortality (Niu et al., 2016a). Another two groups of bees, PBS (n=12) and a non-treatment mock (n=12) were employed as control. Hemolymph of individual bee from each group was collected 3 day after infection (dpi). To prepare the PI stock, 1mg of PI (Sigma) powder was added to 1ml distilled water to make a 1.5mM (1mg/ml) stock. This stock was stored in a 1.5 ml tubes at 4℃protected from light. To prepare WGA/PI staining solution, 100 µl PI stock and 0.1mg WGA-FITC (Sigma) powder was mixed in 100ml 0.2µm filter sterilized 1×phosphate-buffered saline (PBS). For each sample, 7µl hemolymph mixture (5µl collected hemolymph + 2µl PTU) was added to 500µl WGA/PI staining solution and incubated at 37℃for 15min before flow cytometry test.

2.4 Apoptosis analysis by Annexin V

We performed annexin V / PI staining to differentiate between apoptosis or necrosis of hemocytes after IAPV infection. The Annexin and PI staining is often used to identify the apoptosis/necrosis of cells. Cells that stain positive for Annexin V and negative for PI are undergoing apoptosis. Cells that stain positive for both Annexin V and PI are dead cells, either they are in the end stage of apoptosis, or underwent necrosis. Cells that stain negative for both Annexin V and PI are alive and not undergoing measurable apoptosis. *B. terrestris* workers were introduced with IAPV (n=10), PBS (n=10) as described above. Another groups of bees without any treatment were employed as

mock (n=10) control. For each sample, 7µl of collected hemolymph (with PTU) was added to 500µl 1×working solution (provided by the kit) with 5µl PI (provided by kit) and 5µl annexin V (provided by kit, BD Bioscience). Then the solution was transferred to a 5ml tubes and incubated at 37℃for 15min before analysis by flow cytometry.

2.5 Flow cytometry

A BD FACSVerse cytometer (BD Bioscience) with laser 488nm was used to examine the samples. PerCP- Cy5.5-A and FITC-A filters were used to evaluated the PI and FITC (labeled with WGA or Annexin V) signal, respectively. A total of 5000 events were collected for each sample and a threshold value of 25 in forward scatter (FSC) was applied to filter the smaller particles. Data of each sample was recorded by the BD FACs software. FCS files are further analyzed in FCS Express 6 Flow Cytometry software.

2.6 Injection of latex beads to block phagocytosis

Latex beads, polystyrene and with a 0.3 µm diameter mean particle size (Sigma) were washed and resuspended at 1× phosphate buffer saline (PBS) (corresponding to 0.1% solids (w/v)) (Elrod-Erickson et al., 2000). To see the effect of blocking phagocytosis on the IAPV induced mortality, *B.terrestris* workers (n=52) were injected with 5 µl of the beads solution 24h prior to virus infection. Another group of bees (n=48) was injected with same volume of PBS for control. After 24 hours, half of both beads injected bees (n=26) and PBS injected bees (n=24) were infected with IAPV as described above. The rest bees in both groups were injected with PBS for control. Mortality was recorded every day. To check the IAPV accumulation after beads injection, *B. terrestris* workers pre-injected with beads solution (n=12) and PBS (n=10) were injected with IAPV. Viral titers were measured in both fat body and brains at 3dpi.

2.7 RNA extraction, cDNA synthesis and qPCR

B. terrestris workers were put on wet ice for 5~10 min to immobilize before dissection and then brains and fat bodies were collected. Tissue RNA was extracted using the RNeasy mini kit (Qiagen, Venlo, the Netherlands). Five hundred µl of RLT buffer was used to lyse the fat body and brain cells in a tissues lyser with metal beads for 3 min in a 2.0 ML tube. Then the tissue mixture was centrifuged for 5 min at max speed and supernatant was transferred to a filter column (provided by the kit). The remaining steps were performed following the manufacturer's instructions. Genomic DNA was removed by using TURBO DNA-free kit (Ambion, Foster, CA). The quantity and quality of the RNA samples were evluated by a Nanodrop spectrophotometer and 1% agarose gel electrophoresis. Then RNA samples were stored at -80 °C for future use.

cDNA was synthesized with one microgram of RNA by the SuperScript II Reverse Transcriptase (Invitrogen, Waltham, MA) using oligo (dT) primers. qPCR was performed on a CFX Real-Time PCR detection system using GoTaq master mix (Promega, Madison, WI) as previous described. Two internal reference genes, peptidylprolyl isomerase A (PPIA) and 60S ribosomal protein L23 (RPL23), were introduced to normalize the qPCR data (Niu et al., 2014a). The performance of reference genes in each experiment was evaluated by the calculated M and CV value under the qBase frame work (Hellemans et al., 2007)

2.8 Statistics

One-way ANOVA with Tukey's multiple comparison or Kruskal-Wallis test with Dunn's multiple comparison were used for multiple groups mean comparison depending on the normality of the data sets. Unpaired two tailed student *t* test was used for IAPV RNQs comparison. Survival curves were plotted and analyzed by log-ranked analysis

(Kaplan-Meier method). Statistics was done within GraphPad Prism (v 7.02) (GraphPad software).

3. Result

3.1 IAPV infection induces hemocytes with higher PI staining and lower WGA staining

To look at the interaction between viral systemic infection and hemocytes composition, we first compared the particles concentration of hemolymph samples from individual bumblebee. Our results showed that virus infection has no impact on the particles concentration of hemolymph (Kruskal-Wallis test, χ^2=6.183, *p*=0.1031) (Figure 35). Then we looked at the staining patterns of these samples. We can differentiate two groups with different WGA staining in the non-treatment mock (Figure 36A) and PBS injected bees (Figure 36B). The majority of events were observed with high WGA staining, while some cells have less intense WGA staining (gated as G-1). These two groups of events represent viable hemocytes for they are negative for PI staining. A same staining pattern was also observed in the SBPV infected bees (Figure 36C). For

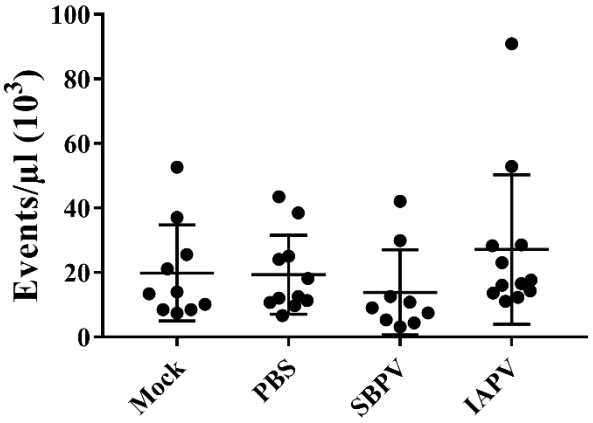

Figure 35. Concertation of particles in hemolymph. Virus infection did not have impact on the concentration of particles of hemolymph samples (Kruskal-Wallis test, χ^2=6.183, *p*=0.1031).

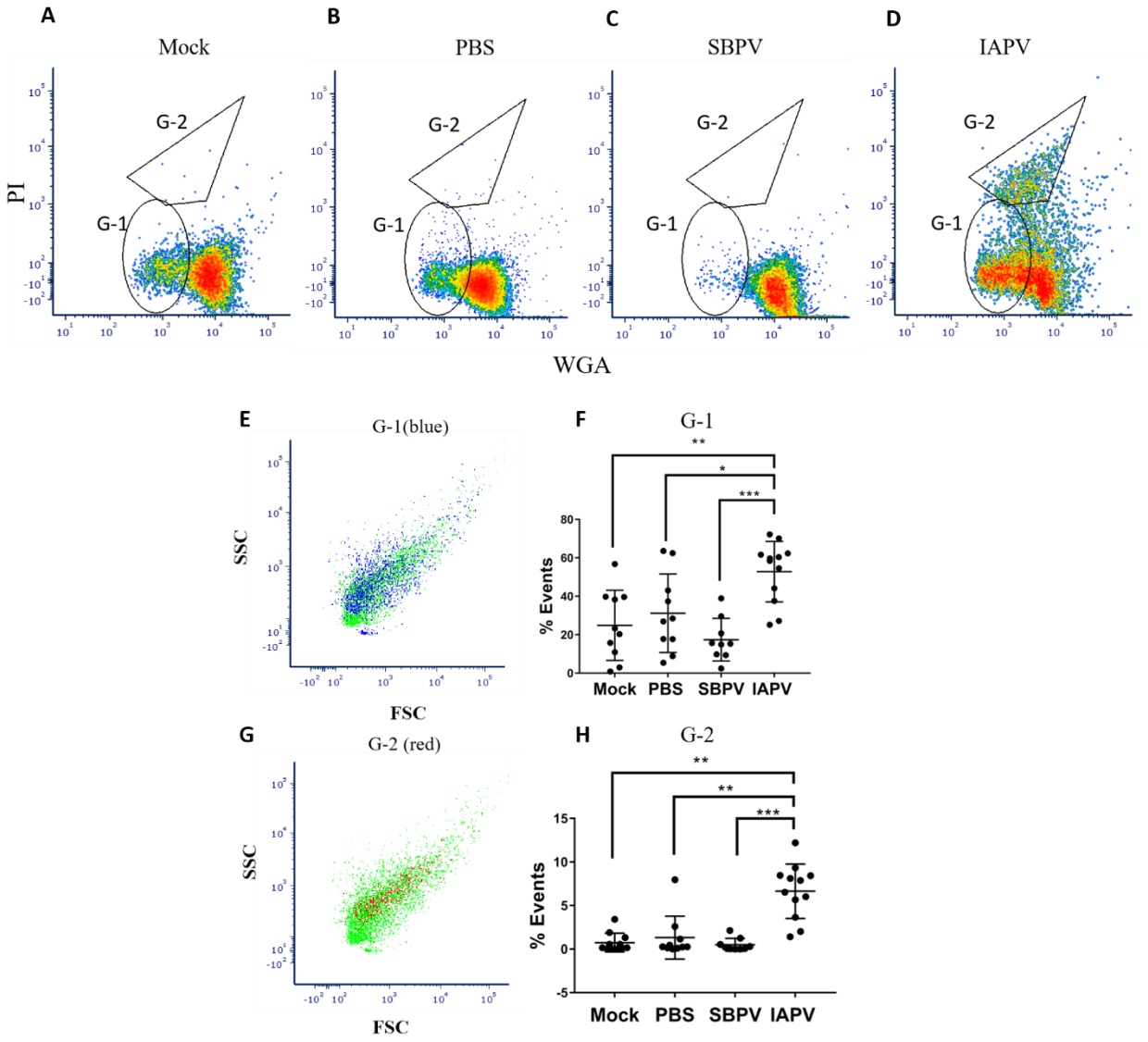

Figure 36. Hemocytes profiling at 3 days after infection (3dpi). (A-D), Density plots of hemocytes stained with PI (Y-axis) and WGA (X-axis). Figures show representatives of samples from four treatment group: Mock (n=10), PBS (n=10), SBPV (n=9) and IAPV (n=12). Gate-1 (G-1) highlights the WGA low and PI negative events. Gate-2 (G-2) highlights the PI positive events. **(E),** SSC vs FSC plots of same sample show in Figure 36D. Blue dots represent the events inside G-1 and green dots represent the other events. (**F),** Comparison of percentage of events in G-1 among four groups. *, ** and *** represent significant difference with *p* value < 0.05, <0.01 and <0.001. Significance was calculated by One-way ANOVA with Tukey's multiple comparison (F=9.453, *p*<0.0001). (**G),** SSC vs FSC plots of same sample show in Figure 2d. Red dots represent the events inside G-2 and green dots represent the other events. **(H),** Comparison of percentage of events in G-2 among four groups. ** and *** represent significant difference with p value < 0.01and < 0.001, respectively. Significance was calculated by Kruskal-Wallis test with Dunn's multiple comparison (χ^2=20, *p*<0.001).

IAPV infection, we saw a clear particles shift towards gate G-1, being WGA low stained cells (ANOVA with Tukey's multiple comparison, F= 9.453, P<0.0001) (Figure 36D). Also, a fraction of particles with PI positive staining (gated as G-2) was observed,

indicating that these cells are dead (Kruskal-Wallis test with Dunn's multiple comparison, χ^2=22, p<0.001). The SSC vs FSC plots, representing particle size and granularity (Figure 36E and G) are used to identify the corresponding particles associated with the different gates (low WGA staining and dead cells) of the same sample shown in Figure 36D. G-1 and G-2 gated events which are highlighted in blue and red, respectively (Figure 36E and G) show no particular difference in size or granularity compared to the ungated ones. Besides, we do notice that the smallest cells with minimal SSC and FSC are less represented by the gating. These results indicated that IAPV infection can induce hemocytes mortality and changes in membrane binding ability with lectin WGA.

3.2 Examination of hemocytes for the evidence of apoptosis/necrosis

We performed Annexin V staining to see if apoptosis or necrosis contribute to the IAPV induced hemocytes mortality. The fluorescence values of PI and Annexin V staining of hemolymph samples from individual bumblebee is shown in Figure 37. Quadrants

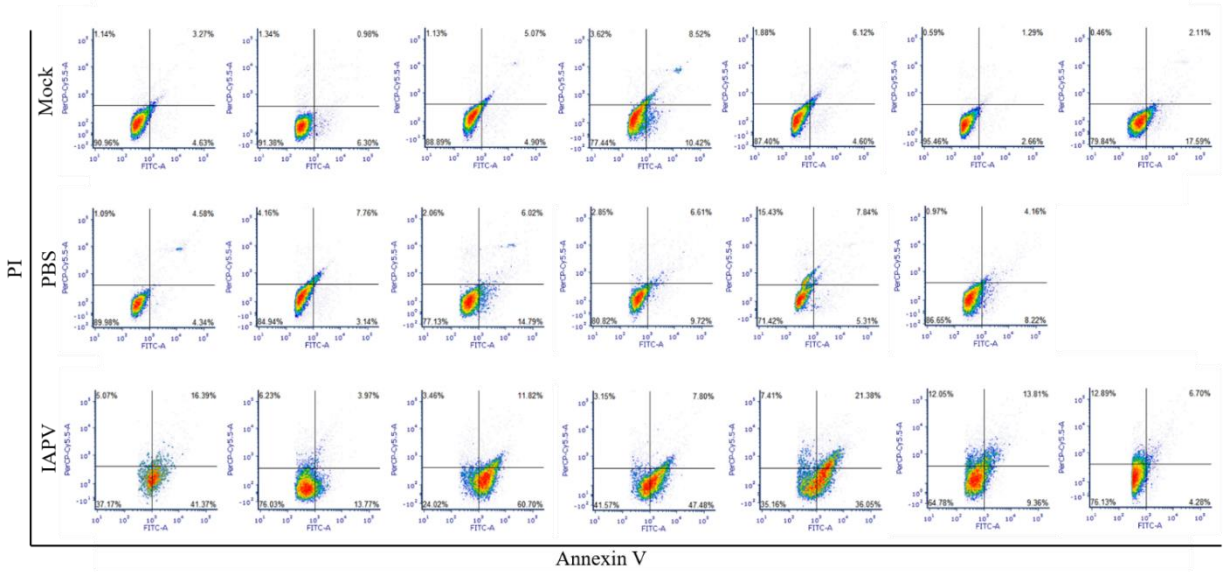

Figure 37. **Bumblebee hemocytes staining by Annexin V and PI.** Hemolymph collected from individual bee treated with IAPV (n=7), PBS (n=6) and non-treatment mock (n=7) at 3dpi was probed with both PI and annexin V and then examined by flow cytometry. Fluorescent measurement obtained from each sample were shown in the PI vs annexin V plot.

were made based on the PI and Annexin V staining pattern of mock samples which are considered as baseline for apoptosis detection. The majority of cells from non-treatment mock and PBS bees are in the lower left quadrant indicating they are not stained with either PI or Annexin V. In the IAPV infected samples, more PI and Annexin V positive hemocytes (upper right quadrant) were observed (ANOVA with Tukey's multiple comparison, F=6.815, *P*=0.0067) (Figure 38B), which is evidence for necrosis

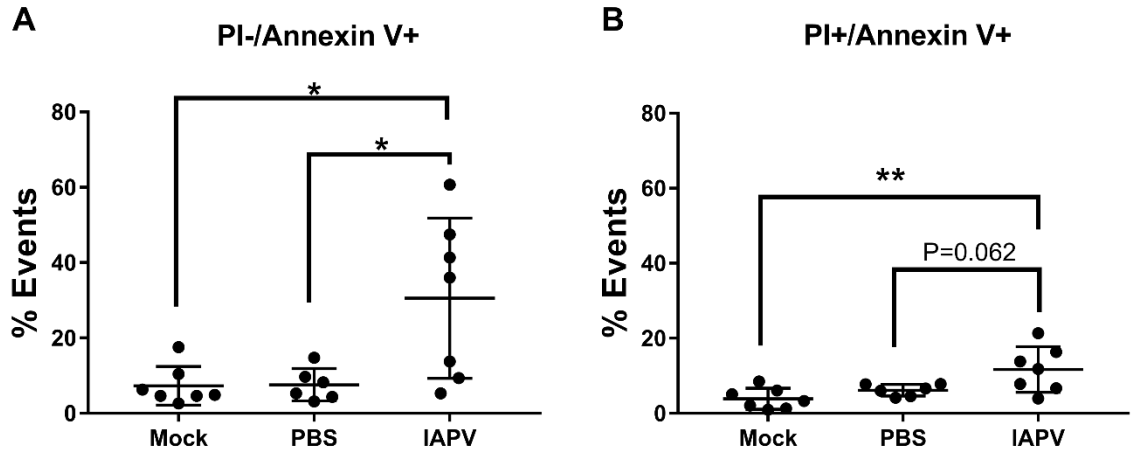

Figure 38. **Percentage of events in the upper right quadrant (PI+/annexin V+) and lower right quadrant (PI-/annexin V+) shown in Figure 37**. **A.** Comparison of percentage of events in the lower right quadrant (PI-/annexin V+) among three treatment groups, mock (n=7), PBS (n=6) and IAPV (n=7). *, ** represent significant difference with *p* value <0.01. Significance was calculated by One-way ANOVA with Tukey's multiple comparison, F=6.991, *P*=0.0061. **B**. Comparison of percentage of events in the upper right quadrant (PI+/annexin V+) among three treatment groups, mock (n=7), PBS (n=6) and IAPV (n=7). ** represent significant difference with *p* value <0.01. Significance was calculated by One-way ANOVA with Tukey's multiple comparison, F=6.815, *P*=0.0067.

(Lamiable et al., 2016). While we did not observe a clear sub-population of cells with only Annexin V staining, which is the typical evidence for apoptosis. Although in the IAPV infected samples, more cells showed a general higher annexin V staining (ANOVA with Tukey's multiple comparison, F=6.991, *P*=0.0061) (Figure 38A), we do not recognize this as conclusive evidence of apoptosis after IAPV infection. As annexin V staining is a snapshot of the dynamics process of the cells losing their membrane integrity towards complete permeability, it is unrealistic to have one population having lost the membrane integrity while not observing a subpopulation being PI positive.

3.3 Exploration of the involvement of phagocytosis upon IAPV infection

One of the main function of hemocytes is phagocytosis which is a conserved cellular defense targeting bacterial, yeast, apoptotic bodies and abiotic particles like synthetic beads (Lavine and Strand, 2002). Whether phagocytosis can contribute to the antiviral immune defense of bumblebee is unclear. Injecting of latex beads into the insect hemocoel blocks the phagocytosis and provides a convenient way to address the

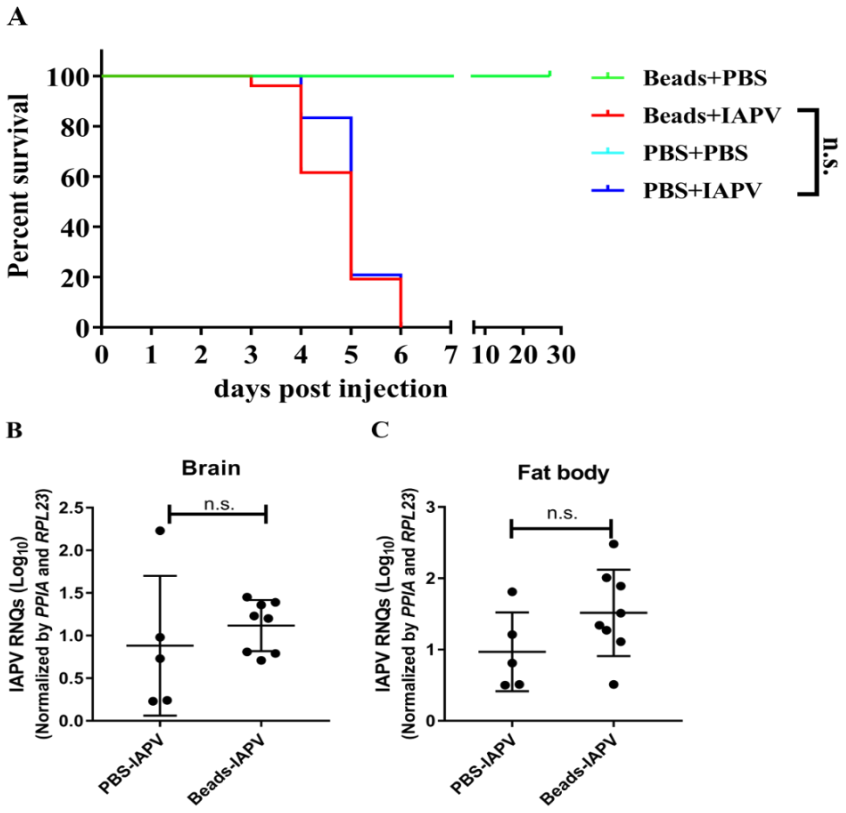

Figure 39. **Effect of latex beads injection on IAPV induced mortality and viral accumulation. A.** Survival of bumblebee workers injected with latex beads or PBS 1 day before challenged with IAPV infection. (log-ranked analysis (Kaplan-Meier method) was used to calculated the significance between groups. **B.** IAPV RNQs at 3 dpi in brains after beads injection and IAPV infection. **C** IAPV RNQs at 3 dpi in fat body after beads injection and IAPV. Significance was calculated by unpaired two tailed student *t* test.

contribution of hemocytes in the host defense (Lamiable et al., 2016). Here, we preinjected latex beads into *B. terrestris* workers and study its effect on the mortality and viral loads after IAPV challenges. Our results showed that beads injection did not affect the survival of bumblebee workers following challenges with IAPV (Figure 39A). Virus infected bees (both beads injected and non-beads injected) were all dead within

6 days after infection, while non-virus infected controls were still alive four weeks after treatment (Figure 39A). Also, beads injection did not result in significant increase of IAPV titers in either brains (Figure 39B) or fat bodies (Figure 39C).

4. Discussion

4.1 Hemocytes mortality induced by IAPV

Our results revealed that a part of the *B. terrestris* hemocytes cell membrane become permeabilized and their nuclei get accessible to PI after IAPV but not SBPV infection, indicating that these cells are damaged or dying. This is likely due to cell necrosis induced after IAPV infection, while the occurrence of apoptosis is not clear in our set up. Virus infection can induce apoptosis/necrosis in insect cells (Clem, 2016; Hay and Kannourakis, 2002; Lamiable et al., 2016), and this process can be visualized by flow cytometry using Annexin V and PI counterstaining (Fan et al., 2013; Lamiable et al., 2016; Marringa et al., 2014). Annexin V binds to the translocated phosphatidylserine (PS) which is a hallmark of apoptosis. In our experiment, Annexin V staining was performed on freshly extracted hemocytes from individual bumblebee. We did not observe apoptosis in the hemocytes. Apoptosis is reported as a host strategy to prevent cells to rupture resulting in the release of viral particles which can then infect new cells (Clem, 2016; Ocampo et al., 2013). But apoptosis in immune cells is less reported and it is not clear whether this sacrifices is beneficial to the host or virus. In *Drosophila,* it is reported that apoptosis of hemocytes can induce shift of host immune status characterized by e.g. more lamellocytes differentiation and induction of Toll pathways, leading to a pro-inflammatory state (Arefin et al., 2015). This indicated that the apoptosis of certain hemocytes types may be expected if changes in hemocytes composition is needed, when confronting certain stresses.

We observed a shift towards lower WGA staining (G-1) in the hemolymph of IAPV infected bumblebee compared to the others. WGA recognizes N-acetylglucosamine (GlcNAc) residues in protein-linked glycans (Burger and Goldburg, 1967) and is often used as a cell membrane probe for tracking insect hemocytes, especially plasmatocytes (Castillo, Robertson, and Strand, 2006; Mortimer et al., 2012; Tirouvanziam et al., 2003). The lower WGA staining may suggest a decreased protein glycosylation on the target cell membrane. Knowing the important role that protein N-glycosylation plays in the cellular mediated defense such as encapsulation (Mortimer et al., 2012), hence the decrease of this protein and lower WGA staining reflect an altered functionality of the hemocytes. One possibility is a host response to the virus. But, this response is not present in SBPV infected bees, although this chronic virus can also replicate and reach high viral titers (Niu. et al., 2016a). An alternative explanation would be that the IAPV infection impairs hemocytes functioning and thereby cellular immunity.

4.2 Hemocytes types vs honeybee

In a recent study, Marringa *et al*., differentiated permeabilized cells (stained with both PI and WGA), plasmatocyes (stained with WGA only) and acellular objects (unstained) from honeybee hemolymph by flow cytometry analysis using PI/WGA staining (Marringa et al., 2014). In our non-challenged mock samples, we mainly observed two groups of cells, i.e. the high- and low- WGA staining cells which correspond to the plasmatocytes and unstained microparticles in Marringa's report, respectively. While the PI permeabilized cells can only be found in our hemolymph samples from IAPV infected bees. We therefore hypothesized that these permeabilized cells observed in Marringa's report may be groups of damaged cells under different conditions, which is a consequence of different sampling strategy. In our case, experiments were

performed on young bees with fixed age (~7 days old) and same nutritional status (see M & M), thus the healthy condition of tested bees is well controlled. While in the report of Marringa *et al*., tested honeybees were randomly sampled from hive, leading to a variable healthy condition due to potential factors such as age, nutritional and pathogenic status. This variability of healthy condition may result in different permeability of hemocytes to PI staining (Hillyer et al., 2005; Hillyer and Strand, 2014; Negri et al., 2015). However, cell typing is not an easy task and requires the utilization of different techniques. Flow cytometry, providing population details, together with typical microscopy analysis may generate more convincing results of hemocytes composition under different conditions. While one should always be careful when correlating data between these two techniques, as the cell population observed by flow cytometry may not be accurately identified by microscope. To reuse cells after cell sorting for further microscopy analysis would provide direct morphological information of same population of cells that seen on the flow cytometry.

4.3 Phagocytosis

Phagocytosis is a major cellular mediated immune defense and has been proved to contribute to the antiviral immunity of *Drosophila melanogaster* against DCV, CrPV and FHV infection (Lamiable et al., 2016; Nainu et al., 2015). In this study, we blocked the phagocytosis of *B. terrestris* to study its involvement in host antiviral defense against IAPV by injection of latex beads. Our results showed that blocking of phagocytosis did not decrease the mortality of workers or increase IAPV loads in tissues, indicating that phagocytosis may not play a major role against IAPV infection. However, studies of *Drosophila* also showed that the involvement of phagocytosis in the antiviral immunity is virus-specific, indicating its potential in dealing with other viruses (Lamiable et al., 2016). Besides, we cannot rule out that the phagocytosis is

not sufficiently blocked for lacking a reliable phagocytosis index. We tried to establish a measurement of phagocytosis by using pHrodo probes, a pH sensitive probe that can fluoresce brightly after pH decreases in active phagosomes. The pHrodo probe labeled to bioparticles (e.g. heat killed *E. coli*, which can be phagocytosed) can be utilized to detect the power of phagocytosis (Lombardo et al., 2013; Miksa et al., 2009; Simons, 2010; Tartaro et al., 2015). However, in our set up we failed to detect an obvious increase of the fluorescence after injection of latex beads by flow cytometry (data not shown). This may be due to the insufficient uptake of pHrodo labeled bioparticles or because the phagosome does not mature into a phagolysosome which provides the optimal acid condition for the probe to fluoresce. Therefore, looking for alternatives of measuring phagocytosis ability in bumblebees is crucial to setup conclusive experiments.

Chapter Ⅶ: Conclusions and future perspectives

1. General conclusion

When studying host-virus interaction one needs to have a clear insight in the limits and assets of one's study system. Within insects several model species are known. The best studied model is the fruit fly, which initially is not used only as a model to study insects, but rather in molecular genetics, being a utile tool with a short generation time and massive off-spring (Jennings, 2011). Honorable second place goes to mosquitos, the vector of many human pathogens and parasites including *Plasmodium* which is the infection agent of Malaria, causing massive human casualties (Barillas-Mury, Wizel, and Han, 2000; Benelli and Mehlhorn, 2016; Gubler, 1998). Entomologists embraced the gained knowledge and could apply it for their own specific interests and scientific questions. In the case of beneficial insects, like bees, the interest in immunity is also linked with the multifactorial problem of bee decline. Immunity is a host defense with costs and benefits, interacting with drivers of declines (see 1.2 in chapter I). This brings us to the first problem when studying host-virus relations: a bee lives in "the real world". It is exposed to biotic and abiotic factors, it is in competition with other bee species, it hosts micro-organisms like bacteria, viruses and eukaryotic parasites. The interactions between a host and these microbes can range between mutualism, commensalism, and parasitism. To study host-virus interactions one must have clear hypotheses before stepping into such complex environments with confounding factors and season variations. These hypotheses can be derived from the study of model insects with lab experiment. Apparently, we are not there yet for the bees, as we cannot just copy & paste the knowledge gained from other model insects. A bee is not a fly, with two pairs of wings instead of one pair and more cute colors. They are simply different animals. Genomic comparisons reveal that the bee immune repertoire is reduced compared to the flies (Barribeau et al., 2015).

This was initially explained by the presence of an extra layer of immunity (i.e. social immunity), as the first genomic information was that of social bees. But as the immune repertoire of solitary bees is also reduced (Barribeau et al., 2015), the need for an own model system in bees is clear. The bumblebee could meet this demand. For *B. terrestris,* feasible rearing techniques are developed, depriving the bee from any contact with the outside world. The adult bee has clear yellow bands, while a newly emerged worker within a colony has a white version instead, at least for one day. Hence, a stock with age fixed bees can be easily obtained. In this dissertation, we used *B. terrestris* workers to study the relation with IAPV. When studying virus-host interactions in insects, a distinction between local and systemic infection needs to be made. Insects have an open circulatory system, which means that infection can go systemic after entering the hemocoel. While a local infection is situated in a specific tissue lining with the outside environment. Viral infection is notorious when being systemic, we therefore first looked for a feasible way to cause systemic infections in the bumblebees. A benefit of the oral infection methodology is that it resembles more closely the natural way of infection. The injection method, although potentially present in bees (discussed in Chapter II), is more artificial.

1.1 Systemic IAPV infection after feeding and injection

We showed that under laboratory conditions, both feeding and artificial injection of Israeli acute paralysis virus (IAPV) can induce systemic infections in bumblebee (*Bombus terrestris*). The oral feeding resulted in high variation among biological replicates, while low doses of virus injections resulted in uniform symptomology and tissue tropism. Based on these results, we therefore used injection to further study the effects of virus infection on different immune pathways of the bees. We do, however, not exclude the usefulness of oral delivery which will have its assets related to other

biological questions. For instance, the breaking of the local immune defense (e.g. epithelial barrier) by viruses, towards a systemic infection invoking clear pathology.

1.2 IAPV tissues infection pattern and paralysis symptoms

While studying IAPV tissues tropism, we noticed some specific symptoms in the acute infected bees. Paralysis symptoms were reported in the honeybee, yet we also observed crippled/immobilized forelegs, prior to the typical symptom of body trembling shortly before death. The onset of these symptoms gave us clear predictive framework, as bees with symptoms would be dead several hours later, while symptomless bees would survive for a day or more. We hypothesized to see clear differences in viral titer and hoped to see relations with specific tissues, highlighting its importance in the virus pathology. However, both symptomatic bees and asymptomatic bees showed similar patterns in IAPV tissues accumulation (brain, midguts, ovary and fat body) and localization (brain), indicating that the viral tissue infection pattern does not contribute to the occurrence of paralysis symptoms.

1.3 The involvement of *Bt*SVC against virus infection

*Bt*SVC represent a specific case in which bee immunity could be differentiated from that of the model insects. Vago, a member of the SVC protein family plays a crosstalk role between the siRNA pathway and Jak/Stat pathway (Deddouche et al., 2008; Paradkar et al., 2012). Both pathways are recruited by the insect immune system upon virus infection. Different arthropods often have multiple SVC proteins, while in most bee species, including *B. terrestris*, there is only one SVC protein identified, whom function is uncharacterized. We could prove the presence of 2 of the 3 specific functional characters of vago, which have been identified in flies and mosquitos (Table 7). One is the antiviral character and the another is the Dicer-2 dependent expression. The cross-linking function with the Jak/Stat pathway could not be proved, but it may

be because we lack a clear end-marker of this pathway upon virus (see 1.3.1 chapter I).

Table. 7. The function of SVC gene in different insect species towards virus infection

	Bumblebees[a,b]	**Flies**[c]	**Mosquitos**[d,e]	**Shrimps**[f,g]
Responding to virus infection	down-regulated[a,b]	up-regulated[c]	up-regulated	up-regulated
Antiviral involvement	yes	yes	yes	?
Links with Dcr2	yes	yes	yes	yes
Links with Jak/Stat	?	?	yes	?
Other links	AMPs	?	?	?

[a,] this study; [b] Niu et al., 2016b; [c] Deddouche et al., 2008; [d] Paradarka et al., 2012
[c] Paradarka et al., 2014; [f] Chen et al., 2011; [g,] Li et al., 2015; "?", indicate undetermined information or lack of data.

We also recorded two unexpected phenomena, one is the down regulation of *BtSVC* upon IAPV infection in different tissues; and two is that silencing *BtSVC* can lower the expression of four antimicrobial peptides (AMP)-coding genes in fat body. Thus, we concluded that SVC in bees can be involved in both host antiviral immunity and AMPs expression. This potential involvement in multiple immune pathways may compensate a smaller immune repertoire of bees. Besides, our results also indicate that the SVCs in the model insects (e.g. flies and mosquitos) are worth of revisiting and a cross species study is needed to fully understand the role that SVC family play in the host immune activities, especially towards the clearance of virus infection.

1.4. The involvement of AMPs against virus infection

The link with *BtSVC* and AMP expression connected viral sensing and anti-viral defenses with typical innate bacterial immune responses. Indeed, the induction of AMPs after viral infection is not universal and generally considered to be a secondary effect of viral infections. The fact that *Bt*SVC, which is involved in antiviral activity against IAPV, can also be involved in the antimicrobial peptides (AMPs) expression

lead to the hypothesis that IAPV can directly induce AMPs expression through the crosstalk function. We tested this and could prove that *hymenoptaecin* is induced after IAPV infection at 1 dpi, and its trend is still visible at 3 dpi. This induction is virus-specific because neither injection of SBPV nor dsGFP can result in similar induction. However, silencing *BtSVC* did not result in different *hymenoptaecin* expression upon IAPV. Therefore, the crosstalk function of SVC towards AMPs regulation upon virus invasion is not clear in our setup and needs more study. Here AMP expression dynamics at earlier time-points would also be valuable.

1.5 The involvement of cellular defense upon IAPV infection

Not able to prove the speculative idea of direct triggering of AMP by viruses directed us to the more traditional explanation. Herein it is believed that viral infections can trigger general inflammation responses, through inducing cell lysis, or as a host defense in cleaning-up the apoptotic bodies to prevent further viral spreading (see chapter VI and chapter VII). This territory is largely unexplored in bee immunity and scarce in insect immunity. Because of lacking cell lines to test some basic assumption of necrotic and apoptotic effects of IAPV on host cells, we decided to explore if cellular immunity is recruited upon virus infection. This question, not directly solving any link between SVCs and viruses and AMP, was rather to bring a new insight into anti-viral defenses in bees. Indeed, within the antiviral immune signaling pathways, the cellular immunity will probably play a prominent role which deserves more studies. Hemocytes, known as the circulating cells in the hemocoel, are the main component of cellular immunity. We used the changes of hemocytes profile as a proxy of responses of cellular immunity to virus infection. By using flow cytometry analysis, we found that IAPV infection is linked with hemocytes mortality and decreased lectin (WGA) binding activity. While SBPV infection has no obvious impact on the hemocytes composition.

This comparison with SBPV infection is useful as this virus causes chronic infection after injection (Niu. et al., 2016a). Second, we tried to infer if phagocytosis, the main cellular immune activity mediated by hemocytes, can be involved in the anti-viral defenses of bees. Our result showed that beads injection (to saturate phagocytosis) did not increase bee mortality nor IAPV titers (in tissues of brains and fat body), thereby we were not able to prove the involvement of phagocytosis in host antiviral defense towards IAPV infection. However, the blocking of phagocytosis in our experiment remained black box, as we lack a reliable method to measure the blocking effect. Thus, further study is needed to establish a reliable method of measuring the phagocytosis ability, which can not only be used as a confirmation of latex beads injection but also a useful indicator of cellular immune responses (see 2.7 in this chapter).

2. Future perspectives

Within this dissertation, we exposed new defense mechanisms within bumblebees to combat against virus infections. It is clear that aside the antiviral defense system RNAi, other pathways also assist to keep viral infection under control. Here we discuss where our results brought us, and look on what's to come. Also, what our result could mean for real bees, meaning those who fly outside and are not poked with needles to get infected with viruses.

2.1 The downstream activation of *Bt*SVC

In Chapter IV we established the antiviral character of *BtSVC* with *in vivo* experiments in bumblebees. This SVC protein is also well conserved in other bees, thus we speculate that its antiviral activity is also well preserved. Further study to identify the antiviral function of SVC in other bee species is encouraged. Special interest should go to the down-stream activation of bee SVC upon virus infection. In *Culex* mosquitos,

*Cq*vago is reported to activate the Jak/Stat pathway to control WNV infection (Paradkar et al., 2014). Although our results failed to establish links between *Bt*SVC and Jak/Stat pathway, we can presume that this link also exists in bees. Niu et al., (2016) did find a relation between *BtSVC* and *Bthop* of the Jak/Stat pathway and silencing *Bthop* resulted in higher SBPV titers (Niu et al., 2016b). However, whether this link between *Bt*SVC and Jak/Stat pathway is through the ligand binding of Domeless, the only identified Jak/Stat receptor in insects to date, is unclear. Previous experiment in mosquitos clearly showed that the silencing of *Domeless* did not have an effect on the antiviral function of *Cq*vago, indicating an unknown receptor linked with Jak/Stat signaling may exist. Therefore, further studies in bumblebee (or other bee species) are required to 1) investigate the relation between *Bt*SVC and Domeless, 2) identify alternative Jak/Stat receptor and 3) provide information on if *Bt*SCV serve the ligand of this receptor.

Our results also suggested links between *Bt*SVC and AMPs, placing *Bt*SVC as a potential regulator targeting multiple immune pathways including the NF-κB signaling pathways. So far there is no report showing SVC can be linked with NF-κB signaling pathways like Toll and IMD. While in *D. melanogaster*, several SVCs including *Dm*vago (CG2081, CG2444, CG31997 and CG14132) (Sheldon et al., 2007) are reported to be responsive to bacterial infection. Moreover, *Bt*SVC acid amino sequence is closely related to CG31997 (see chapter 4). Thus, further studies towards identifying the role of NF-κB pathways in the antiviral defense of bumblebee and the interaction with *Bt*SVC are required.

2.2 Systemic immune communicator?

In mosquito, there is evidence showing *Cq*vago is secreted and has an interferon (IFN)-like cytokine function (Paradkar et al., 2012). In mammalian cells, IFNs are a

multifunctional family of cytokines that can be induced in virus infected cells by engagement of viral molecules with pattern recognition receptors (PRRs) and induce innate immune responses in infected cells and neighboring cells through the Jak/Stat pathway (Fleming, 2016; Raftery and Stevenson, 2017). It is not clear whether SVC in bumblebee can also follow a similar secretion manner. However, we do know that the signal peptide at the N-terminal side of SCV is conserved and therefore direction toward the secretory pathway is possible (Niu et al., 2016b). To prove this, further experiments on SVC protein level are required. Here we listed the potential experimental procedure and few things worth noting towards this direction (Figure 40).

Throughout our work, we mainly observed reduced expression of *BtSVC* after IAPV infection. While virus infection in flies and mosquitos normally resulted in increased SVC expression (Deddouche et al., 2008; Paradkar et al., 2012). Following the expression of *Bt*SVC at protein level will give a better insight in its expression dynamics. Here the choice of tissues to follow is important. Our results observed the functional role of *Bt*SVC in fat body, thus fat body is proposed to produce and secrete *Bt*SVC upon virus infection. Hemolymph is another important tissue to check for it is often associated with the systemic immune responses. These two tissues are key resources of *Bt*SVC and link the protein with systemic immune responses. Besides, gut, trachea, secretory tract can also be sources if *Bt*SVC is responsive in local immunity, thus a detection of base line expression of SVC in bee tissues is also helpful.

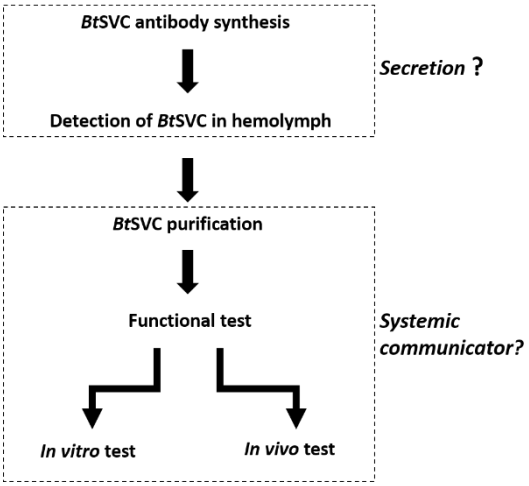

Figure. 40 Experimental procedure to further study *Bt*SVC.

Temporal responses in relation to different stressors (e.g. bacterial infection, age, nutritional status…) will give further insight about the diversified role suggested by its influence on multiple targets (our results) and expression profile of multiple SVCs in *D. melanogaster* (Sheldon et al., 2007). Ultimately to understand which stressor are related with *Bt*SVC expression and if it is restricted to immune stressors or if it has a broader function. Thus, pure *Bt*SVC is needed and this can be accomplished by the protein expression system, for instance by the insect cell-bacolovirus system. Purified *Bt*SVC can then be used for function verification. Two levels of test are highly recommended, one is *in vitro, Bt*SVC can be directly added to the cell cultural medium. Then the cell mortality and viral titers can be observed after infection, but also its influence on the RNA levels or protein expression. However, lacking a cell line for bee species is a major issue. Considerable effort has been done to make bee cell lines, with some publications showing successful results (Carrillo-Tripp et al., 2016; Goblirsch, Spivak, and Kurtti, 2013). However, when these cells were cultivated by the broader scientific community, the initial good performance was quickly lost. Using other cell lines e.g. S2, may be helpful to check if the antiviral function of *Bt*SVC is conserved between species but may not give direct conclusion when negative results are observed. *In vivo* tests can be performed, especially if expression profiles of *Bt*SVC in hemolymph has been observed. For example, if *Bt*SVC is observed to be induced in the hemolymph upon virus infection, then purified *Bt*SVC can be injected into the host hemocoel prior to viral infection, to see the effect of pre-activation of SVC mediated antiviral activity on virus infection.

2.3 Local immunity and the natural infection route

Injection of few viral particles quickly led to bee mortality, while at least 2×10^7 virus particles are needed to have similar effect when feeding IAPV. These results indicated

that initial infection routes are critical for virus pathogenesis. Singh et al. (2010) presented that virus transmission from infected honeybees towards bumblebees was probably occurring by oral/fecal transmission routes though sharing floral resources (Singh et al., 2010). These infections did not result in overt symptoms in bees, therefor it seems that an immune response is initiated following the oral infection, not clearing the viruses, but keeping it under control. In honeybees, it has been well described how covert infection (without clear symptomology) can change into overt infection with obvious symptoms. Here the ectoparasite *Varroa destructor* often plays an important role. When the mite punctures the adult or pupae; viruses are directly delivered into the host hemocoel, circumventing local immune systems and directly exposing internal tissues under viral infection. The presence of mites breaks the normal virus-host dynamics and makes it beneficial to virus infection. Therefore, future study of viral infection in bumblebee and other wild bee species may not only focus on the already balanced virus-bee interactions, but also the potential balance breaker(s) which can be parasites and other species that closely interact with bees. Such studies can also be very helpful to reveal the naturally infected route of IAPV in bumblebees, especially towards the occurrence of overt infection. Without a better understanding of the IAPV infection route in the nature, it is difficult to determine the tissue tropism and related immune responses (both local and systemic).

2.4. AMPs regulation upon viral infection, a response to inflammation?

The induction of AMPs after virus infection is considered to be a secondary effect caused by virus infection and not by direct virus sensing. In chapter V, we tried to prove that the AMPs induction can be regulated by *Bt*SVC, an antiviral modulator that function after direct virus sensing by Dicer-2. Unfortunately, silencing *BtSVC* did not impact the *hymenoptaecin* induction upon IAPV infection. Therefor we predicted other

immune pathways associated with these secondary effects needed to be present. In Chapter VI, we showed that the IAPV infection is linked with hemocytes mortality and changes of hemocytes membrane staining pattern. These changes in hemolymph may activate a chain of reactions, which is also associated with the production of AMPs (Zambon et al., 2005). One theory is that, infected hemocytes/tissue cells and cells undergoing apoptosis can be recognized as aberrant and targeted by the hemocyte for phagocytosis. Other infected cell that are not recognized by hemocytes are lysed due to virus replication, releasing internal cellular compounds (e.g. endogenous DNA) into the hemocoel and may activate the Toll/IMD (Zambon et al., 2005) (Figure 41). The activated Toll/IMD can then increase the production of AMPs which are secreted

into hemolymph, a signal of systemic infection. The enhanced AMPs production can in turn activate more hemocytes cells to clean the cell debris and eliminate the infected cells more efficiently (Figure 41). Here hemocytes play a critical part in the surveillance of healthy and damaged cell membranes and send signal to fat body cells as well. Once the cell is recognized as abnormal, hemocytes can be activated to produce cytokine like receptor upd 3 and Spaetzle (Spz) to activate the Jak/Stat and Toll pathways in fat body cells, resulting in the production of AMPs (Agaisse et al., 2003; Panayidou and Apidianakis, 2013). Thus, the loss of these important immune cells may not only result in an impaired cellular activity such as phagocytosis and encapsulation but can also significantly reduce host systemic immune communication

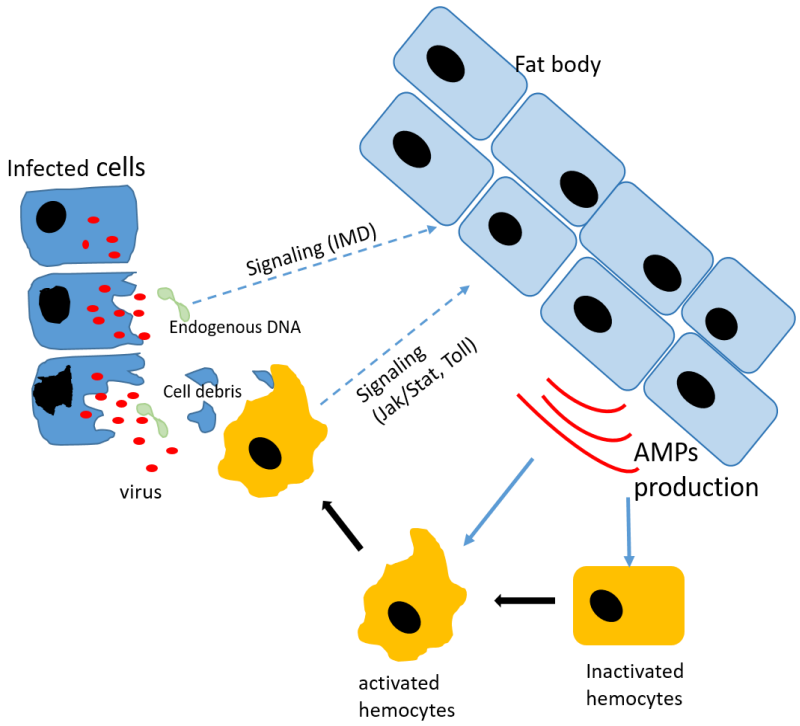

Figure 41. Model for the involvement of AMPs in the antiviral defense of bumblebee. Viral replication in the infected cells leads to apoptosis or cell lysis. Cell lysis release internal cellular components and debris. Released material can then signal to activate IMD and Toll pathways in the fat body and local cellular responses (e.g. phagocytosis). Activated hemocytes signal to activate Jak/Stat and Toll pathways in the fat body cells. The activated Toll and IMD in the fat body result in the production of AMPs which are secreted into the hemolymph and cause global activation of cellular responses. More activated hemocytes enhance the cellular mediated activity and clean up the infected cells more efficiently. Purple arrows indicate the signaling to activate humoral responses. Blue arrows indicate the signaling to activate the cellular responses. Figure restyled from (Zambon *et al.*, 2005).

as well. This may explain why injection of low amounts of IAPV can induce an acute infection in a short period, while injection of SBPV does not.

2.5 New strategy in hemocytes typing?

To date, our understanding of cellular defense in insect antiviral activity is very limited. One major issue is the uncertainty of hemocytes composition (e.g. types, numbers). Here it is difficult to give uniform morphological descriptions of insect hemocytes, due to different development stages and functionalities associated. The insect hemocyte profile can be dynamic over different species and even within the same species, a large variation is noticed determining on age, sex, nutritional status, pathogen infections, etc. (Lavine and Strand, 2002; Negri et al., 2015). The traditional strategy of studying hemocytes composition mainly includes microscope-based hemocytes differentiation and number counting, which can be subjective and time consuming. Such basic descriptive study is needed in different bees. However, changes of hemocytes activity (e.g. membrane activity, metabolic activity) which can be important indicators of hemocytes condition, are often not detected when using this traditional method. Thus, additional strategies are required towards effective and comprehensive surveillance of hemocytes composition. The utilization of flow cytometry may well serve this purpose. Flow cytometry allows real-time analysis of cellular composition, cell signaling, and other relevant immunological pathways, thus providing an accessible tool for rapid diagnostic and assessment (Abraham and Aubert, 2016; Ahluwalia, Wallace, and Peereboom, 2012). The combination of flow cytometry with microscopy have potential to be used as a routine strategy when typing cells. Here flow cytometry with cell sorting can sort hemocytes based on their staining property (often an evidence of similar function) and scatter plots, allowing to further analyze the fractioned cell types under microscope for morphology. This will help us to recognize

hemocytes from both functional level and morphological level. One difficulty of this strategy is to correlate results between the two techniques. This requires cell reviving after flow cytometry to cultivate enough cells for the following microscopy test. However, the staining performance and flow cytometry analysis may have adverse effect on the cells and lead to low productivity of cell reviving. Therefore, direct characterization by flow cytometry would be better. However, a recent study in the honeybee showed a high within samples variation when using PI/WGA counterstaining to differentiate hemocytes (Marringa et al., 2014). This calls for an improvement of the current methodology of using flow cytometry for hemocytes categorization in insect, here we give our suggestions in this direction,

1. Standardized samples. We presume that the high variation observed from individual samples may be a consequence of different bee's condition. Therefore, standardizing the bee condition will be crucial to reduce inter samples variability. This can be easily achieved by using age, nutrition and microclimate conditioned individual bumblebees.

2. Cell based staining strategy. The staining strategy of insect hemocytes is still very primitive. This is mainly because of lacking information of cell membrane proteins (e.g. glycoproteins) for labeling. In mammalian cells, the combination of multiple antibody targeting different membrane proteins is routinely used for blood cells differentiation by flow cytometry (Starkey et al., 1988; Terstappen et al., 1990). To achieve this in insects, the first step may be the identification of extracellular protein profile of hemocytes by RNA-Seq or proteome analysis. Based on these profiles, a detailed categorization can be started. Here fluorescence microscopy and polychromatic flow cytometry are needed to determine the best markers combination when differentiating hemocytes cells.

2.6 Diagnostics of bee health?

Within bee research, there is a great interest to have a health indicator which can be very useful when studying the effect of drivers for bee decline in real world. One direction here is to find universal biomarker (indicator) through RNA-Seq, proteomics and metabolomics analysis. Many research groups are engaged in this direction. However, the bee hemocytes profile can also be a potential description of host health condition, which value is largely ignored. By using standardized hemocytes profiling methods (described in 2.5 of this chapter), a screening of subpopulation of hemocytes based on their membrane staining patterns (with fluorescent (antibody) markers) can be setup. These results will form a basis of hemocytes marker set which can be used for hemocytes profiling. To develop a routine diagnostic method, correlation study between hemocytes profiles and different stresses is needed. This requires the examination of large numbers of hemocytes samples under standardized conditions (age, nutritional status, pathogen infection, microclimates…), establishing a hemocytes profile data bank. Polychromatic flow cytometry analysis will first run on samples with single stressors exposed in lab conditions, but later on supplemented with profiles of bees from different environmental conditions. Now the data banking can really start, sampling bees from different environment, determining their hemocyte profile and measuring their parasite and virus infection profile, and also other biotic and abiotic factors associated with their environment. Such databases should ultimately lead toward a bee health passport which is useful to study stressor and synergy of stressor in bee decline (Figure 42).

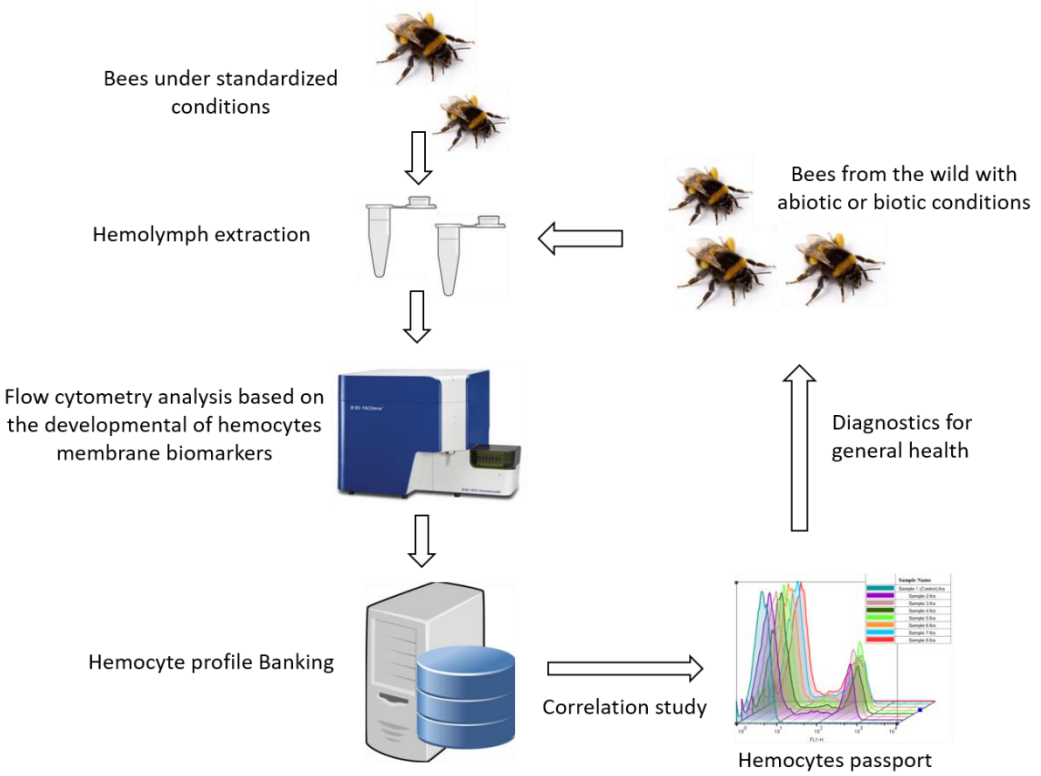

Figure 42 Establishment of a hemocytes profile data bank and passport

2.7 Phagocytosis index.

Aside from hemocyte typing and measuring changes, studying their actual functions will gain more insight in their role in immunity. Hemocytes mediated phagocytosis is the main activity of these linked with immunity (Lamiable et al., 2016; Nainu et al., 2015). In *Drosphila*, flies with genetic depletion of hemocytes (hemocytes loss) can be used for functional study of phagocytosis (Lamiable et al., 2016). In other insects, physical methods, e.g. injection of latex beads are often used to block phagocytosis. No matter which kind of blocking methods is used, a valid way of measuring blocking efficiency is needed. However, such information is missing in most studies (including ours in chapter 5). Here we listed two proposed strategies for potential phagocytosis measurement.

Using phrodo probe

pH-rodo, a kind of pH sensitive probe, is non-fluorescent outside the cell but fluorescent brightly in the phagolysosome (Figure 43). Therefore, the pHrodo-labeled bio-particles (e.g. hest killed *E. coli*) can be used to detect the power of phagocytosis (Bahrini et al., 2015; Tartaro et al., 2015). The mechanism is simple: bio-particles are aiming to induce phagocytosis however if the hemocytes are already occupied by, for instance, pre-injection of latex beads, the following bio-particles injection cannot induce equal phagocytosis (to non-pre-injection of beads), resulting in a decreased fluorescence. The decreased fluorescence can be used as a phagocytosis index. However, when applying this method *in vivo*, we did not find obvious fluorescence changes by using flow cytometry (data not shown). One possibility is that the phagosome does not mature into phagolysosome which can digest the up-taken particles, thus lacking the optimal acid condition for the pH-rodo probes to fluorescent.

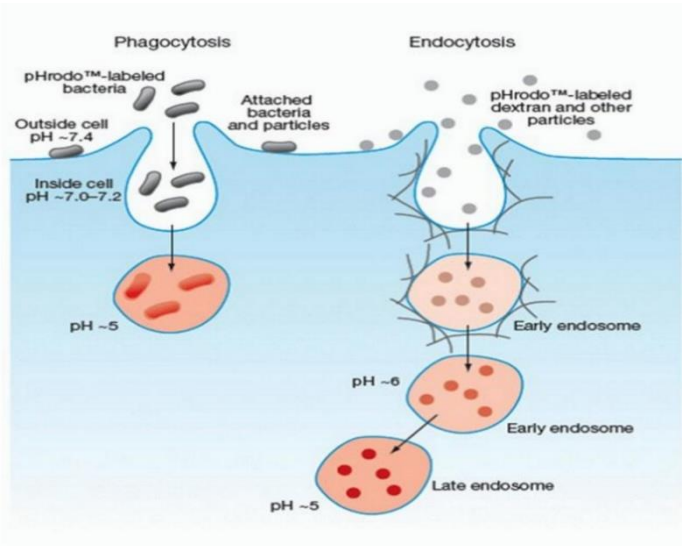

Figure 43. Schematic of pHrodo™ dye-based Detection of Phagocytosis and Endocytosis
Particles (microorganisms or other bio molecules) labeled with pHrodo™ dye are added to cells. Some remain in solution or become non-specifically attached to cell—they do not fluoresce because of the neutral pH of the extracellular environment. Some are taken up by phagocytosis or endocytosis and become encapsulated in vesicles. As vesicles are processed, pH decreases and the pHrodo™ -labeled particles fluoresce brightly.

Using flow cytometry and fluorescent beads

Another method is to use fluorescent beads. The strategy is also simple: the injected fluorescent beads (Starkey et al.) are phagocytosed by living hemocytes which is highlighted by fluorescent staining of either nuclei or cytoplasm. Then by using flow

cytometry, it allows to sort cells undergoing phagocytosis (events with red and green) and those do not (events green).

$$\textbf{\textit{Phagocytosis index (PI)}} = \frac{\textbf{\textit{Events(Red+Green)}}}{\textbf{\textit{All Events}}} \textbf{\textit{ \%}}$$

Then phagocytosis index can be calculated as the percentage of double fluorescent events in total events. However, this method may not reflect the real phagocytosis events for the fluorescent beads attached to the hemocytes can also be considered as taken up.

References List

Abraham, R.S. and Aubert, G., 2016. Flow Cytometry, a Versatile Tool for Diagnosis and Monitoring of Primary Immunodeficiencies. Clin Vaccine Immunol 23, 254-71.

Agaisse, H., Petersen, U.-M., Boutros, M., Mathey-Prevot, B. and Perrimon, N., 2003. Signaling Role of Hemocytes in Drosophila JAK/STAT-Dependent Response to Septic Injury. Developmental Cell 5, 441-450.

Ahluwalia, M.S., Wallace, P.K. and Peereboom, D.M., 2012. Flow cytometry as a diagnostic tool in lymphomatous or leukemic meningitis: ready for prime time? Cancer 118, 1747-53.

Allen, M.F. and Ball, B.V., 1995. Characterisation and serological relationships of strains of Kashmir bee virus. Ann. Appl. Biol. 126, 471-484.

Amann, R.I., Binder, B.J., Olson, R.J., Chisholm, S.W., Devereux, R. and Stahl, D., 1990. Combination of 16S rRNA-targeted oligonucleotide probes with flow cytometry for analyzing mixed microbial populations. Applied and environmental microbiology 56, 1919-1925.

Arefin, B., Kucerova, L., Krautz, R., Kranenburg, H., Parvin, F. and Theopold, U., 2015. Apoptosis in Hemocytes Induces a Shift in Effector Mechanisms in the Drosophila Immune System and Leads to a Pro-Inflammatory State. PloS one 10, e0136593.

Arrese, E.L. and Soulages, J.L., 2010. Insect fat body: energy, metabolism, and regulation. Annual review of entomology 55, 207-225.

Avadhanula, V., Weasner, B.P., Hardy, G.G., Kumar, J.P. and Hardy, R.W., 2009. A novel system for the launch of alphavirus RNA synthesis reveals a role for the Imd pathway in arthropod antiviral response. PLoS pathogens 5, e1000582.

Azzami, K., Beier, H., Ritter, W. and Tautz, J., 2012. Infection of honey bees with acute bee paralysis virus does not trigger humoral or cellular immune responses. Arch Virol 157, 689-702.

Bahrini, I., Song, J.H., Diez, D. and Hanayama, R., 2015. Neuronal exosomes facilitate synaptic pruning by up-regulating complement factors in microglia. Sci Rep 5, 7989.

Bailey, L. and Ball, B.V., 1991. Honey bee pathology. American Press, London.

Bailey, L., Gibbs, A.J. and Wood, R.D., 1963. Two viruses from adult honey bees (*Apis mellifera* Linnaeus). Virology 21, 390-395.

Bailey, L. and Milne, R.G., 1969. The multiplication regions and interaction of acute and chronic bee-paralysis viruses in adult honey bees. The Journal of general virology 4, 9-14.

Bailey, L. and Woods, R.D., 1974. Three previously undescribed viruses from the honey bee. J. Gen. Virol. 25, 175-186.

Barillas-Mury, C., Wizel, B. and Han, Y.S., 2000. Mosquito immune responses and malaria transmission: lessons from insect model systems and implications for vertebrate innate immunity and vaccine developmen. Insect biochemistry and molecular biology 30, 429-442.

Baron, G.L., Raine, N.E., Brown, M.J.F. and Osborne, J., 2014. Impact of chronic exposure to a pyrethroid pesticide on bumblebees and interactions with a trypanosome parasite. Journal of Applied Ecology 51, 460-469.

Barribeau, S.M., Sadd, B.M., du Plessis, L., Brown, M.J., Buechel, S.D., Cappelle, K., Carolan, J.C., Christiaens, O., Colgan, T.J., Erler, S., Evans, J., Helbing, S., Karaus, E., Lattorff, H.M., Marxer, M., Meeus, I., Napflin, K., Niu, J., Schmid-Hempel, R., Smagghe, G., Waterhouse, R.M., Yu, N., Zdobnov, E.M. and Schmid-Hempel, P., 2015. A depauperate immune repertoire precedes evolution of sociality in bees. Genome biology 16, 83.

Bates, D., Mächler, M., Bolker, B. and Walker, S., 2015. Fitting Linear Mixed-Effects Models Usinglme4. J Stat Softw 67.

Benelli, G. and Mehlhorn, H., 2016. Declining malaria, rising of dengue and Zika virus: insights for mosquito vector control. Parasitol Res 115, 1747-54.

Blanchard, P., Ribiere, M., Celle, O., Lallemand, P., Schurr, F., Olivier, V., Iscache, A.L. and Faucon, J.P., 2007. Evaluation of a real-time two-step RT-PCR assay for quantitation of Chronic bee paralysis virus (CBPV) genome in experimentally-infected bee tissues and in life stages of a symptomatic colony. Journal of virological methods 141, 7-13.

Boncristiani, H.F., Evans, J.D., Chen, Y., Pettis, J., Murphy, C., Lopez, D.L., Simone-Finstrom, M., Strand, M., Tarpy, D.R. and Rueppell, O., 2013. In vitro infection of pupae with Israeli acute paralysis virus suggests disturbance of transcriptional homeostasis in honey bees (Apis mellifera). PloS one 8, e73429.

Boncristiani, H.F., Jr., Di Prisco, G., Pettis, J.S., Hamilton, M. and Chen, Y.P., 2009. Molecular approaches to the analysis of deformed wing virus replication and pathogenesis in the honey bee, Apis mellifera. Virology journal 6, 221.

Bosco-Drayon, V., Poidevin, M., Boneca, I.G., Narbonne-Reveau, K., Royet, J. and Charroux, B., 2012. Peptidoglycan sensing by the receptor PGRP-LE in the *Drosophila* gut induces immune responses to infectious bacteria and tolerance to microbiota. Cell Host Microbe 12, 153-65.

Boulant, S., Stanifer, M. and Lozach, P.Y., 2015. Dynamics of virus-receptor interactions in virus binding, signaling, and endocytosis. Viruses 7, 2794-2815.

Brown, M.J., Loosli, R. and Schmid-Hempel, P., 2000. Condition-dependent expression of virulence in a trypanosome infecting bumblebees. Oikos 91, 421-427.

Brutscher, L.M., Daughenbaugh, K.F. and Flenniken, M.L., 2015. Antiviral Defense Mechanisms in Honey Bees. Curr Opin Insect Sci 10, 71-82.

Brutscher, L.M. and Flenniken, M.L., 2015. RNAi and Antiviral Defense in the Honey Bee. J Immunol Res 2015, 941897.

Buchon, N., Broderick, N.A., Poidevin, M., Pradervand, S. and Lemaitre, B., 2009. Drosophila intestinal response to bacterial infection: activation of host defense and stem cell proliferation. Cell Host Microbe 5, 200-11.

Buchona, N., Poidevinb, M., Kwonc, H.-M., Guilloua, A.L., Sottasa, V., Leec, B.L. and Lemaitrea, B., 2009. A single modular serine protease integrates signals from pattern-recognition receptors upstream of the *Drosophila* Toll pathway. Proceedings of the National Academy of Sciences of the United States of America 106, 12442–12447.

Burger, M.M. and Goldburg, A.R., 1967. Identification of a tumor-specific determinant on neoplastic cell surfaces. Proceedings of the National Academy of Sciences of the United States of America 57, 359-366.

Cameron, S.A., Lozier, J.D., Stange, J.P., Koch, J.B., Cordes, N., Solter, L.F. and Griswold, T.L., ,, 2011. Patterns of widespread decline in North American bumble bees. Proceedings of the National Academy of Sciences of the United States of America 108, 662-667.

Cappelle, K., Smagghe, G., Dhaenens, M. and Meeus, I., 2016. Israeli acute paralysis virus infection leads to an enhanced RNA interference response and not its suppression in the bumblebee *Bombus terrestris*. Viruses 8, 334.

Carrillo-Tripp, J., Dolezal, A.G., Goblirsch, M.J., Miller, W.A., Toth, A.L. and Bonning, B.C., 2016. In vivo and in vitro infection dynamics of honey bee viruses. Sci Rep 6, 22265.

Castillo, J.C., Robertson, A.E. and Strand, M.R., 2006. Characterization of hemocytes from the mosquitoes Anopheles gambiae and Aedes aegypti. Insect biochemistry and molecular biology 36, 891-903.

Chen, Y.H., Jia, X.T., Zhao, L., Li, C.Z., Zhang, S., Chen, Y.G., Weng, S.P. and He, J.G., 2011. Identification and functional characterization of Dicer2 and five single VWC domain proteins of *Litopenaeus vannamei*. Dev Comp Immunol 35, 661-71.

Chen, Y.P. and J.D., E., 2007. Historical presence of Israeli acute paralysis virus in the United States. Am. Bee J. 147, 1027-1028.

Chen, Y.P., Pettis, J.S., Collins, A. and Feldlaufer, M.F., 2006. Prevalence and transmission of honeybee viruses. Applied and environmental microbiology 72, 606-11.

Chen, Y.P., Pettis, J.S., Corona, M., Chen, W.P., Li, C.J., Spivak, M., Visscher, P.K., DeGrandi-Hoffman, G., Boncristiani, H., Zhao, Y., vanEngelsdorp, D., Delaplane, K., Solter, L., Drummond, F., Kramer, M., Lipkin, W.I., Palacios, G., Hamilton, M.C., Smith, B., Huang, S.K., Zheng, H.Q., Li, J.L., Zhang, X., Zhou, A.F., Wu, L.Y., Zhou, J.Z., Lee, M.L., Teixeira, E.W., Li, Z.G. and Evans, J.D., 2014. Israeli acute paralysis virus: epidemiology, pathogenesis and implications for honey bee health. PLoS pathogens 10, e1004261.

Chen, Y.P. and Siede, R., 2007. Honey Bee Viruses. Adv Virus Res 70, 33-80.

Cheon, H.M., Shin, S.W., Bian, G., Park, J.H. and Raikhel, A.S., 2006. Regulation of lipid metabolism genes, lipid carrier protein lipophorin, and its receptor during immune challenge in the mosquito *Aedes aegypti*. J Biol Chem 281, 8426-35.

Choi, I.K. and Hyun, S., 2012. Conserved microRNA miR-8 in fat body regulates innate immune homeostasis in *Drosophila*. Dev Comp Immunol 37, 50-4.

Choi, Y.S., Choo, Y.M., Lee, K.S., Yoon, H.J., Kim, I., Je, Y.H., Sohn, H.D. and Jin, B.R., 2008. Cloning and expression profiling of four antibacterial peptide genes from the bumblebee Bombus ignitus. Comp Biochem Physiol B Biochem Mol Biol 150, 141-6.

Christina, I.Z., SchuÈ tz, C.S., Katzenberger, J.D., Bauer, M. and Pankratz, M.J., 2002. Nutrient control of gene expression in *Drosophila*: microarray analysis of starvation and sugar-dependent response. The EMBO Journal 21, 6162-6173.

Clem, R.J., 2016. Arboviruses and apoptosis: the role of cell death in determining vector competence. The Journal of general virology 97, 1033-6.

Corbet, S.A., Fussel, M., Ake, R., Fraser, A., Gunson, C., Savage, A. and Smith, K., 1993. Temperature and the pollinating activity of social bees. Ecol Entomol 18, 17-30.

Core, A., Runckel, C., Ivers, J., Quock, C., Siapno, T., Denault, S., Brown, B., Derisi, J., Smith, C.D. and Hafernik, J., 2012. A new threat to honey bees, the parasitic phorid fly *Apocephalus borealis*. PloS one 7, e29639.

Costa, A., Jan, E., Sarnow, P. and Schneider, D., 2009. The Imd pathway is involved in antiviral immune responses in Drosophila. PloS one 4, e7436.

Cox-Foster D.L., Conlan S., Holmes, E.C., Palacios G., Evans J.D., Moran N.A., Quan P.L., Briese T., Hornig M., Geiser D.M., Martinson V., vanEngelsdorp D., Kalkstein A.L., Drysdale A., Hui J., Zhai J., Cui L., Hutchison S.K., Simons J.F., Egholm M., Pettis J.S. and W.I., L., 2007. A Metagenomic Survey of Microbes in Honey Bee Colony Collapse Disorder. Science 318, 283-287.

Dall, D.J., 1987. Multiplication of Kashmir bee virus in pupae of the honeybee, *Apis mellifera*. Journal of invertebrate pathology 49, 279-290.

Danihlík, J., Aronstein, K. and Petřivalský, M., 2016. Antimicrobial peptides: a key component of honey bee innate immunity. Journal of Apicultural Research 54, 123-136.

de Brito Sanchez, M.G., Lorenzo, E., Su, S., Liu, F., Zhan, Y. and Giurfa, M., 2014. The tarsal taste of honey bees: behavioral and electrophysiological analyses. Frontiers in behavioral neuroscience 8, 25.

de Graaf, D.C., Dauwe, R., Walravens, K. and Jacobs, F.J., 2002. Flow cytometric analysis of lectin-stained haemocytes

of the honeybee (Apis mellifera). Apidologie 33, 571-579.

De Luca, P.A. and Vallejo-Marin, M., 2013. What's the 'buzz' about? The ecology and evolutionary significance of buzz-pollination. Curr Opin Plant Biol 16, 429-35.

de Miranda, J.R., Cordoni, G. and Budge, G., 2010a. The Acute bee paralysis virus-Kashmir bee virus-Israeli acute paralysis virus complex. Journal of invertebrate pathology 103 Suppl 1, S30-47.

de Miranda, J.R., Dainat, B., Locke, B., Cordoni, G., Berthoud, H., Gauthier, L., Neumann, P., Budge, G.E., Ball, B.V. and Stoltz, D.B., 2010b. Genetic characterization of slow bee paralysis virus of the honeybee (Apis mellifera L.). The Journal of general virology 91, 2524-30.

Deddouche, S., Matt, N., Budd, A., Mueller, S., Kemp, C., Galiana-Arnoux, D., Dostert, C., Antoniewski, C., Hoffmann, J.A. and Imler, J.L., 2008. The DExD/H-box helicase Dicer-2 mediates the induction of antiviral activity in drosophila. Nature immunology 9, 1425-32.

DeGrandi-Hoffman, G. and Chen, Y., 2015. Nutrition, immunity and viral infections in honey bees. Current Opinion in Insect Science 10, 170-176.

Denholm, C.H. 1999. Inducible honey bee viruses associated with *Varroa jacobsoni*, Keele University, Keele, UK.

Di Prisco, G., Pennacchio, F., Caprio, E., Boncristiani, H.F., Jr., Evans, J.D. and Chen, Y., 2011. *Varroa destructor* is an effective vector of Israeli acute paralysis virus in the honeybee, *Apis mellifera*. The Journal of general virology 92, 151-155.

Ding, S.W., 2010. RNA-based antiviral immunity. Nat Rev Immunol 10, 632-44.

Dostert, C., Jouanguy, E., Irving, P., Troxler, L., Galiana-Arnoux, D., Hetru, C., Hoffmann, J.A. and Imler, J.L., 2005. The Jak-STAT signaling pathway is required but not sufficient for the antiviral response of drosophila. Nature immunology 6, 946-53.

El Chamy, L., Leclerc, V., Caldelari, I. and Reichhart, J.M., 2008. Sensing of 'danger signals' and pathogen-associated molecular patterns defines binary signaling pathways 'upstream' of Toll. Nature immunology 9, 1165-70.

Eleftherianos, I., Xu, M., Yadi, H., Ffrench-Constant, R.H. and Reynolds, S.E., 2009. Plasmatocyte-spreading peptide (PSP) plays a central role in insect cellular immune defenses against bacterial infection. J Exp Biol 212, 1840-8.

Elrod-Erickson, M., Mishra, S. and Schneider, D., 2000. Interactions between the cellular and humoral immune responses in *Drosophila*. Curr Biol 10, 781-784.

Engelhard, E.K. and Volkman, L.E., 1995. Developmental resistance in fourth instar *Trichoplusia ni* orally inoculated with *Autographa californica* m nuclear polyhedrosis virus. Virology 209, 384-389.

Erler, S., Popp, M. and Lattorff, H.M., 2011. Dynamics of immune system gene expression upon bacterial challenge and wounding in a social insect (Bombus terrestris). PloS one 6, e18126.

Fan, J., Xie, Y., Xue, J., Zhang, Y. and Yang, Q., 2013. Cellular apoptosis of hemocytes from Dendrolimus tabulaeformis Tsai et Liu larvae induced with the secondary metabolites of Beauveria brongniartii (Sacc.) Petch. PloS one 8, e71600.

Farris, S.M. and Sinakevitch, I., 2003. Development and evolution of the insect mushroom bodies: towards the understanding of conserved developmental mechanisms in a higher brain center. Arthropod Structure & Development 32, 79-101.

Fauser-Misslin, A., Sadd, B.M., Neumann, P., Sandrock, C. and Osborne, J., 2014. Influence of combined pesticide and parasite exposure on bumblebee colony traits in the laboratory. Journal of Applied Ecology 51, 450-459.

Ferreira, A.G., Naylor, H., Esteves, S.S., Pais, I.S., Martins, N.E. and Teixeira, L., 2014. The Toll-dorsal pathway is required for resistance to viral oral infection in *Drosophila*. PLoS pathogens 10, e1004507.

Fievet, J., Tentcheva, D., Gauthier, L., de Miranda, J., Cousserans, F., Colin, M.E. and Bergoin, M., 2006. Localization of deformed wing virus infection in queen and drone Apis mellifera L. Virology journal 3, 16.

Fleming, S.B., 2016. Viral Inhibition of the IFN-Induced JAK/STAT Signalling Pathway: Development of Live Attenuated Vaccines by Mutation of Viral-Encoded IFN-Antagonists. Vaccines (Basel) 4.

Flenniken, M.L. and Andino, R., 2014. Non-specific dsRNA-mediated antiviral response in the honey bee. PloS one 8, e77263.

Fujiyuki, T., Matsuzaka, E., Nakaoka, T., Takeuchi, H., Wakamoto, A., Ohka, S., Sekimizu, K., Nomoto, A. and Kubo, T., 2009. Distribution of Kakugo virus and its effects on the gene expression profile in the brain of the worker honeybee Apis mellifera L. Journal of virology 83, 11560-8.

Fürst, M.A., McMahon, D.P., Osborne, J.L., Paxton, R.J. and Brown, M.J., 2014. Disease associations between honeybees and bumblebees as a threat to wild pollinators. Nature 506, 364-366.

Galbraith, D.A., Yang, X., Nino, E.L., Yi, S. and Grozinger, C., 2015. Parallel epigenomic and transcriptomic responses to viral infection in honey bees (Apis mellifera). PLoS pathogens 11, e1004713.

Galiana-Arnoux, D., Dostert, C., Schneemann, A., Hoffmann, J.A. and Imler, J.L., 2006. Essential function in vivo for Dicer-2 in host defense against RNA viruses in drosophila. Nature immunology 7, 590-7.

Ganesan, S., Aggarwal, K., Paquette, N. and Silverman, N., 2011. NF-kappaB/Rel proteins and the humoral immune responses of Drosophila melanogaster. Curr Top Microbiol Immunol 349, 25-60.

Garibaldi, L.A., Steffan-Dewenter, I., Winfree, R. and Aizen, M.A., 2014. Wild pollinators enhance fruit set of crops regardless of honey bee abundance. Science 339, 1608-1611.

Genersch, E., Yue, C., Fries, I. and de Miranda, J.R., 2006. Detection of Deformed wing virus, a honey bee viral pathogen, in bumble bees (Bombus terrestris and Bombus pascuorum) with wing deformities. Journal of invertebrate pathology 91, 61-3.

Ghosh, R.C., Ball, B.V., Willcocks, M.M. and Carter, M.J., 1999. The nucleotide sequence of sacbrood virus of the honey bee: an insect picorna-like virus. The Journal of general virology 80, 1541-1549.

Gobert, V., Gottar, M., Matskevich, A.A., Rutschmann, S., Royet, J., Belvin, M., Hoffmann, J. and Ferrandon, D., 2003. Dual activation of the Drosophila Toll pathway by two pattern recognition receptors. Science 302, 2126-2130.

Goblirsch, M.J., Spivak, M.S. and Kurtti, T.J., 2013. A cell line resource derived from honey bee (Apis mellifera) embryonic tissues. PloS one 8, e69831.

Goldsworthy, G., Opoku-Ware, K. and Mullen, L., 2002. Adipokinetic hormone enhances laminarin and bacterial lipopolysaccharide-induced activation of the prophenoloxidase cascade in the African migratory locust, *Locusta migratoria*. Journal of insect physiology 48, 601-608.

Gottar, M., Gobert, V., Matskevich, A.A., Reichhart, J.M., Wang, C., Butt, T.M., Belvin, M., Hoffmann, J.A. and Ferrandon, D., 2006. Dual detection of fungal infections in Drosophila via recognition of glucans and sensing of virulence factors. Cell 127, 1425-37.

Goulson, D., 2003. Bumblebees, their behaviour and ecology Oxford University Press Inc. New York, United States.

Goulson, D., Lye, G.C. and Darvill, B., 2008. Decline and conservation of bumble bees. Annual review of entomology 53, 191-208.

Goulson, D., Nicholls, E., Botias, C. and Rotheray, E.L., 2015. Bee declines driven by combined stress from parasites, pesticides, and lack of flowers. Science 347, 1255957.

Gubler, D.J., 1998. Dengue and Dengue Hemorrhagic Fever. Clin Microbiol Rev 11, 480-496.

Gupta, A.P., 1985. Cellular elements in the hemolymph Pergamon Press,, New York.

Hakim, R.S., Baldwin, K. and Smagghe, G., 2010. Regulation of midgut growth, development, and metamorphosis. Annual review of entomology 55, 593-608.

Hay, S. and Kannourakis, G., 2002. A time to kill : viral manipulation of the cell death program. The Journal of general virology 83, 1547-1564.

Hedges, L.M. and Johnson, K.N., 2008. Induction of host defence responses by Drosophila C virus. The Journal of general virology 89, 1497-501.

Hellemans, J., Mortier, G., De Paepe, A., Speleman, F. and Vandesompele, J., 2007. qBase relative quantification framework and software for management and automated analysis of real-time quantitative PCR data. Genome biology 8, R19.

Heuer, C.M., Kollmann, M., Binzer, M. and Schachtner, J., 2012. Neuropeptides in insect mushroom bodies. Arthropod Struct Dev 41, 199-226.

Hillyer, J.F., Schmidt, S.L., Fuchs, J.F., Boyle, J.P. and Christensen, B.M., 2005. Age-associated mortality in immune challenged mosquitoes (Aedes aegypti) correlates with a decrease in haemocyte numbers. Cell Microbiol 7, 39-51.

Hillyer, J.F. and Strand, M.R., 2014. Mosquito hemocyte-mediated immune responses. Curr Opin Insect Sci 3, 14-21.

Imler, J.L., 2014. Overview of Drosophila immunity: a historical perspective. Dev Comp Immunol 42, 3-15.

Irving, P., Ubeda, J.M., Doucet, D., Troxler, L., Lagueux, M., Zachary, D., Hoffmann, J.A., Hetru, C. and Meister, M., 2005. New insights into Drosophila larval haemocyte functions through genome-wide analysis. Cell Microbiol 7, 335-50.

Jennings, B.H., 2011. Drosophila – a versatile model in biology & medicine. Materials Today 14, 190-195.

Jensen, R.A., 2001. Orthologs and paralogs - we need to get it right. Genome biology 2.

Kerr, J.T., Pindar, A., Galpern, P., Packer, L., Potts, S.G., Roberts, S.M., Rasmont, P., Schweiger, O., Colla, S.R., Richardson, L.L., Wagner, D.L., Gall, L.F., Sikes, D.S. and A., P., 2015. Climate change impacts on bumblebees converge across continents. Science 349, 177-180.

Kim, V.N., Han, J. and Siomi, M.C., 2009. Biogenesis of small RNAs in animals. Nat Rev Mol Cell Biol 10, 126-39.

Kingsolver, M.B., Huang, Z. and Hardy, R.W., 2013. Insect antiviral innate immunity: pathways, effectors, and connections. Journal of molecular biology 425, 4921-36.

Kleinjung, J., Romein, J., Lin, K. and Heringa, J., 2004. Contact-based sequence alignment. Nucleic Acids Res 32, 2464-73.

Lamiable, O., Arnold, J., de Faria, I.J., Olmo, R.P., Bergami, F., Meignin, C., Hoffmann, J.A., Marques, J.T. and Imler, J.L., 2016. Analysis of the Contribution of Hemocytes and Autophagy to Drosophila Antiviral Immunity. Journal of virology 90, 5415-26.

Lanot, R., Zachary, D., Holder, F. and Meister, M., 2001. Postembryonic hematopoiesis in Drosophila. Dev Biol 230, 243-57.

Lanzi, G., de Miranda, J.R., Boniotti, M.B., Cameron, C.E., Lavazza, A., Capucci, L., Camazine, S.M. and Rossi, C., 2006. Molecular and biological characterization of deformed wing virus of honeybees (Apis mellifera L.). Journal of virology 80, 4998-5009.

Lavine, M.D. and Strand, M.R., 2002. Insect hemocytes and their role in immunity. Insect biochemistry and molecular biology 32, 1295-1309.

Lee, P.E. and Furgala, B., 1965. Chronic bee paralysis virus in the nerve ganglia of the adult honey bee. Journal of invertebrate pathology 7, 170-174.

Lee, P.E. and Furgala, B., 1967. Viruslike particles in adult honeybee (*Apis mellifera* Linnaues). Virology 32, 11-17.

Lemaitre, B., 2004. Landmark: The road to Toll. Nat Rev Immunol 4, 521-527.

Lemaitre, B. and Hoffmann, J., 2007. The host defense of *Drosophila melanogaster*. Annu Rev Immunol 25, 697-743.

Levashina, E.A., Moita, L.F., Blandin, S., Vriend, G., Lagueux, M. and Kafatos, F.C., 2001. Conserved role of a complement-like protein in phagocytosis revealed by dsRNA knockout in cultured cells of the mosquito, *Anopheles gambiae*. Cell 104, 709-718.

Levitt, A.L., Singh, R., Cox-Foster, D.L., Rajotte, E., Hoover, K., Ostiguy, N. and Holmes, E.C., 2013. Cross-species transmission of honey bee viruses in associated arthropods. Virus research 176, 232-40.

Li, C., Li, H., Chen, Y., Chen, Y., Wang, S., Weng, S.P., Xu, X. and He, J., 2015. Activation of Vago by interferon regulatory factor (IRF) suggests an interferon system-like antiviral mechanism in shrimp. Sci Rep 5, 15078.

Li, J.L., Cornman, R.S., Evans, J.D., Pettis, J.S., Zhao, Y., Murphy, C., Peng, W.J., Wu, J., Hamilton, M., Boncristiani, H.F., Jr., Zhou, L., Hammond, J. and Chen,

Y.P., 2014. Systemic spread and propagation of a plant-pathogenic virus in European honeybees, Apis mellifera. mBio 5, e00898-13.

Li, Y., Xiang, Q., Zhang, Q., Huang, Y. and Su, Z., 2012. Overview on the recent study of antimicrobial peptides: origins, functions, relative mechanisms and application. Peptides 37, 207-15.

Li, Z., Chen, Y., Zhang, S., Chen, S., Li, W., Yan, L., Shi, L., Wu, L., Sohr, A. and Su, S., 2013. Viral infection affects sucrose responsiveness and homing ability of forager honey bees, Apis mellifera L. PloS one 8, e77354.

Lihoreau, M., Latty, T. and Chittka, L., 2012. An exploration of the social brain hypothesis in insects. Front Physiol 3, 442.

Locke, B., Forsgren, E., Fries, I. and de Miranda, J.R., 2012. Acaricide treatment affects viral dynamics in *Varroa destructor*-infested honey bee colonies via both host physiology and mite control. Applied and environmental microbiology 78, 227-235.

Lombardo, F., Ghani, Y., Kafatos, F.C. and Christophides, G.K., 2013. Comprehensive genetic dissection of the hemocyte immune response in the malaria mosquito Anopheles gambiae. PLoS pathogens 9, e1003145.

Longworth, M.S., Walker, J.A., Anderssen, E., Moon, N.S., Gladden, A., Heck, M.M., Ramaswamy, S. and Dyson, N.J., 2012. A shared role for RBF1 and dCAP-D3 in the regulation of transcription with consequences for innate immunity. PLoS Genet 8, e1002618.

Manley, R., Boots, M. and Wilfert, L., 2015. Emerging viral disease risk to pollinating insects: ecological, evolutionary and anthropogenic factors. The Journal of applied ecology 52, 331-340.

Maori, E., Lavi, S., Mozes-Koch, R., Gantman, Y., Peretz, Y., Edelbaum, O., Tanne, E. and Sela, I., 2007. Isolation and characterization of Israeli acute paralysis virus, a dicistrovirus affecting honeybees in Israel: evidence for diversity due to intra- and inter-species recombination. The Journal of general virology 88, 3428-3438.

Maori, E., Paldi, N., Shafir, S., Kalev, H., Tsur, E., Glick, E. and Sela, I., 2009. IAPV, a bee-affecting virus associated with Colony Collapse Disorder can be silenced by dsRNA ingestion. Insect Molecular Biology 1, 55-60.

Marringa, W.J., Krueger, M.J., Burritt, N.L. and Burritt, J.B., 2014. Honey bee hemocyte profiling by flow cytometry. PloS one 9, e108486.

Martin, S.J., Highfield, A.C., Brettell, L., Villalobos, E.M., Budge, G.E., Powell, M., Nikaido, S. and Schroeder, D.C., 2012. Global Honey Bee Viral Landscape Altered by a Parasitic Mite. Science 336, 1306-1306.

Martinson, V.G., Moy, J. and Moran, N.A., 2012. Establishment of characteristic gut bacteria during development of the honeybee worker. Applied and environmental microbiology 78, 2830-40.

McMahon, D.P., Fürst, M.A., Caspar, J., Theodorou, P., Brown, M.J. and Paxton, R.J., 2015. A sting in the spit: widespread cross-infection of multiple RNA viruses across wild and managed bees. The Journal of animal ecology 84, 615-624.

McMenamin, A.J. and Genersch, E., 2015. Honey bee colony losses and associated viruses. Current Opinion in Insect Science 8, 121-129.

Meeus, I., de Miranda, J.R., de Graaf, D.C., Wackers, F. and Smagghe, G., 2014. Effect of oral infection with Kashmir bee virus and Israeli acute paralysis virus on bumblebee (*Bombus terrestris*) reproductive success. Journal of invertebrate pathology 121, 64-69.

Menail, A.H., Piot, N., Meeus, I., Smagghe, G. and Loucif-Ayad, W., 2016. Large pathogen screening reveals first report of *Megaselia scalaris* (Diptera: Phoridae) parasitizing *Apis mellifera intermissa* (Hymenoptera: Apidae). Journal of invertebrate pathology 137, 33-7.

Merkling, S.H. and van Rij, R.P., 2013. Beyond RNAi: antiviral defense strategies in Drosophila and mosquito. Journal of insect physiology 59, 159-70.

Michener, C.D., 2007. The bees of the world, 2nd ed. John Hopkins University Press, 434 Baltimore.

Miksa, M., Komura, H., Wu, R., Shah, K.G. and Wang, P., 2009. A novel method to determine the engulfment of apoptotic cells by macrophages using pHrodo succinimidyl ester. J Immunol Methods 342, 71-7.

Mockel, N., Gisder, S. and Genersch, E., 2011. Horizontal transmission of deformed wing virus: pathological consequences in adult bees (Apis mellifera) depend on the transmission route. The Journal of general virology 92, 370-7.

Mommaerts, V., Reynders, S., Boulet, J., Besard, L., Sterk, G. and Smagghe, G., 2010. Risk assessment for side-effects of neonicotinoids against bumblebees with and without impairing foraging behavior. Ecotoxicology 19, 207-15.

Mommaerts, V., Wackers, F. and Smagghe, G., 2013. Assessment of gustatory responses to different sugars in harnessed and free-moving bumblebee workers (Bombus terrestris). Chemical senses 38, 399-407.

Mortimer, N.T., Kacsoh, B.Z., Keebaugh, E.S. and Schlenke, T.A., 2012. Mgat1-dependent N-glycosylation of membrane components primes Drosophila melanogaster blood cells for the cellular encapsulation response. PLoS pathogens 8, e1002819.

Müller., S., Matthiesen., S.H. and Nielsen., K.V. 2009. Preparation of FFPE Tissue Slides for Solid Tumor FISH Analysis. In: Kumar., G.L. and Rudbeck., L. (Eds),

Immunohistochemical (IHC) Staining Methods, Dako North America, California pp. 67-74.

Myles, K.M., Wiley, M.R., Morazzani, E.M. and Adelman, E.N., 2008. Alphavirus-derived small RNAs modulate pathogenesis in disease vector mosquitoes. Proceedings of the National Academy of Sciences of the United States of America 105, 19938–19943.

Nainu, F., Tanaka, Y., Shiratsuchi, A. and Nakanishi, Y., 2015. Protection of Insects against Viral Infection by Apoptosis-Dependent Phagocytosis. J Immunol 195, 5696-706.

Negri, P., Maggi, M., Ramirez, L., Szawarski, N., De Feudis, L., Lamattina, L. and Eguaras, M., 2015. Cellular immunity in Apis mellifera: studying hemocytes brings light about bees skills to confront threats. Apidologie 47, 379-388.

Nehme, N.T., Quintin, J., Cho, J.H., Lee, J., Lafarge, M.C., Kocks, C. and Ferrandon, D., 2011. Relative roles of the cellular and humoral responses in the Drosophila host defense against three gram-positive bacterial infections. PloS one 6, e14743.

Niu, J., Cappelle, K., de Miranda, J.R., Smagghe, G. and Meeus, I., 2014a. Analysis of reference gene stability after Israeli acute paralysis virus infection in bumblebees *Bombus terrestris*. Journal of invertebrate pathology 115, 76-79.

Niu, J., Meeus, I., Cappelle, K., Piot, N. and Smagghe, G., 2014b. The immune response of the small interfering RNA pathway in the defense against bee viruses. Current Opinion in Insect Science 6, 22-27.

Niu, J., Meeus, I. and Smagghe, G., 2016b. Differential expression pattern of Vago in bumblebee (*Bombus terrestris*), induced by virulent and avirulent virus infections. Sci Rep 6, 34200.

Niu., J., Smagghe., G., Coninck., D.I.D., Nieuwerburgh., F.V., Deforce., D. and Meeus., I., 2016a. In vivo study of Dicer-2-mediated immune response of the small interfering RNA pathway upon systemic infections of virulent and avirulent viruses in Bombus terrestris. Insect Biochemistry & Molecular biology 70, 127-137.

Ocampo, C.B., Caicedo, P.A., Jaramillo, G., Ursic Bedoya, R., Baron, O., Serrato, I.M., Cooper, D.M. and Lowenberger, C., 2013. Differential expression of apoptosis related genes in selected strains of Aedes aegypti with different susceptibilities to dengue virus. PloS one 8, e61187.

Otterstatter, M.C. and Thomson, J.D., 2007. Contact networks and transmission of an intestinal pathogen in bumble bee (Bombus impatiens) colonies. Oecologia 154, 411-21.

Otterstatter, M.C. and Whidden, T.L., 2004. Patterns of parasitism by tracheal mites (*Locustacarus buchneri*) in natural bumble bee populations. Apidologie 35, 351-357.

Palacios, G., Hui, J., Quan, P.L., Kalkstein, A., Honkavuori, K.S., Bussetti, A.V., Conlan, S., Evans, J., Chen, Y.P., vanEngelsdorp, D., Efrat, F., Pettis, J., Cox-Foster, D., Holmes, E.C., Briese, T. and W.I., L., 2008. Genetic Analysis of Israel Acute Paralysis Virus: Distinct Clusters Are Circulating in the United States. Journal of virology 82, 6209–6217.

Pan, X., Zhou, G., Wu, J., Bian, G., Lu, P., Raikhel, A.S. and Xi, Z., 2012. Wolbachia induces reactive oxygen species (ROS)-dependent activation of the Toll pathway to control dengue virus in the mosquito Aedes aegypti. Proceedings of the National Academy of Sciences of the United States of America 109, E23-31.

Panayidou, S. and Apidianakis, Y., 2013. Regenerative inflammation: lessons from Drosophila intestinal epithelium in health and disease. Pathogens 2, 209-31.

Paradkar, P.N., Duchemin, J.B., Voysey, R. and Walker, P.J., 2014. Dicer-2-dependent activation of Culex Vago occurs via the TRAF-Rel2 signaling pathway. PLoS Negl Trop Dis 8, e2823.

Paradkar, P.N., Trinidad, L., Voysey, R., Duchemin, J.B. and Walker, P.J., 2012. Secreted Vago restricts West Nile virus infection in *Culex* mosquito cells by activating the Jak-STAT pathway. Proceedings of the National Academy of Sciences of the United States of America 109, 18915-18920.

Park, C., Kang, H.S., Jeong, J., Kang, I., Choi, K., Yoo, M.S., Kim, Y.H., Kang, S.W., Lim, H.Y., Yoon, B.S. and Chae, C., 2016. In-situ Hybridization for the Detection of Sacbrood Virus in Infected Larvae of the Honey Bee (Apis cerana). J Comp Pathol 154, 258-62.

Parmentier, L., Smagghe, G., de Graaf, D.C. and Meeus, I., 2016. Varroa destructor Macula-like virus, Lake Sinai virus and other new RNA viruses in wild bumblebee hosts (Bombus pascuorum, Bombus lapidarius and Bombus pratorum). Journal of invertebrate pathology 134, 6-11.

Passarelli, A.L., 2011. Barriers to success: how baculoviruses establish efficient systemic infections. Virology 411, 383-92.

Peng, W., Li, J., Boncristiani, H., Strange, J.P., Hamilton, M. and Chen, Y., 2011. Host range expansion of honey bee Black Queen Cell Virus in the bumble bee, Bombus huntii. Apidologie 42, 650-658.

Piot, N., Snoeck, S., Vanlede, M., Smagghe, G. and Meeus, I., 2015. The effect of oral administration of dsRNA on viral replication and mortality in *Bombus terrestris*. Viruses 7, 3172-3185.

R Core Team. 2016. R: A language and environment for statistical computing, R Foundation for Statistical Computing, Vienna, Austria.

Raftery, N. and Stevenson, N.J., 2017. Advances in anti-viral immune defence: revealing the importance of the IFN JAK/STAT pathway. Cell Mol Life Sci 74, 2525-2535.

Ramirez, J.L. and Dimopoulos, G., 2010. The Toll immune signaling pathway control conserved anti-dengue defenses across diverse *Ae. aegypti* strains and against multiple dengue virus serotypes. Dev Comp Immunol 34, 625-9.

Ribeiro, C. and Brehelin, M., 2006. Insect haemocytes: what type of cell is that? Journal of insect physiology 52, 417-29.

Ronald, P.C. and Beutler, B., 2010. Plant and animal sensors of conserved microbial signatures. Science 330, 1061-1064.

Runckel, C., Flenniken, M.L., Engel, J.C., Ruby, J.G., Ganem, D., Andino, R. and DeRisi, J.L., 2011. Temporal analysis of the honey bee microbiome reveals four novel viruses and seasonal prevalence of known viruses, Nosema, and Crithidia. PloS one 6, e20656.

Ryabov, E.V., Wood, G.R., Fannon, J.M., Moore, J.D., Bull, J.C., Chandler, D., Mead, A., Burroughs, N. and Evans, D.J., 2014. A virulent strain of deformed wing virus (DWV) of honeybees (*Apis mellifera*) prevails after *Varroa destructor*-mediated, or in vitro, transmission. PLoS pathogens 10, e1004230.

Ryu, J.H., Kim, S.H., Lee, H.Y., Bai, J.Y., Nam, Y.D., Bae, J.W., Lee, D.G., Shin, S.C., Ha, E.M. and Lee, W.J., 2008. Innate immune homeostasis by the homeobox gene caudal and commensal-gut mutualism in *Drosophila*. Science 319, 777-782.

Ryu, J.H., Nam, K.B., Oh, C.T., Nam, H.J., Kim, S.H., Yoon, J.H., Seong, J.K., Yoo, M.A., Jang, I.H., Brey, P.T. and Lee, W.J., 2003. The homeobox gene caudal regulates constitutive local expression of antimicrobial peptide genes in *Drosophila epithelia*. Mol Cel Biol 24, 172-185.

Sabin, L.R., Hanna, S.L. and Cherry, S., 2010. Innate antiviral immunity in Drosophila. Current opinion in immunology 22, 4-9.

Sanchez-Contreras, M. and Vlisidou, I., 2008. The Diversity of Insect-bacteria Interactions and its Applications for Disease Control. Biotechnology and Genetic Engineering Reviews 25, 203-244.

Sanchez-Vargas, I., Scott, J.C., Poole-Smith, B.K., Franz, A.W., Barbosa-Solomieu, V., Wilusz, J., Olson, K.E. and Blair, C.D., 2009. Dengue virus type 2 infections of Aedes aegypti are modulated by the mosquito's RNA interference pathway. PLoS pathogens 5, e1000299.

Savina, A., Jancic, C., Hugues, S., Guermonprez, P., Vargas, P., Moura, I.C., Lennon-Dumenil, A.M., Seabra, M.C., Raposo, G. and Amigorena, S., 2006. NOX2 controls phagosomal pH to regulate antigen processing during crosspresentation by dendritic cells. Cell 126, 205-18.

Shah, K.S., Evans, E.C. and Pizzorno, M.C., 2009. Localization of deformed wing virus (DWV) in the brains of the honeybee, Apis mellifera Linnaeus. Virology journal 6, 182.

Sheldon, T.J., Miguel-Aliaga, I., Gould, A.P., Taylor, W.R. and Conklin, D., 2007. A novel family of single VWC-domain proteins in invertebrates. FEBS Lett 581, 5268-74.

Shen, M., Cui, L., Ostiguy, N. and Cox-Foster, D., 2005. Intricate transmission routes and interactions between picorna-like viruses (Kashmir bee virus and sacbrood virus) with the honeybee host and the parasitic varroa mite. The Journal of general virology 86, 2281-2289.

Simons, E.R., 2010. Measurement of phagocytosis and of the phagosomal environment in polymorphonuclear phagocytes by flow cytometry. Curr Protoc Cytom Chapter 9, Unit9 31.

Singh, R., Levitt, A.L., Rajotte, E.G., Holmes, E.C., Ostiguy, N., Vanengelsdorp, D., Lipkin, W.I., Depamphilis, C.W., Toth, A.L. and Cox-Foster, D.L., 2010. RNA viruses in hymenopteran pollinators: evidence of inter-Taxa virus transmission via pollen and potential impact on non-*Apis* hymenopteran species. PloS one 5, e14357.

Siu, R.W., Fragkoudis, R., Simmonds, P., Donald, C.L., Chase-Topping, M.E., Barry, G., Attarzadeh-Yazdi, G., Rodriguez-Andres, J., Nash, A.A., Merits, A., Fazakerley, J.K. and Kohl, A., 2011. Antiviral RNA interference responses induced by Semliki Forest virus infection of mosquito cells: characterization, origin, and frequency-dependent functions of virus-derived small interfering RNAs. Journal of virology 85, 2907-17.

Souza-Neto, J.A., Sim, S. and Dimopoulos, G., 2009. An evolutionary conserved function of the JAK-STAT pathway in anti-dengue defense. Proceedings of the National Academy of Sciences of the United States of America 106, 17841–17846.

Starkey, P.M., Sargent, I.L. and Redman, C.W.G., 1988. Cell populations in human early pregnancy decidua: characterization and isolation of large granular lymphocytes by flow cytometry. Immunology 65, 129-134.

Strand, M.R., 2008. The insect cellular immune response. Insect Science 15, 1-14.

Stuart, L.M. and Ezekowitz, R.A., 2005. Phagocytosis: elegant complexity. Immunity 22, 539-50.

Takahasia, K., Ochiaib, M., Horiuchia, M., Kumetaa, H., Oguraa, K., Ashidab, M. and Inagakia, F., 2009. Solution structure of the silkworm □GRP/GNBP3 N-terminal domain reveals the mechanism for □-1,3-glucan-specific recognition. Proceedings of the National Academy of Sciences of the United States of America 106, 11679-11684.

Tartaro, K., VanVolkenburg, M., Wilkie, D., Coskran, T.M., Kreeger, J.M., Kawabata, T.T. and Casinghino, S., 2015. Development of a fluorescence-based in vivo phagocytosis assay to measure mononuclear phagocyte system function in the rat. J Immunotoxicol 12, 239-46.

Tassetto, M., Kunitomi, M. and Andino, R., 2017. Circulating Immune Cells Mediate a Systemic RNAi-Based Adaptive Antiviral Response in Drosophila. Cell 169, 314-325 e13.

Terstappen, L., Johnsen, S., Segers-Nolten, I. and Loken, M.R., 1990. Identification and characterization of plasma cells in normal human bone marrow by high-resolution flow cytometry. Blood 76, 1739-1747.

Tirouvanziam, R., Davidson, C.J., Lipsick, J.S. and Herzenberg, L.A., 2003. Fluorescence-activated cell sorting (FACS) of *Drosophila* hemocytes reveals important functional similarities to mammalian leukocytes. Proceedings of the National Academy of Sciences of the United States of America 101, 2912-2917.

Tomancak, P., Beaton, A., Weiszmann, R., Kwan, E., Shu, S., Lewis, S.E., Richards, S., Ashburner, M., Hartenstein, V., Celniker, S.E. and Rubin, G.M., 2002. Systematic determination of patterns of gene expression during *Drosophila* embryogenesis. Genome biology 3, research0088.1–0088.14.

Valanne, S., Wang, J.H. and Ramet, M., 2011. The *Drosophila* Toll signaling pathway. J Immunol 186, 649-56.

van Rij, R.P., Saleh, M.C., Berry, B., Foo, C., Houk, A., Antoniewski, C. and Andino, R., 2006. The RNA silencing endonuclease Argonaute 2 mediates specific antiviral immunity in Drosophila melanogaster. Genes Dev 20, 2985-95.

Van Steenkiste, D., Raes, H. and Jacobs, F., 1988. Hemocytes of adult honey bees (*Apis mellifera*). Ann. Soc. R. Zool. Belgique, 234-235.

Vandesompele, J., De Preter, K., Pattyn, F., Poppe, B., Van Roy, N., De Paepe, A. and Speleman, F., 2002. Accurate normalization of real-time quantitative RT-PCR data by geometric averaging of multiple internal control genes. Genome biology 3, 0034.1.

Velthuis, H.H.W. and van Doorn, A., 2006. A century of advances in bumblebee domestication and the economic and environmental aspects of its commercialization for pollination. Apidologie 37, 421-451.

Wang, H., Meeus, I. and Smagghe, G., 2016. Israeli acute paralysis virus associated paralysis symptoms, viral tissue distribution and *Dicer-2* induction in bumblebee workers (*Bombus terrestris*). The Journal of general virology 97, 1981-1989.

Wang, X., Aliyari, R., Li, W., Li, H., Kim, K., Carthew, R., Atkinson, P. and Ding, S., 2006. RNA interference directs innate immunity against viruses in adult drosophila. Science 312, 452-454.

Washburn, J.O., Kirkpatrick, B.A. and Volkman, L.E., 1995. Comparative pathogenesis of *Autographa californica* m nuclear polyhedrosis virus in larvae of *Trichoplusia ni* and *Heliothis virescens* Virology 209, 561-568.

Washburn, J.O., Lyons, E.H., Haas-Stapleton, E.J. and Volkman, L.E., 1999. Multiple nucleocapsid packaging of *Autographa californica* nucleopolyhedrovirus accelerates the onset of systemic infection in *Trichoplusia ni*. Journal of virology 73, 411-416.

Williams, P.H. and Osborne, J.L., 2009. Bumblebee vulnerability and conservation world-wide. Apidologie 40, 367-387.

Wilson, R.C. and Doudna, J.A., 2013. Molecular mechanisms of RNA interference. Annu Rev Biophys 42, 217-39.

Xi, Z., Ramirez, J.L. and Dimopoulos, G., 2008a. The *Aedes aegypti* Toll Pathway Controls Dengue Virus Infection. PLoS pathogens 4.

Xi, Z., Ramirez, J.L. and Dimopoulos, G., 2008b. The *Aedes aegypti* toll pathway controls dengue virus infection. PLoS pathogens 4, e1000098.

Xu, J., Mon, H., Kusakabe, T., Li, Z., Zhu, L., Iiyama, K., Masuda, A., Mitsudome, T. and Lee, J.M., 2013. Establishment of a soaking RNA interference and Bombyx mori nucleopolyhedrovirus (BmNPV)-hypersensitive cell line using Bme21 cell. Applied microbiology and biotechnology 97, 10435-44.

Ye, T. and Zhang, X., 2013. Involvement of Ran in the regulation of phagocytosis against virus infection in S2 cells. Dev Comp Immunol 41, 491-7.

Yue, D., Nordhoff, M., Wieler, L.H. and Genersch, E., 2008. Fluorescence *in situ* hybridization (FISH) analysis of the interactions between honeybee larvae and *Paenibacillus larvae*, the causative agent of American foulbrood of honeybees (*Apis mellifera*). Environmental microbiology 10, 1612-1620.

Zaidman-Remy, A., Herve, M., Poidevin, M., Pili-Floury, S., Kim, M.S., Blanot, D., Oh, B.H., Ueda, R., Mengin-Lecreulx, D. and Lemaitre, B., 2006. The *Drosophila* amidase PGRP-LB modulates the immune response to bacterial infection. Immunity 24, 463-73.

Zambon, R.A., Nandakumar, M., Vakharia, V.N. and Wu, L.P., 2005. The Toll pathway is important for an antiviral response in *Drosophila*. Proceedings of the National Academy of Sciences of the United States of America 102, 7257-7262.

Zhu, F. and Zhang, X., 2013. The Wnt signaling pathway is involved in the regulation of phagocytosis of virus in Drosophila. Sci Rep 3, 2069.

Summary

Bumblebees (*Bombus spp*.), key pollinators of many agricultural crops and wild flowers across the globe and essential for a balance ecosystem, are declining at an alarming rate. Causes for this loss are complex and thought to be a combined effect of multiple stressors. The recent emerging of RNA viruses in bumblebees caught scientific attention for its notorious reputation in another well-known pollinator species, *Apis mellifera*. This calls for a comprehensive understanding of the interaction between these viruses and the bumblebee host. In this thesis, we mainly applied lab experiments to investigate: 1) the symptom and tissues infection pattern of Israeli acute paralysis virus (IAPV) in bumblebee *Bombus terrestris* workers; 2) the involvement of host innate immune system in the antiviral defense activity.

Under laboratory conditions, oral feeding and artificial injection are two most widely used virus delivery methods. Whether these two delivery methods can have impact on the viral tissues infection patterns is not clear. Our result showed that injection of low amounts of IAPV can induce acute mortality while feeding with much higher amounts cause both acute and chronic mortality. We also observed a higher variability of IAPV titers among biological replicates, and less clear tissues tropism in feeding than injection during the systemic infection, making the method feeding less optimal to study systemic infection. Besides, IAPV can be visualized in the similar functional regions of brains (e.g. mushroom bodies and optical lobes) after both injection and feeding. Surprisingly, we did not detect a clear viral signal in the columnar cells of the gut epithelium after either injection or feeding, which is a possible evidence of local defense. Therefore, studies with oral infection methods are advisable to infer the importance of local immunity and its central role as a barrier towards systemic infections.

After injection with IAPV, *B. terrestris* workers showed a clear front legs paralysis symptoms, prior to the typical symptom e.g. body trembling which is often observed shortly before death. Interestingly, not all viral infected bees can show these paralysis symptoms. Our results showed that symptomatic bees and asymptomatic bees share similar patterns in IAPV tissues accumulation (in brain, midguts, ovary and fat body) and localization (in brain). We could not proof that virus tissue infection pattern contribute to the occurrence of these paralysis symptoms.

Upon viral infection, siRNA and Jak/Stat pathways are recruited by the host to mitigate the virus infection. Vago, a protein which belongs to the single von Willebrand factor C-domain proteins (SVCs), can play a crosstalk role between the two pathways. Within hymenopteran species we noticed a reduced repertoire of SVCs, in most bee species there is just one SVC protein which function is uncharacterized. Our results showed that silencing this *SVC* gene lead to increased IAPV titers in fat body of *B. terrestris*, indicating that SVC is involved in the host antiviral defense. This antiviral role is mediated by Dicer-2, a key player of the siRNA pathway, as silencing *Dicer-2* lowered the *BtSVC* expression and increased the IAPV titers.

We also observed a lower expression of antimicrobial peptides (AMP) genes in fat body with silenced *BtSVC* expression, suggesting a potential links of *Bt*SVC with AMP expression. However, *Bt*SVC does not seem to interact with AMPs induction upon IAPV infection, indicating that *Bt*SVC is only involved in the basal AMP expression.

Aside from the antiviral immune signaling pathways, cellular immunity can also contribute to the insect antiviral immune defense, which mechanism is yet to be clear. Hemocytes, known as the circulating cells in the hemocoel, are the main component of cellular immunity. Therefore, changes of hemocytes profile can be used as a proxy of cellular response against virus infection. By using flow cytometry analysis, we found

that IAPV infection can induce hemocytes mortality and decreased lectin (WGA) binding activity, while another RNA virus SBPV did not. We also provided evidence of cell necrosis after IAPV infection, although the evidence of apoptosis is not clear in our setup. Besides, latex beads injection (to block phagocytosis) did not increase the mortality nor IAPV titers (in tissues of brains and fat body). The involvement of phagocytosis in host antiviral defense towards IAPV infection is not clear at this stage. Future studies towards understanding the role that cellular immunity plays in the host antiviral defense is therefore needed.

Samenvatting

Hommels (Bombus sp.) zijn essentiële bestuivers van verschillende gewassen wereldwijd. De globale achteruitgang van deze species kan vertrekkende gevolgen hebben voor de bestuiving van deze gewassen en het ecosysteem in het algemeen. De precieze oorzaak achter hun achteruitgang blijkt echter een complex gegeven en wordt vermoedelijk veroorzaakt door een combinatie van verschillende stressoren. De recentelijke ontdekking van RNA virussen in hommels leidde dan ook tot heel wat aandacht in de wetenschappelijke wereld, dit aangezien deze virussen die gekend zijn bij de honingbij daar vaak desastreuse gevolgen hebben. Studies die de interactie tussen deze virussen en de hommel bestuderen zijn daarom nodig zodat een goed beeld gevormd kan worden van de impact van deze virussen op hommels. In dit proefschrift werd deze interactie voornamelijk bestudeerd aan de hand van labo experimenten. Als eerste werden de symptomen en infectiepatronen van Israeli acute paralysis virus (IAPV) onderzocht bij *Bombus terrestris* werksters. In een tweede luik werd de rol van het aangeboren immuunsysteem bij de antivirale afweermechanismen onderzocht.

Orale toediening en kunstmatige injectie zijn de twee meest gebruikte technieken om een gastheer te infecteren onder laboratoriumcondities. Er is echter weinig geweten over de invloed van deze toedieningstechnieken op het infectiepatroon van een virus. Onze resultaten tonen dat injectie van een lage dosis IAPV resulteert in een acute mortaliteit. Orale toediening van een veel hogere dosis IAPV leidde tot zowel een acute als chronische mortaliteit. Orale toediening resulteerde in een hoge variabiliteit van de virus titer in weefsels tussen de biologische herhalingen. Daarnaast was er bij orale toediening van IAPV een minder duidelijk weefseltropisme vergeleken met injectie. Bij zowel orale toediening als injectie kon IAPV teruggevonden worden in gelijkaardige regio’s van de hersenen (nl. de mushroom bodies en de optische lobes).

Tot onze verbazing resulteerde geen van beide toedieningstechnieken in een viraal signaal in de columnaire cellen van het darmepitheel, wat een mogelijk bewijs is van een lokale antivirale reactie. Orale toediening van virus wordt dan ook aangeraden voor studies die de rol van lokale immuniteit en het belang hiervan als barrière voor systemische infecties bestuderen.

Injectie van IAPV resulteerde in verlamming van de voorpoten gevolgd door de typische symptomen welke vaak worden gezien vlak voor het sterven, nl. het trillen van het hele lichaam. Echter niet alle geïnfecteerde hommels vertoonden deze verlammingsverschijnselen. Onze resultaten tonen dat zowel symptomatische als asymptomatische hommels een gelijkaardige IAPV weefsel accumulatie (in de hersenen, de middendarm, de eierstokken en het vetweefsel) en lokalisatie in de hersenen vertonen. We konden echter niet aantonen dat het infectiepatroon van het virus doorheen de weefsels bijdraagt tot de geobserveerde verlammingsverschijnselen.

Na virale infectie worden de siRNA en de Jak/Stat pathway geactiveerd door de host om de infectie te bestrijden. Vago, een proteïne behorende tot de “single von Willebrand factor C-domain proteins” (SVCs), zou een rol kunnen spelen in de communicatie tussen beide pathways. Binnen de hymenopteren blijkt het aantal SVCs gereduceerd te zijn. In de meeste bijensoorten wordt slechts één SVC proteïne teruggevonden, de functie hiervan is echter nog niet gekend. Onze resultaten tonen dat het silencen van dit SVC gen een verhoogde IAPV titer veroorzaakt in het vetweefsel van *B. terrestris*. Dit illustreert de rol van SVC in het antiviraal afweermechanisme van de gastheer. De rol van SVC wordt gemedieerd door Dicer-2, welke een belangrijke rol heeft in de siRNA pathway, aangezien het silencen van

Dicer-2 resulteerde in een verlaagde expressie van BtSCV en een verhoogde IAPV titer.

Daarnaast werd ook een verlaagde expressie van antimicrobiële peptiden (AMP) opgemerkt bij het silencen van BtSVC. Dit zou kunnen wijzen op een link tussen BtSVC en AMP expressie. BtSVC blijkt echter niet te interageren met de AMP expressie bij IAPV infectie, wat wijst op het feit dat BtSVC enkel betrokken is bij de basale expressie van AMPs.

Naast de antivirale immuunrespons signalisatie pathways kan cellulaire immuniteit echter ook bijdragen tot de antivirale immuunrespons in insecten, hoewel de precieze mechanismen hierachter nog niet gekend zijn. Hemocyten, dit zijn de cellen die vrij circuleren in het hemoceel, zijn de hoofdcomponent van de cellulaire immuniteit. Verandering van de samenstelling van hemocyten kan daarom gebruikt worden als een proxy de cellulaire respons na virale infectie. Aan de hand van flow cytrometry analyses konden we aantonen dat IAPV infectie mortaliteit bij hemocyten veroorzaakt en een verlaagde lectine (WGA) bindingsactiviteit. Infectie met SBPV, een ander RNA virus, veroorzaakte deze effecten echter niet. IAPV infectie resulteerde in celnecrose. Het inbrengen van latex kralen om fagocytose te blokkeren resulteerde niet in een verhoogde mortaliteit of hogere IAPV titer in de hersenen of het vetweefsel. De rol van fagocytose bij antivirale afweermechanismen na IAPV infectie is echter nog niet opgehelderd. Verdere studies zijn daarom nodig om de rol van de cellulaire immuunrespons bij antivirale afweer in de gasteer grondig te onderzoeken.

Curriculum Vitae

Haidong Wang

Lab of Agrozoology

Faculty of Bioscience Engineering, Ghent University

Coupure links 653, 9000 Ghent, Belgium

Email: haidong.wang@ugent.be, Tel: 32-09-264-6146 (work)/32-0486928906 (home)

Personal info

Nationality: China
Place of Birth: Zibo, Shandong
Date of Birth: 22/09/1987
Email: haidong.wang@ugent.be/wanghd2826@gmail.com

Education

Oct.2013-now, PhD student in Applied Biology Science, Ghent University, Belgium. Supported by Chinese scholarship council (CSC) and co-funding of Ghent University (BOF-UGent).

Sep.2010-June 2013, Master in Forest Protection, Northwest A&F University, China. Thesis title: Molecular cloning and expression of P450 genes from *Dastarcus helophoroides*

Sep. 2006-June 2010, Bachelor in Horticulture, Shandong Agriculture University, China.

Research

Oct. 2013-now, Virus-host interaction of Israeli acute paralysis virus and bumblebee *Bombus terrestris*

Sep.2010-July.2013, Molecular cloning and expression of P450 genes in *Dastarcus helophoroides*

Publications with this thesis

Wang, H., Smagghe, G. & Meeus. I., 2017. The role of von Willebrand factor C-domain protein (SVC) in bumblebee immunity (*Bombus terrestris*) is more than antiviral defense. *Under review*.

Wang, H., Smagghe, G. & Meeus. I., 2017. Differential expression of antimicrobial peptides in *Bombus terrestris* workers upon Israeli acute paralysis virus (IAPV). *Under review*

Wang, H., Meeus, I., Piot, N. & Smagghe, G., 2017. Systemic Israeli acute paralysis virus (IAPV) infection in bumblebee (*Bombus terrestris*) through feeding and injection Journal of Invertebrate Pathology *Under review*

Wang, H., Meeus. I. & Smagghe, G., 2016. Israeli acute paralysis virus associated paralysis symptoms, viral tissue distribution and Dicer-2 induction in bumblebee workers (*Bombus terrestris*). Journal of General Virology. 97, 1981-1989

Acknowledgments

A famous speecher once said that if he is asked to give a 5min speech, he needs to prepare for a week, however, when it comes to a speech of two hours, no preparation is needed. At this very moment, I really feel what he feels. Indeed, it is a difficult job to include the thanks of four years in only two pages of a book where the rest 98% of the contents of this book are scientific. I will try my best.

First of course, I have to thank my promoter, Prof. Guy Smagghe. You brought me to the stage and gave me the opportunity to perform. If I look back now, this opportunity has changed my life completely. So, thank you Guy!

Ivan, as my co-promoter, we had some really good time together (both in the lab and bar…). If Guy is the one who brought me to the stage, then you are the one who taught me to dance. I really enjoyed the discussions (both scientific ones and political ones…) with you. Your ideas often inspired me and made me think in a different way. You are an excellent supervisor and a great friend!

To my dissertation committee, Prof. dr. ir. Peter Bossier, Dr. ir. Olivier Christiaens, Dr. ir. Tom Defoirdt, Prof. Dirk de Graaf, Prof. Dr. Luc Swevers, and Prof. Daisy Vanrompay, thank you for correcting my thesis and offering professional advices.

In our lab, I had the luck to work with some really nice people. Leen, Bjorn, Rik, Didier, and Stephanie, thank you for providing support to my work in the lab. You guys are always the first one to turn to when I ran into technical problems.

Through collaborations, I also had nice memories with people outside our department. Anneke, thank you for offering me assistance in sectioning work in my first two years, I really miss the time in Melle! Tom, thank you for doing flow cytometry test for me and I know you are often very busy.

To my bumblebee group, Ivan, Kevin, Anneleen, Niels, Maxime, Matti, Tian, Kleber, Luoluo, and Adinda, and those who already graduated, Jinzhi, Kaat, Jafa, Annelies and Laurian, I will always treasure the time we had! Kaat, thank you for guiding me (even for a short time) in my first year with cell work! Anneleen and Niels, thanks for offering me the language support with the Dutch summary of this thesis.

To my party group, Clauvis, Jinzhi, kathy, Ruben, Dora and all the foreign friends in Block B and other department in ugent and Belgium, thank you guys for giving me so many nice and crazy nights!

To my sweet Chinese group, you make me feel just like home, I will always treasure the time we had (especially those during the lunch and at the weekends)!

Special thanks must go to Na and Jinzhi. I learned a lot from you two. You both are excellent scientists! I do appreciate your help and guidance during my PhD career. Fan and An, as my former roommates, we had some really nice moments together, especially in the kitchen!

Of course, I must thank the Chinese Scholarship Council (CSC) and the BOF co-founding (ugent) for providing me financial support during my PhD study!

Before the end, I would like to thank all the professors, colleagues and friends that once brought me happiness and gave me a hand in the past four years. Forgive me that I cannot mention each of your name here, but your faces and the memory we shared will always in my mind!

At last, thank you mum and dad, for supporting every choice I have made in my life. Love you both! **爸，妈，谢谢你们一直以来对我毫无保留的支持，我爱你们！**